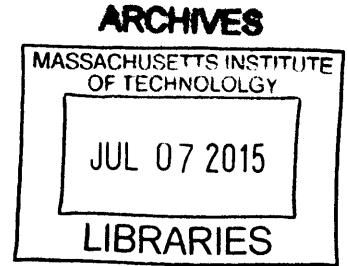# Intelligent Network Selection and Energy Reduction for Mobile Devices

by

Shuo Deng

B.S., Automation, Tsinghua University (2009)

S.M., Computer Science, Massachusetts Institute of Technology (2012)

Submitted to the Department of Electrical Engineering and Computer Science

in partial fulfillment of the requirements for the degree of

Doctor of Philosophy in Computer Science

at the

Massachusetts Institute of Technology

June 2015

©Massachusetts Institute of Technology 2015. All rights reserved.

Author . . . . **Signature redacted** . . . .

Department of Electrical Engineering and Computer Science

May 20, 2015

Certified by . . . **Signature redacted** . . . .

Hari Balakrishnan

Professor

Thesis Supervisor

Accepted by . . . . . **Signature redacted** . . . .

Leslie A. Kolodziejski

Chair, Department Committee on Graduate Theses

Intelligent Network Selection and Energy Reduction for Mobile Devices

by

Shuo Deng

Submitted to the Department of Electrical Engineering and Computer Science on

May 20, 2015, in partial fulfillment of the requirements for the degree of

Doctor of Philosophy in Computer Science

ABSTRACT

The popularity of mobile devices has stimulated rapid progress in both Wi-Fi and cellular technologies. Before LTE was widely deployed, Wi-Fi speeds dominated cellular network speeds. But that is no longer true today. In a study we conducted with a crowd-sourced measurement tool used by over 1,000 users in 16 countries, we found that 40% of the time LTE outperforms Wi-Fi, and 75% of the time the difference between LTE and Wi-Fi throughput is higher than 1 Mbits/s.

Thus, instead of the currently popular "always prefer Wi-Fi" policy, we argue that mobile devices should use the best available combination of networks: Wi-Fi, LTE, or both. Selecting the best network combination, however, is a challenging problem because: 1) network conditions vary with both location and time; 2) many network transfers are short, which means that the decision must be made with low overhead; and, 3) the best choice is determined not only by best network performance, but also constrained by practical factors such as monetary cost and battery life.

In this dissertation, we present Delphi, a software controller for network selection on mobile devices. Delphi makes intelligent network selection decisions according to current network conditions and monetary cost concerns, as well as battery-life considerations. Our experiments show that Delphi reduces application network transfer time by 46% for web browsing and by 49% for video streaming, compared with Android's default policy of always using Wi-Fi when it is available. Delphi can also be configured to achieve high

throughput while being energy efficient; in this configuration, it achieves $1.9\times$ the through-put of Android's default policy while only consuming 6% more energy.

Delphi improves performance but uses the cellular network more extensively than the status quo, consuming more energy than before. To address this problem, we develop a general method to reduce the energy consumption of cellular interfaces on mobile devices. The key idea is to use the statistics of data transfers to determine the best times at which to put the radio in different power states. These techniques not only make Delphi more useful in practice but can be deployed independently without Delphi to improve energy efficiency for any cellular-network-enabled devices. Experiments show that our techniques reduce energy consumption by 15% to 60% across various traffic patterns.

Dissertation Supervisor: Hari Balakrishnan
Title: Professor

To Xinming and my parents

Contents

List of Figures

11

12

13

16

List of Tables

17

Previously Published Material

This dissertation includes material from the following publications:

1. Shuo Deng, Ravi Netravali, Anirudh Sivaraman, Hari Balakrishnan. "WiFi, LTE, or Both? Measuring Multi-Homed Wireless Internet Performance", ACM IMC 2014. (Chapter 2)

2. Shuo Deng, Anirudh Sivaraman, Hari Balakrishnan. "All Your Network Are Belong to Us: A Transport Framework for Mobile Network Selection", HotMobile 2014. (Chapter 3)

3. Shuo Deng, Alvin Cheung, Sam Madden, Hari Balakrishnan."Multi-Network Control Framework for Mobile Applications", ACM S3 2013. (Chapter 3)

4. Shuo Deng, Anirudh Sivaraman, Hari Balakrishnan. "Delphi: A Software Controller for Mobile Network Selection", *Submitted for publication*. (Chapter 3)

5. Shuo Deng, Hari Balakrishnan. "Traffic-Aware Techniques to Reduce 3G/LTE Wireless Energy Consumption", ACM CoNEXT 2012. (Chapter 4)

   The dataset used in Chapters 2 and 3 is available at `http://web.mit.edu/cell-vs-wifi`.

Acknowledgments

I would like to thank my advisor, Hari Balakrishnan, for his guidance and advice in the past six years, and also for being open-minded and supportive about my career choice. During these years, I learned much from Hari, including how to tackle new research problems, pitch ideas, and give presentations. I believe these skills will be valuable not only for my research but also for my future life, no matter what career path I choose.

I would also like to thank my thesis committee members, Sam Madden and Dina Katabi. As my academic advisor, Sam has given me guidance not only on graduate courses but also on research. Dina offered me the opportunity to give practice talks during her group meeting, and provided valuable feedback.

I would also like to thank my labmates and colleagues. Katrina LaCurts's dedication to research has really inspired me. I feel fortunate to have worked with her on her cloud computing project, from which I learned a great deal about how to conduct research. I have also worked closely with Alvin Cheung, Anirudh Sivaraman, Ravi Netravali, and Tiffany Chen. They brought fun, motivation, and relief to my research. I also want to thank Lenin Ravindranath, Raluca Ada Popa, Keith Winstein, Jonathan Perry, Amy Ousterhout for giving me valuable feedback and detailed comments on writing papers.

My research has benefited from our collaboration with Foxconn. I feel fortunate to have worked with Foxconn engineers: Leon Lee, Ethan Kuo, Edward Lu, and Sigma Huang. Without their hard work and expertise in network engineering, it would have been hard to deploy my algorithms on commercial devices.

My parents have supported me unconditionally throughout my life. Their life stories taught me to always be focused and determined and keep inner peace. I thank my grand-father and grandmother for being supportive of my study abroad. Special thanks goes to

my husband, Xinming Chen, who has been my 24/7 technical and emotional support all through graduate school, and who gave up a cozy life in China to end our long-distance relationship and start a new page of life together in the United States.

Chapter 1

Introduction

By the end of 2014, the number of mobile-connected devices had exceeded the world's population [74]. The popularity of these devices has stimulated further rapid progress in both Wi-Fi and cellular technology. Now the 802.11 standard provides a Wi-Fi link rate as high as 1 Gbps [1]. Cellular networks have advanced from EDGE to 3G to LTE, or 4G, with peak downlink speed also in the order of 1 Gbps [2].

Despite all these high-speed wireless technologies being widely deployed, the lack of an intelligent network selection mechanism prevents mobile device users from fully exploiting available network resources. Today's mobile operating systems typically hard-code the decision of which network to use when confronted with multiple choices. If the user has previously associated with an available Wi-Fi network, the mobile device uses that over a cellular option. This choice often leads to frustrating results. For example, when walking outdoors, users often find their device connecting to a Wi-Fi access point inside a building and experience poor performance when the right answer is to use the cellular network. Even inside homes and buildings, a static choice is not always the best: there are rooms where the Wi-Fi network might be much slower than the cellular network, depending on other users, time of day, and other factors. Thus, network selection for mobile devices needs to be done dynamically since Wi-Fi and cellular networks are not evenly distributed, either spatially or temporally.

Moreover, in practice, users care not just about performance but also about the monetary cost of using wireless networks as well as battery life. These factors increase the difficulty

of the network-selection problem. Indeed, one reason many current mobile devices always prefer Wi-Fi over cellular is because Wi-Fi is generally free, whereas cellular is generally not. However, for some users with a monthly cellular data plan, the downside of being too conservative with using cellular networks is that they may end up paying a subscription fee every month while using little of their data plan budget. Meanwhile, the economics of cellular data plans are changing. After being offered beginning in 2007, "unlimited" plans were halted in 2011 by several carriers (although pre-existing users could hold on to them). Since 2013, however, unlimited plans have made a resurgence, especially in Tier-2 operators, where 45% of the users have such plans today [74]. In addition, an increasing number of major app providers like Facebook, Google, and WhatsApp, have proposed and are deploying "zero rating" plans so that mobile device users will not be charged when these apps generate cellular traffic [83]. Thus, an intelligent network selection mechanism should be able to cope with different monetary cost models.

Another major concern is energy consumption. It is well known that the cellular radio consumes significant amounts of energy; on the iPhone 6 Plus, for example, the stated internet-use time is "up to 12 hours on 3G or LTE" (i.e., when the 3G radio is on and in "typical" use) and the talk-time is "up to 24 hours".[1] On the Nexus 5, the equivalent numbers are "up to 7 hours on LTE for internet-use" and "up to 17 hours for talk time"[2]. Thus, to improve overall user experience, an intelligent network selection mechanism should not merely aim for increasing the network speed.

This dissertation begins with a measurement study analyzing the network performance of mobile devices in the real world. This measurement study also shows that significant improvements may be achieved if network selection is done properly. Then, we present Delphi, a software controller for network selection on mobile devices. Delphi makes intelligent network selection decisions according to current network conditions, monetary cost concerns, as well as battery level. Delphi's design is based on data collected during the measurement study. We also implement Delphi and show that it can improve network performance in real-world experiments. Finally, we take a deeper look into the causes of high

---

[1]http://www.apple.com/iphone-6/specs/

[2]https://support.google.com/nexus/answer/3467463?hl=en&ref_topic= 3415523

energy consumption when a mobile device uses the cellular network, and develop software solutions to improve the energy-efficiency of cellular interfaces.

1.1 Measuring Wi-Fi and Cellular Networks

We conducted a set of measurements using a crowd-sourced network measurement tool as well as with controlled experiments (§2). The conclusions from this measurement study are as follows:

1. Over 73% of the time, the throughput of one of the networks was higher than the other by at least 1 Mbit/s. When the throughput difference was at least 1 Mbit/s, LTE/4G had higher throughput 56% of the time, and Wi-Fi 44% of the time; that is, it was roughly split down the middle. The throughput differentials depended on the transfer size, due to the dynamics of TCP congestion control.

2. Over 83% of the time, the round-trip latency of one of the networks was higher than the other by at least 100 ms.

3. Multipath TCP (MPTCP) [77], which uses multiple interfaces whenever possible, did not always out-perform single-path TCP connections. A key factor in MPTCP's performance was the *choice of primary subflow*, that is, the network on which the initial connection and data transfer is done. This choice has a strong effect on the throughput, particularly for short and medium-sized transfers.

These conclusions left a key question open: *How do we design a practical software module for mobile devices to select the best network for applications?* This question is important for both single-path and multi-path TCP transfers.

1.2 Network Selection for Multi-homed Mobile Devices

To answer this question, we designed *Delphi* (§3), a mobile software controller that helps mobile applications select the best network among available choices for their data transfers. Our starting point is from the perspective of users and applications rather than the transport layer or the network. Depending on the objectives of interest, Delphi makes different

decisions about which network to use and in what order.

We consider three objectives (though the framework handles other objectives as well):

1. minimize the time to complete an application-level transfer (the ratio of transfer size to transfer throughput);

2. minimize the energy per byte of the transfer, which usually (but not always) entails picking only one network; and

3. minimize the monetary cost per byte of the transfer.

Delphi provides a framework to optimize these and similar objectives. This problem is challenging because the answer changes with time, and depends on location and user movement.

Delphi has four components:

1. *Network Performance Predictor* estimates the latency and throughput of different networks by running a machine-learning predictor using features obtained from the Network Monitor.

2. The *Network Monitor* uses passive observations of wireless network properties such as the Received Signal Strength Indicator (RSSI) and channel quality, lightweight active probes, and an adaptive method that uses active probes only when passive indicators suggest a significant change in conditions.

3. *Traffic Profiler* provides an estimate of the length of transfers; this component is required because throughput depends on the size of the transfer.

4. *Network Selector* uses network performance predictions, transfer lengths, and the specified objectives for application transfers to determine which network to use for each transfer.

Our evaluation shows that:

1. In our simulations over traces collected from 22 locations, Delphi improved the median throughput by 2.1× compared with always using Wi-Fi, the default policy on Android devices today. Delphi can also be configured to achieve high throughput while being energy-efficient; in this mode, it achieves 1.9× throughput while consuming only 6% more energy compared with Android's default policy.

2. When running with unmodified applications, Delphi reduces applications' network

transfer time by 46% for web browsing and by 49% for video streaming, compared with Android's default policy.

3. Delphi is also proactive in switching networks when the device is moving. It can detect that the network that is currently in use is performing worse than the alternatives and can switch before the connection breaks. In our experiment, Delphi switched networks 30 seconds earlier than the MPTCP handover mode proposed in [57] did.

1.3 Reducing the Energy Consumed by the Cellular Interface
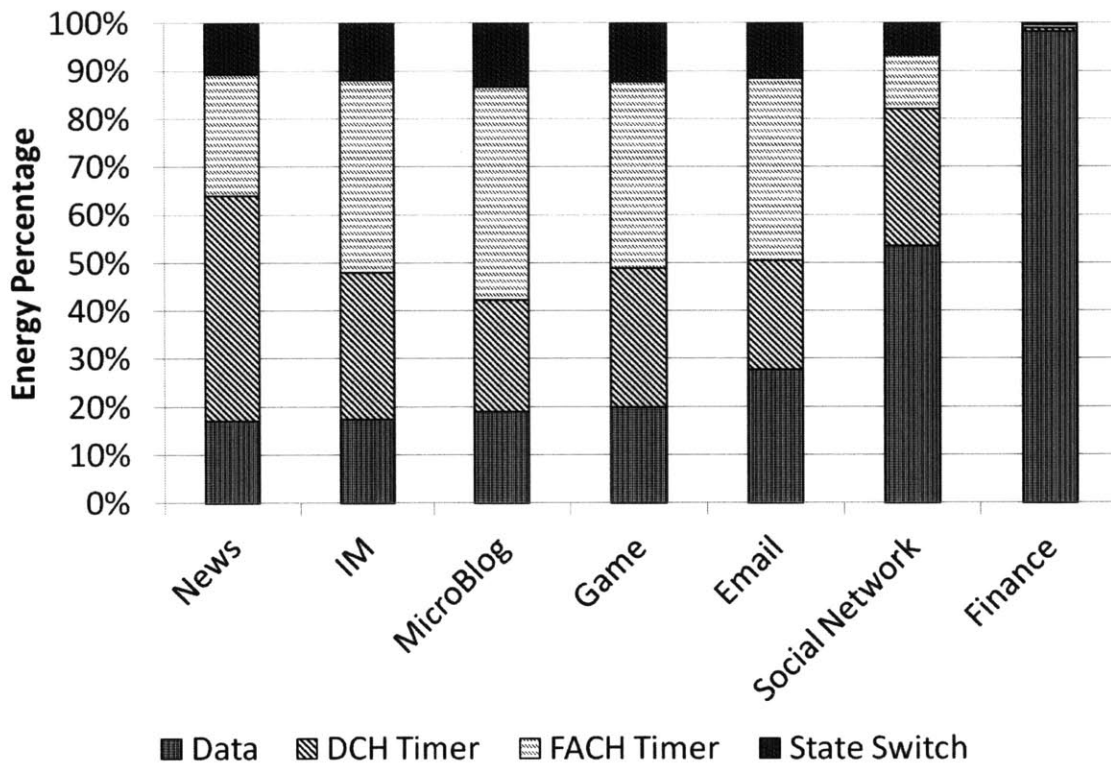
Figure 1-1: Energy consumed by the 3G interface. "Data" corresponds to a data transmission; "DCH Timer" and "FACH Timer" are each the energy consumed with the radio in the idle states specified by the two timers, and "State Switch" is the energy consumed in switching states. These timers and state switches are described in §4.2.

The results in our measurement study indicate that cellular networks should be used

27

more often to achieve better performance. However, it is well known that the 3G/LTE radio consumes significant amounts of energy. We show the measured values of 3G energy consumption for multiple Android applications in Figure 1-1.[3] This bar graph shows the percentage of energy consumed by different 3G radio states. For most of these applications (which are all background applications that can generate traffic without user input, except for Facebook), less than 30% of the energy consumed was during the actual transmission or reception of data. Previous research arrived at a similar conclusion [14]: about 60% of the energy consumed by the 3G interface is spent when the radio is not transmitting or receiving data.

In Chapter 4, we develop a solution to reduce 3G/LTE energy consumption. Unlike currently deployed methods that simply switch between radio states after fixed time intervals—an approach known to be rather crude and sub-optimal [81, 15, 40, 66]—our approach is to observe network traffic activity on the mobile device and switch between the different radio states by adapting to the workload. We apply statistical learning techniques to predict network activity and make transitions that are suggested by the statistical models. This approach is well-suited to the emerging *fast dormancy* mechanism [3, 4] that allows a radio to rapidly move between the Active and Idle states and vice versa. Our goal is to reduce the energy consumed by networked background applications on mobile devices.

1.4 Contributions

This dissertation makes the following contributions:

1. Our measurement study analyzes mobile network performance in the real world. This measurement study also demonstrates that significant potential improvement may be achieved if network selection is done properly.

2. The design and implementation of Delphi demonstrates a way to coordinate different concerns when making network interface selections. Inside Delphi, we employ machine learning methods to make network selections. The machine learning models

---

[3]An HTC G1 phone connected to a power monitor [43], with only one application running, at one indoor location.

are trained using network performance data we collected during the measurement study. In the future, as wireless networks advance, the specific parameters we trained for the current solution or even the machine learning algorithm may not be applicable to make good network selections; however, our modular design makes sure that the algorithms can be easily replaced. Thus, as long as there are co-existing networks whose performances are not evenly distributed spatially or temporally, Delphi's framework can always be applicable.

3. Both our network selection and energy-efficient solutions require no modification to the application running on the mobile devices. Thus, they can be easily deployed and improve the performance and user experience of millions of apps already deployed.

1.5 Outline

The rest of this dissertation is organized as follows. Chapter 2 describes our measurement study on the performance of Wi-Fi and cellular networks as well as transferring data on both networks. Chapter 3 presents the design, implementation and evaluation for Delphi. Chapter 4 analyzes the energy-efficiency issue of cellular networks in detail and presents our solution to reduce energy consumption. Chapter 5 concludes the dissertation and discusses directions for future work.

Chapter 2

Measurement Study

Access to Wi-Fi and cellular wireless networks is *de rigueur* on mobile devices today. With the emergence of LTE, cellular performance is starting to rival the performance of Wi-Fi. Moreover, when Wi-Fi signal quality is low or in crowded settings, the anecdotal experience of many users is that cellular performance may in fact be considerably better than Wi-Fi performance. But just how good are LTE and Wi-Fi networks in practice, and how do they compare with each other? Should applications and transport protocols strive to select the best network, or should they simply always use Multi-Path TCP (MPTCP) [77]?

To answer these questions, we implemented a crowd-sourced network measurement tool (§ 2.1) to understand the flow-level performance of TCP over Wi-Fi and LTE in the wild from 16 different countries over a nine-month period, encompassing 3,632 distinct 1-Mbyte TCP flows. We used this data to measure transfer times for different amounts of data transferred.

MPTCP is not widely deployed yet on most phones.[1] As a result, we manually measured flow-level MPTCP performance and compared it with the performance of TCP running exclusively over Wi-Fi or LTE in 20 different locations, in 7 cities in the United States (§ 2.2). Finally, to complement our empirical flow-level analysis, we used an existing record-and-replay tool to analyze (§ 2.3) and run (§ 2.4) mobile apps on emulated cellular and Wi-Fi links, using it to study the impact of network selection on application

---

[1]The Apple iOS is an exception [49]. MPTCP is observed to be used for Siri. MPTCP on iOS operates in master-backup mode using Wi-Fi as the primary path, falling back to a cellular path only if Wi-Fi is unavailable.
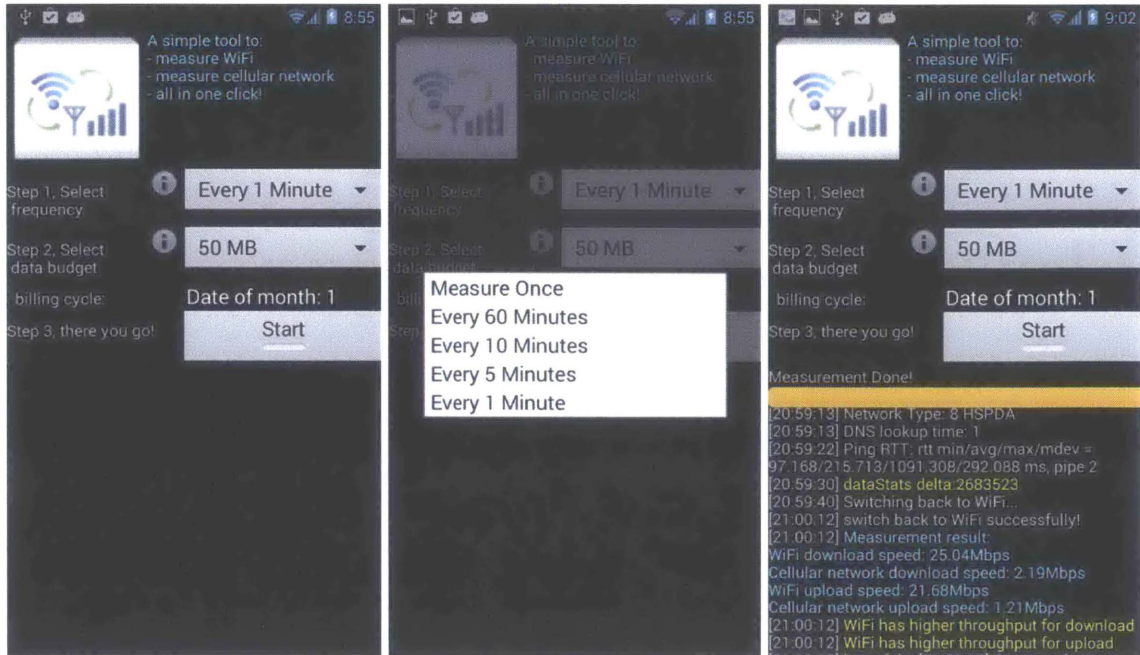
Figure 2-1: *Cell vs. Wi-Fi* User Interface.

performance.

2.1 Cell vs. Wi-Fi Measurement

In September 2013, we published an Android app on Google Play, called *Cell vs. Wi-Fi* (`http://web.mit.edu/cell-vs-wifi`). *Cell vs. Wi-Fi* measures end-to-end Wi-Fi and cellular network performance and uses these measurements to tell smartphone users if they should be using the cellular network or Wi-Fi at the current time and location. The app also serves as a crowd-sourced measurement tool by uploading detailed measurement data to our server, including packet-level traces. Over a nine-month period after the app was published, it attracted over 750 downloads. We collected over 10 GB of measurement data from 3,632 distinct TCP connections over this duration from these users.

2.1.1 Cell vs. Wi-Fi App

Figure 2-1 shows the user interface of *Cell vs. Wi-Fi*. Users can choose to measure network performance periodically or once per click. Users can also set an upper bound on the
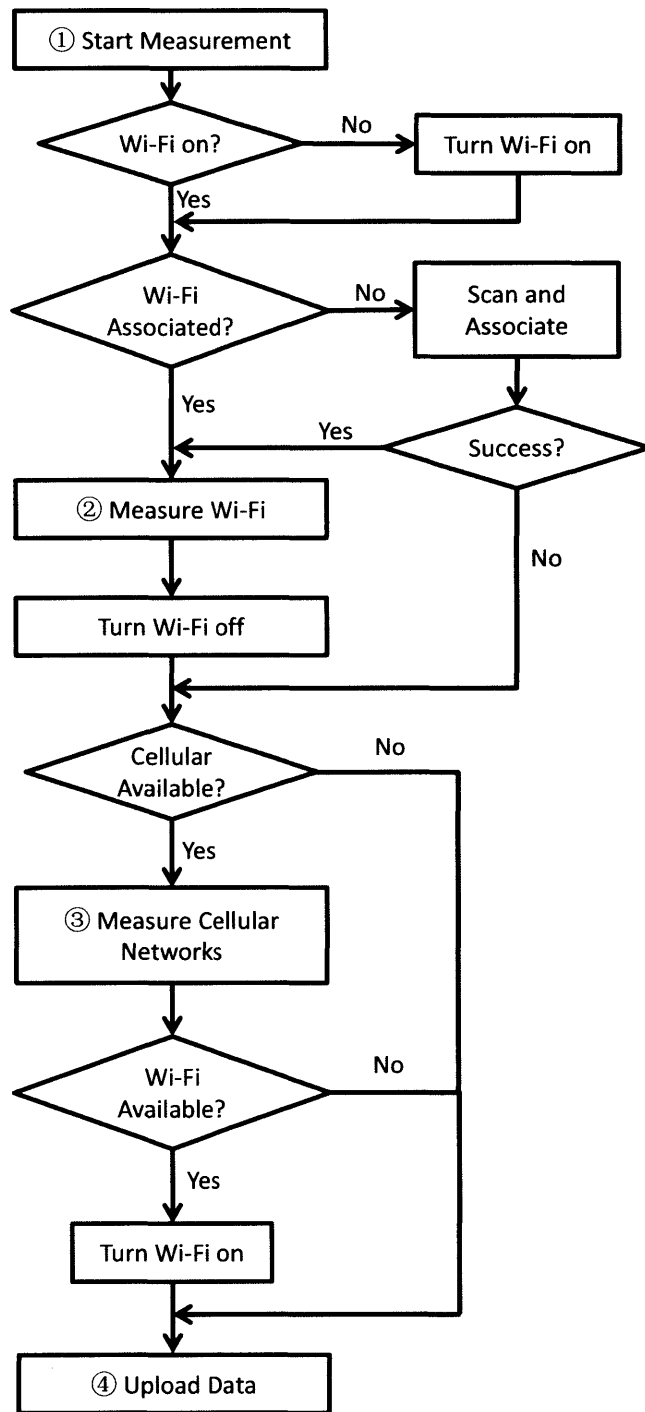
Figure 2-2: *Cell vs. Wi-Fi*: single measurement collection run.

amount of cellular data that the app can consume, especially for devices on a limited cellular data plan.

The flow chart in Figure 2-2 shows a single measurement collection run. When the user clicks the Start button, or the pre-set periodic measurement timer expires, one run of measurement collection starts, shown as Step ① in the figure. If Wi-Fi is available, and the phone successfully associates with an Access Point (AP), *Cell vs. Wi-Fi* collects packet-level tcpdump traces for a 1-Mbyte TCP upload and a 1-Mbyte TCP download between the mobile device and our server at MIT.

After measuring Wi-Fi, *Cell vs. Wi-Fi* turns off the Wi-Fi interface on the phone and attempts to connect to the cellular network. If the user has turned off the cellular data network, *Cell vs. Wi-Fi* aborts the cellular measurement. If *Cell vs. Wi-Fi* successfully connects to the cellular network, then in Step ③ it collects a similar set of packet-level tcpdump traces for both an upload and a download. Once both Wi-Fi and cellular network measurements are finished, in Step ④ *Cell vs. Wi-Fi* uploads the data collected during this measurement run, together with the user ID (randomly generated when a smartphone user uses the app for the first time) and the phone's geographic location, to our server at MIT.

More information about *Cell vs. Wi-Fi* can be found at http://web.mit.edu/ cell-vs-wifi.

2.1.2 Results

Cell vs. Wi-Fi collected network-performance data from locations in five continents: North America, South America, Europe, Africa, and Asia. We observed that some users use this app to measure only Wi-Fi or LTE performance, but not both. We do not consider these measurement runs because our goal is to compare LTE and Wi-Fi performance at nearly the same place and time. To ensure that we measured only performance of LTE or an equivalent high-speed cellular network, such as HSPA+, we used the Android network-type API [12] and picked only those measurement runs that used LTE or HSPA+. When using the term *LTE* in this dissertation, we mean either LTE or HSPA+. After these filtering steps, our dataset contains over 1,606 complete runs of measurement, that is, both LTE and Wi-Fi transfers in both directions.

In Table 2.1, we group nearby runs together using a *k*-means clustering algorithm, with

Location Name	(Lat, Long)	# of Runs	LTE %
US (Boston, MA)	(42.4, -71.1)	884	10%
Israel	(31.8, 35.0)	276	55%
US (Portland)	(45.6, -122.7)	164	45%
Estonia	(59.4, 27.4)	124	71%
South Korea	(37.5, 126.9)	108	66%
US (Orlando)	(28.4, -81.4)	92	35%
US (Miami)	(26.0, -80.2)	84	52%
Malaysia	(4.24, 103.4)	76	68%
Brazil	(-23.6, -46.8)	56	4%
Germany	(52.5, 13.3)	40	20%
Spain	(28.0, -16.7)	40	80%
Thailand (Phichit)	(16.1, 100.2)	40	80%
US (New York)	(40.9, -73.8)	24	33%
Japan	(36.4, 139.3)	16	25%
Sweden	(59.6, 18.6)	16	0%
Thailand (Chiang Mai)	(18.8, 99.0)	16	75%
US (Chicago)	(42.0, -88.2)	16	25%
Hungary	(47.4, 16.8)	8	0%
Italy	(44.2, 8.3)	8	0%
US (Salt Lake City)	(40.8, -111.9)	8	0%
Colombia	(7.1, -70.7)	4	0%
US (Santa Fe)	(35.9, -106.3)	4	0%

Table 2.1: Geographical coverage and diversity of the crowd-sourced data collected from 16 countries using *Cell vs. Wi-Fi*, ordered by number of runs collected. The last column shows the percentage of runs in which LTE's throughput is higher than Wi-Fi's throughput.

a cluster radius of $r = 100$ kilometers (i.e., all runs in each group are within 200 kilometers of each other). For each location group, we also list the percentage of measurement runs where LTE has higher throughput than Wi-Fi does.

Figure 2-3 shows the CDF of difference in throughput between Wi-Fi and LTE on the uplink and the downlink. We can see that the throughput difference can be larger than 10 Mbit/s in either direction. The gray region shows 42% (uplink) and 35% (downlink) of the data samples whose LTE throughput is higher than Wi-Fi throughput. If we combine uplink and downlink together, 40% of the time LTE outperforms Wi-Fi. Figure 2-4 shows the CDF of ping RTT difference between LTE and Wi-Fi. During our measurement, we sent 10 pings and took the average RTT value. The shaded area shows that in 20% of

35
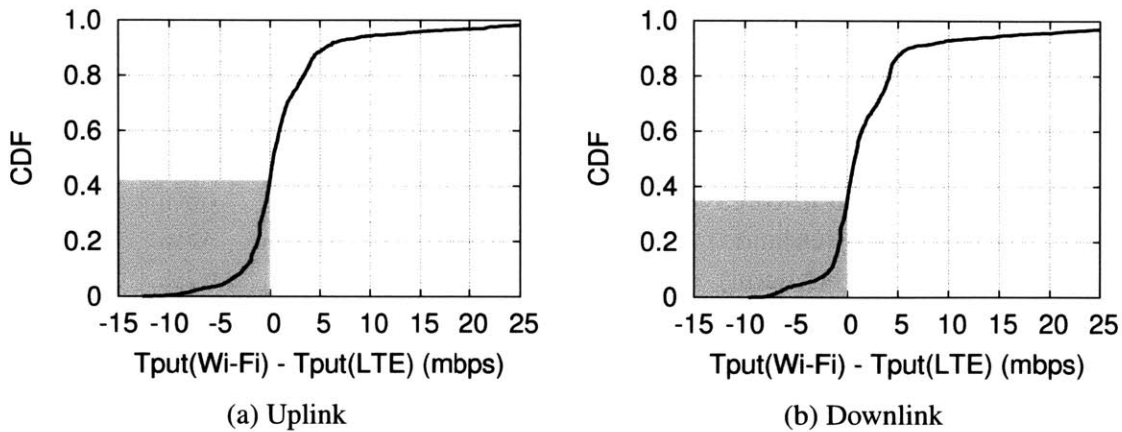
(a) Uplink (b) Downlink

Figure 2-3: CDF of difference between Wi-Fi and LTE throughput. The gray region shows 42% (uplink) and 35% (downlink) of the data samples whose LTE throughput is higher than Wi-Fi throughput.
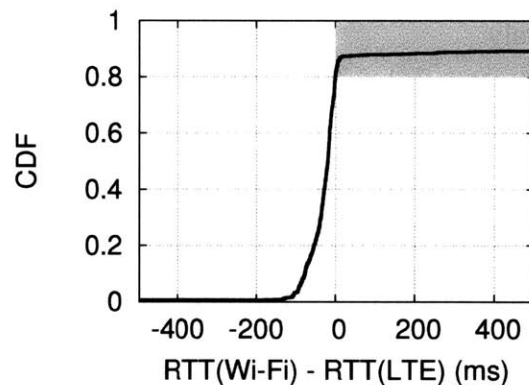
Figure 2-4: CDF of the difference between average Ping RTT with Wi-Fi and LTE. The gray region shows 20% of the data samples whose LTE RTT is lower than Wi-Fi RTT.

our measurement runs, LTE has a lower ping RTT than Wi-Fi does, although the cellular network is commonly assumed to have higher delays.

The simple network selection policy used by mobile devices today forces applications to use Wi-Fi whenever available. However, our measurement results indicate that a more flexible network selection policy will improve the network performance of mobile applications.

36

2.2 MPTCP Measurements

When Wi-Fi and cellular networks offer comparable performance, or when each varies significantly with time, it is natural to use both simultaneously. Several schemes transmitting data on multiple network interfaces have been proposed in the past [84, 62, 54, 77]. Among these, the most widespread is MPTCP [77]. MPTCP can be used in two modes [57]: *Full-MPTCP* mode, which transmits data on all available network interfaces at any time, and *Backup* mode, which transmits data on only one network interface at a time, falling back to the other interface only if the first interface is down. Unless stated otherwise, all experiments in this chapter used MPTCP in Full-MPTCP mode. For completeness, we compare the two modes in § 2.2.6. We used a modified version of *Cell vs. Wi-Fi* to carry out MPTCP measurements. We observed the following:

1. We found that MPTCP throughput for short flows depends significantly on the network selected for the primary subflow[2] in MPTCP; for example, changing the network (LTE or Wi-Fi) for the primary subflow changes the average throughput of a 10 KByte flow by 60% in the median (Figure 2-12 in § 2.2.4).

2. For long flows, selecting the proper congestion control algorithm is also important. For example, using different congestion control algorithms (coupled or decoupled) changes the average throughput of a 1 MByte flow by 34% in the median (Figure 2-17 in § 2.2.5).

3. MPTCP's Backup mode is typically used for energy efficiency: keeping fewer interfaces active reduces energy consumption overall. However, we found that for MPTCP in Backup mode, if LTE is set to the backup interface, very little energy can be saved for flows that last shorter than 15 seconds (§ 2.2.6).

2.2.1 MPTCP Overview

MPTCP initiates a connection in a manner similar to regular TCP: it picks one of the available interfaces and establishes a TCP connection using a SYN-ACK exchange with the server over that interface. Every TCP connection that belongs to a MPTCP connection

---

[2]We define subflows in § 2.2.1.

is called an MPTCP *subflow*. The first established subflow is called the *primary subflow*.

We used the Linux MPTCP implementation for our measurements [52] (Ubuntu Linux 13.10 with Kernel version 3.11.0, with the MPTCP Kernel implementation version v0.88). In this implementation, MPTCP initiates the primary subflow on the interface used as the default route on the machine. Once the primary subflow is established, if there are other interfaces available, MPTCP creates an additional subflow using each new interface and combines the new subflow with the existing subflows on the same MPTCP connection.[3] For example, a mobile device can establish an MPTCP primary subflow through Wi-Fi to the server and then add an LTE subflow to the server. To terminate the connection, each subflow is terminated using four-way FIN-ACKs, similar to TCP. In § 2.2.4 we study the effect of choosing different interfaces for the primary subflow on MPTCP performance.

There are two kinds of congestion-control algorithms used by MPTCP: *decoupled* and *coupled*. In decoupled congestion control, each subflow increases and decreases its congestion window independently, as if they were independent TCP flows [19]. In coupled congestion control, each subflow in an MPTCP connection increases its congestion window based on ACKs both from itself and from other subflows [77, 37] in the same MPTCP connection. In § 2.2.5 we compare the coupled and decoupled algorithms and find that using different congestion control algorithms has less impact on throughput compared with selecting the correct interface for primary subflows for short flows. However, for long flows, changing congestion control algorithms results in a substantial throughput difference.

2.2.2   Measurement Setup

Figure 2-5 shows the MPTCP measurement setup. The MPTCP client is a laptop running Ubuntu 13.10 with MPTCP installed. We tethered two smartphones to the laptop, one in "airplane" mode with Wi-Fi enabled, and the other with Wi-Fi disabled but connected to LTE (either the Verizon or the Sprint LTE network). The MPTCP server is located at MIT, with a single Ethernet interface, also running Ubuntu 13.10 with MPTCP installed.

We installed a modified version of *Cell vs. Wi-Fi* on both phones. The phone with Wi-Fi

---

[3]For simplicity, here we explain only how MPTCP works when the server is single-homed (like the server in our experiments), and the client alone is multi-homed.
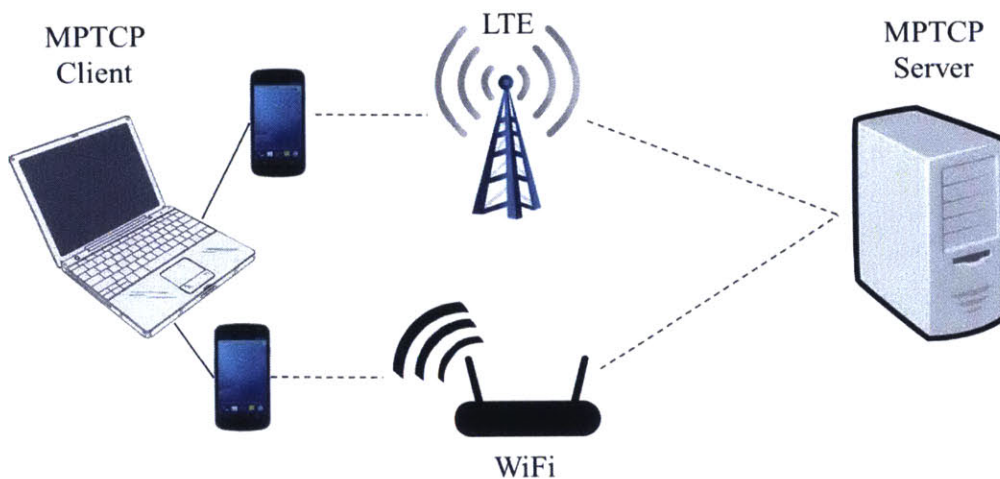
Figure 2-5: Setup of MPTCP measurement.

enabled measures only Wi-Fi performance (Step ② in Figure 2-2). The phone connected to LTE measures only cellular network performance (Step ③ in Figure 2-2).

The experimental setup also allows us to measure the energy consumption separately for each interface, which we present in § 2.2.6.

Each measurement run comprises the following:

1. Single-path TCP upload and download using modified *Cell vs. Wi-Fi* through LTE.
2. Single-path TCP upload and download using modified *Cell vs. Wi-Fi* through Wi-Fi.
3. MPTCP upload and download in Full-MPTCP mode with LTE as the primary sub-flow.
4. MPTCP upload and download in Full-MPTCP mode with Wi-Fi as the primary sub-flow.

We conducted the measurements at 20 different locations on the east and west coasts of the United States, shown in Table 2.2. At each city, we conducted our measurement at places where people would often use mobile devices: cafes, shopping malls, university campuses, hotel lobbies, airports, and apartments. At 7 of the 20 locations, we measured both Verizon and Sprint LTE networks using both MPTCP congestion-control algorithms: decoupled and coupled. At the other 13 locations, we were able to measure only the Verizon LTE network with coupled congestion control.

In Figure 2-6, we compare the Wi-Fi and LTE throughput distributions for the data we

39

ID	City	Description
1	Amherst, MA	University Campus, Indoor
2	Amherst, MA	University Campus, Outdoor
3	Amherst, MA	Cafe, Indoor
4	Amherst, MA	Downtown, Outdoor
5	Amherst, MA	Apartment, Indoor
6	Boston, MA	Cafe, Indoor
7	Boston, MA	Shopping Mall, Indoor
8	Boston, MA	Subway, Outdoor
9	Boston, MA	Airport, Indoor
10	Boston, MA	Apartment, Indoor
11	Boston, MA	Cafe, Indoor
12	Boston, MA	Downtown, Outdoor
13	Boston, MA	Store, Indoor
14	Santa Babara, CA	Hotel Lobby, Indoor
15	Santa·Babara, CA	Hotel Room, Indoor
16	Santa Babara, CA	Conference Room, Indoor
17	Los Angeles, CA	Airport, Indoor
18	Washington, D.C.	Hotel Room, Indoor
19	Princeton, NJ	Hotel Room, Indoor
20	Philadelphia, PA	Hotel Room, Indoor

Table 2.2: Locations where MPTCP measurements were conducted.

(a) Uplink

(b) Downlink
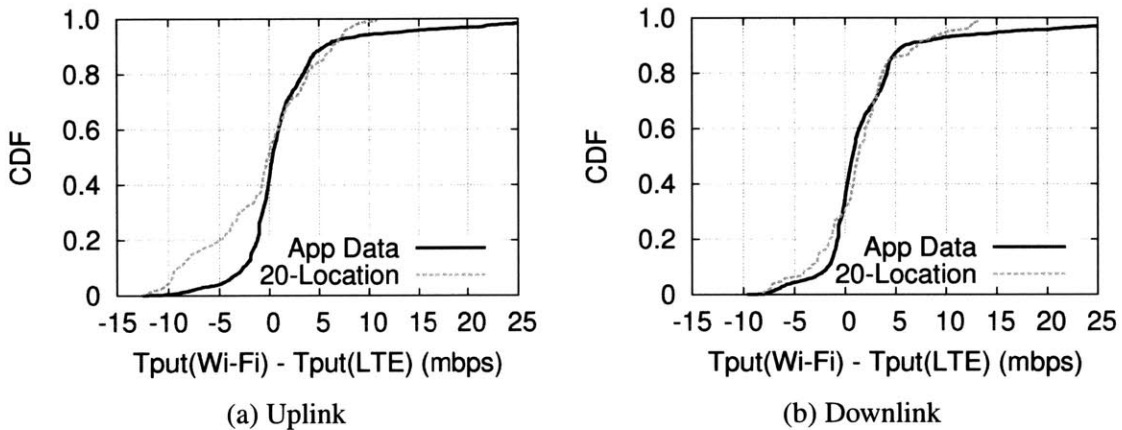
Figure 2-6: CDF for Wi-Fi and LTE throughput measured using regular TCP at 20 locations (shown as "20-Location") compared with the CDF in Figure 2-3 (shown as "App Data").

collected at these 20 locations and the data collected from *Cell vs. Wi-Fi* in § 2.1. We can see that for both upload and download, the "20-Location" CDF curves are close to the CDF

curves from § 2.1, implying that the 20 locations that were selected have similar variability in network conditions as the *Cell vs. Wi-Fi* dataset. For simplicity, in the rest of § 2.2, we show only results of downlink flows from the server to the client.

2.2.3 TCP vs. MPTCP
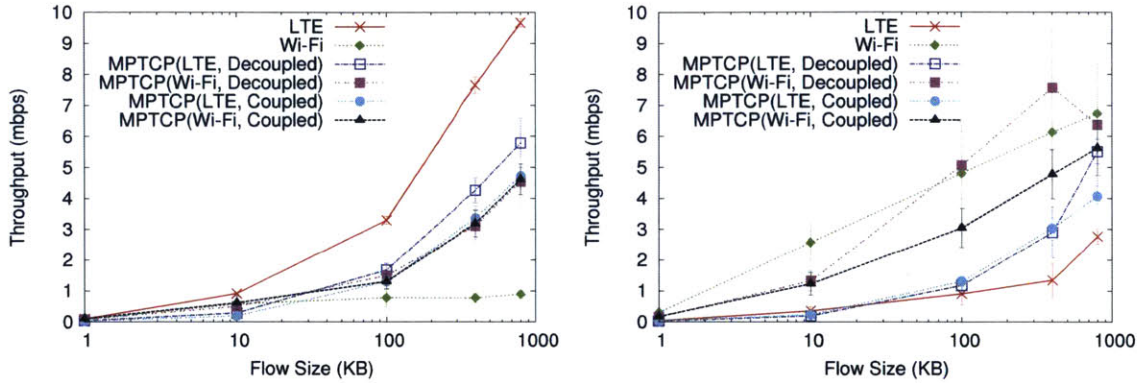
(a) MPTCP performs worse than single TCP.   (b) MPTCP performs better than single TCP.

Figure 2-7: MPTCP throughput vs single-path TCP throughput at 2 representative locations. Figure 2-7a shows a case in which MPTCP throughput is lower than the best throughput of single-path TCP. Figure 2-7b shows a case where MPTCP throughput (in this case, MPTCP (Wi-Fi, decoupled)) is higher than that of single-path TCP for large flow sizes.

A natural question pertaining to MPTCP is how the performance of MPTCP compares with the best single-path TCP performance achievable by an appropriate choice of networks alone. To answer this, we looked at all four MPTCP variants (two congestion control algorithms times two choices for the network used by the primary subflow) and both single-path TCP variants (Wi-Fi and LTE) as a function of flow size. Figure 2-7 illustrates two qualitatively different behaviors.

Figure 2-7a shows a case in which the performance of MPTCP is always worse than the best single-path TCP regardless of flow size. This occurs in a particularly extreme scenario in which a large disparity in link speeds between the two networks (LTE and Wi-Fi) leads to degraded MPTCP performance irrespective of flow size. On the other hand, Figure 2-7b shows an alternative scenario where MPTCP is better than the best single-path TCP at larger flow sizes. In both cases, however, picking the right network for single-path
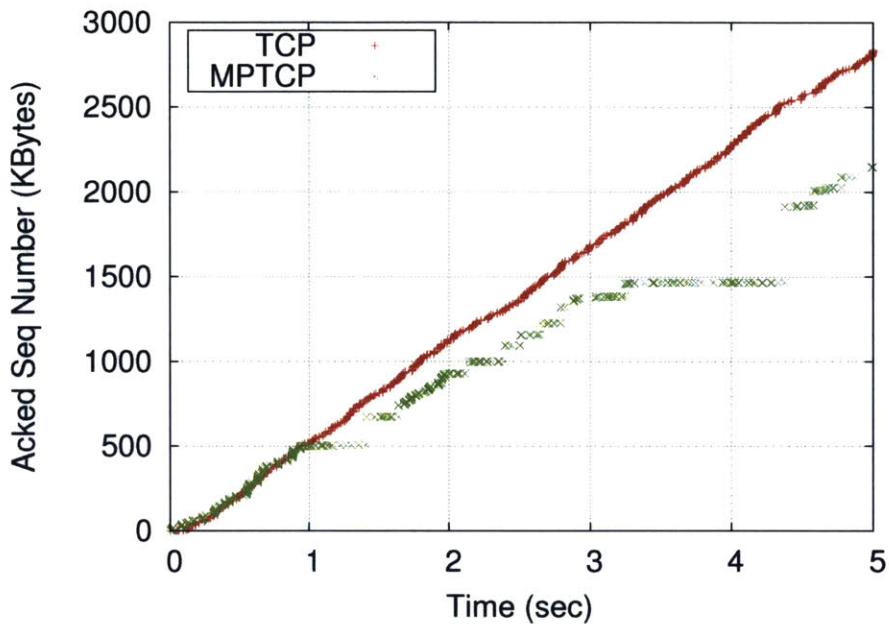
Figure 2-8: Acknowledged data vs. time for TCP and MPTCP.

(a) Sender Side
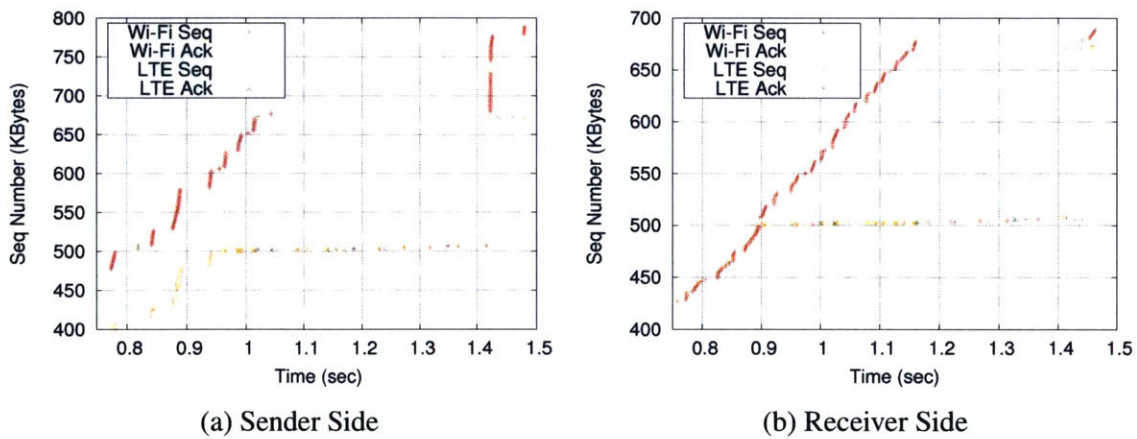
(b) Receiver Side

Figure 2-9: MPTCP sent and acknowledged data sequence number vs. time on sender and receiver side.

TCP is preferable to using MPTCP for smaller flows. These results suggest that it may not always be advisable to use both networks, and an adaptive policy that automatically picks the networks to transmit on and the transport protocol to use would improve performance relative to any static policy.

To investigate why MPTCP do not give higher throughput in certain cases, we con-

ducted experiments in a lab environment where Wi-Fi has a much higher link speed than LTE has. Figure 2-8 shows the ACK packet seen on the sender side when using Wi-Fi for single-path TCP and using Wi-Fi and LTE for MPTCP. We can see that between time 1.0 second and 1.5 seconds, the MPTCP sender sees fewer ACKs; thus, the average throughput decreases. To explain why MPTCP slows down at time 1.0 second, Figure 2-9 shows the MPTCP data sequence numbers sent out and ACK sequence numbers received on its Wi-Fi subflow and LTE subflow. We can see that in Figure 2-9a MPTCP starts sending data on the LTE subflow at time 0.82 seconds. It sends out 10 back-to-back packets (with sequence numbers from 514008 bytes to 519720 bytes) because the initial congestion control window is set to 10 by default. The LTE subflow receives the first ACK at time 1.02 seconds, that is, the RTT for LTE subflow is 0.2 seconds, much longer than Wi-Fi subflow's RTT (which is 0.03 seconds on average during this transfer). However, as shown in Figure 2-9b, due to long delays on the LTE subflow, it receives the first three data packets on the LTE subflow at 1.0, 1.02, and 1.16 seconds, respectively. Since MPTCP sends ACKs with the highest in-order received sequence number, it keeps sending ACKs with sequence number 515436 to the sender although the Wi-Fi subflow has sent out packets with higher sequence numbers. This causes the Wi-Fi subflow to stop sending higher sequence number packets and to start retransmitting packets with sequence number 515436 at time 1.18 seconds. The retransmission phase ends at time 1.45 seconds because there are 10 packets scheduled to be sent on the LTE subflow at the beginning, and the sender needs to make sure all 10 packets are received before it can transmit further packets. In this case, seven packets are retransmitted on the Wi-Fi subflow. This effect is mentioned as "head-of-line blocking" in previous work [58].

One possible approach to reduce throughput degradation caused by head-of-line blocking is to reduce the initial congestion control window; thus, the Wi-Fi subflow will retransmit fewer packets. To verify this assumption, we configured the initial congestion control window for MPTCP to be 1 and ran the same experiment. The results are shown in Figures 2-10 and 2-11. We can see that in Figure 2-11a because only one packet is sent on the LTE subflow at time 0.31 seconds, and is ACKed at time 0.47 seconds, there is no more retransmission on the Wi-Fi path due to head-of-line blocking.
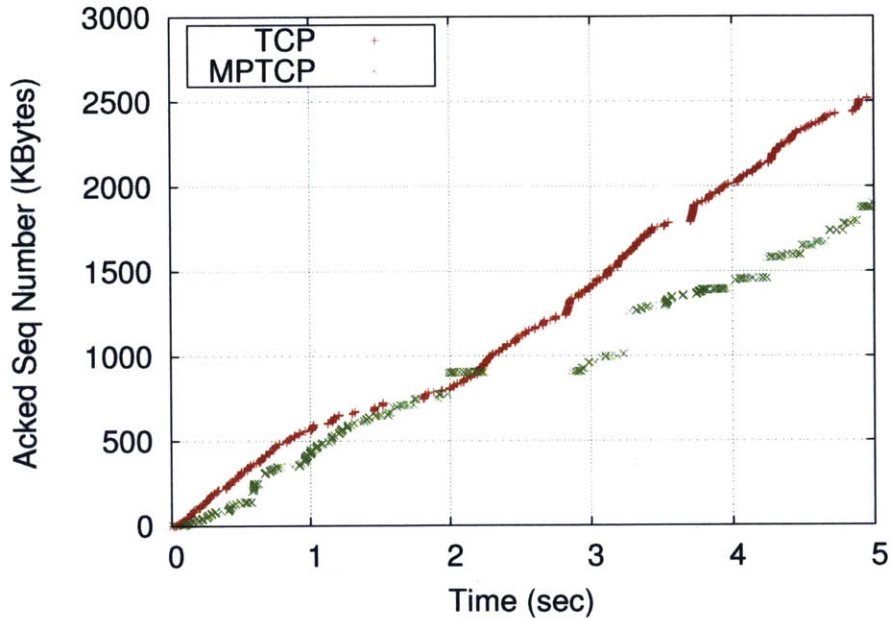
Figure 2-10: Acknowledged data vs. time for TCP and MPTCP when initial congestion control window is 1 MSS.

(a) Sender Side   (b) Receiver Side
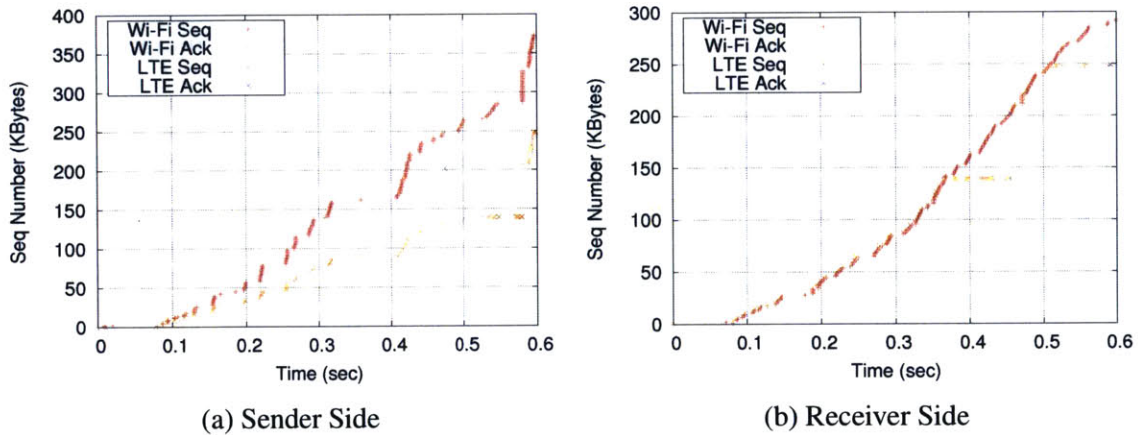
Figure 2-11: MPTCP sent and acknowledged data sequence number vs. time on sender and receiver side, when initial congestion control window is 1 MSS.

2.2.4 Primary Flow Measurement

We then studied how the choice of the network for the primary subflow can affect MPTCP throughput for different flow sizes. To show this quantitatively, we calculate the relative throughput difference as:
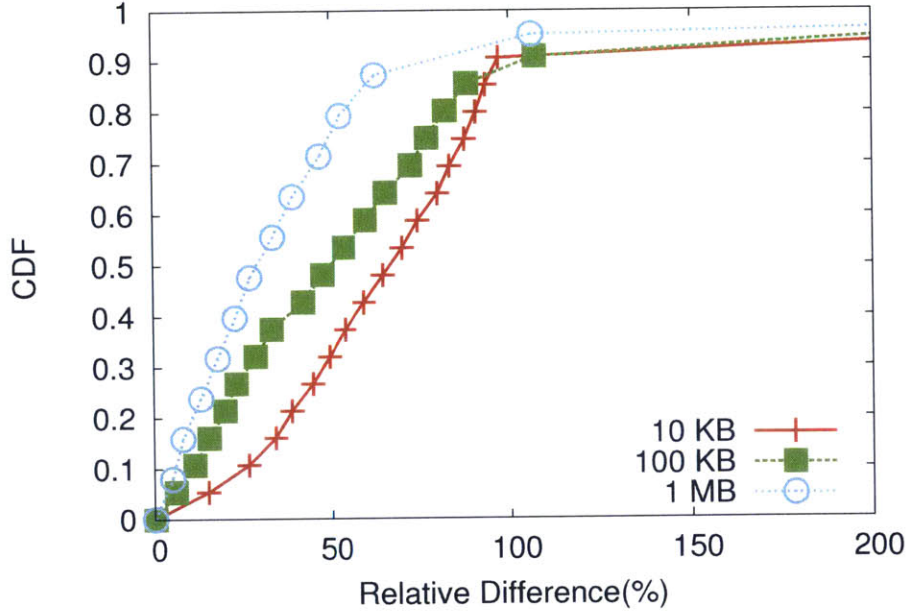
Figure 2-12: CDF of relative difference between $MPTCP_{LTE}$ and $MPTCP_{Wi-Fi}$, for different flow sizes. The median relative difference for each flow size is: 60% for 10 KBytes, 49% for 100 KBytes and 28% for 1MByte. Thus, throughput for smaller flow sizes is more affected by the choice of the network for the primary subflow.

$$\frac{|MPTCP_{LTE} - MPTCP_{Wi-Fi}|}{MPTCP_{Wi-Fi}}.$$

Here, $MPTCP_{LTE}$ is the throughput achieved by MPTCP using LTE for the primary subflow, and $MPTCP_{Wi-Fi}$ is the throughput achieved by MPTCP using Wi-Fi for the primary subflow (in this subsection, we ran MPTCP using only *decoupled* congestion control). Figure 2-12 shows the CDF of the relative throughput difference for three flow sizes: 10 KBytes, 100 KBytes, and 1 MByte. We see that using different networks for the primary subflow has the greatest effect on smaller flow sizes.

2.2.4.1 MPTCP Throughput Evolution Over Time

To understand how using different networks for the primary subflow affects MPTCP throughput evolution over time, we collected `tcpdump` traces at the MPTCP client during the measurement. From the traces, we calculated the average throughput from the time the MPTCP session was established, to the current time t. In Figures 2-13 and 2-14, we plot
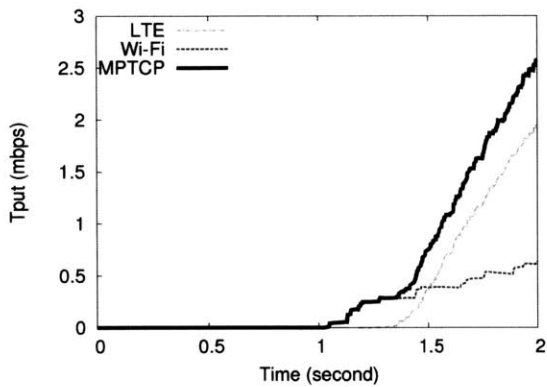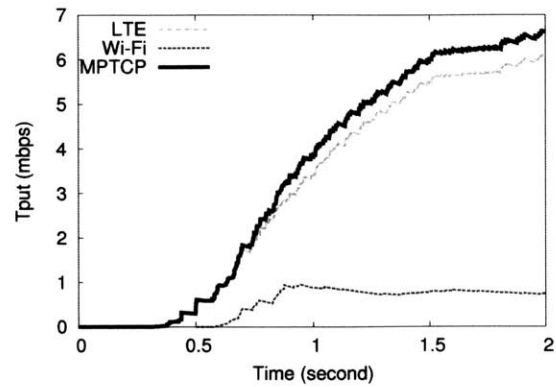
(a) Using Wi-Fi for the primary subflow   (b) Using LTE for the primary subflow

Figure 2-13: MPTCP throughput over time, measured at a location where LTE had higher throughput than Wi-Fi had. MPTCP throughput grows faster over time when using LTE for the primary subflow.
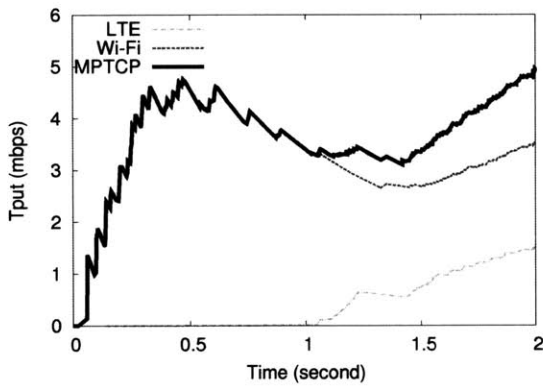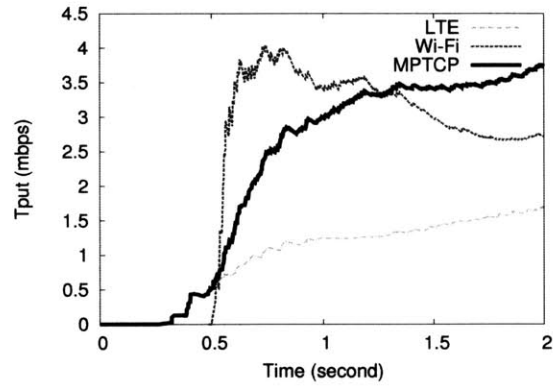
(a) Using Wi-Fi for the primary subflow   (b) Using LTE for the primary subflow

Figure 2-14: MPTCP throughput over time, measured at a location where Wi-Fi had higher throughput than LTE had. MPTCP throughput grows faster over time when using Wi-Fi for the primary subflow.

the average throughput as a function of time. Each sub-figure shows the throughput of the entire MPTCP session (shown as MPTCP) and the throughput of the individual Wi-Fi and LTE subflows.

Figure 2-13 shows traces collected at a location where LTE had much higher throughput than Wi-Fi had. At time 0, the client sent the SYN packet to the server. In Figure 2-13a, it took the client 1 second to receive the SYN-ACK packet from the server over Wi-Fi. MPTCP throughput was the same as the throughput of the Wi-Fi subflow until the LTE

46

subflow was established. Because LTE had much higher throughput at this location and time, once the subflow was established on LTE, it quickly increased its throughput (and therefore MPTCP's throughput). By contrast, in Figure 2-13b, the client received the SYN-ACK faster, and MPTCP throughput increased more quickly because the first subflow was on the higher-throughput LTE network. Because of the smaller SYN-ACK RTT and higher throughput on the first primary subflow, the MPTCP connection using LTE for the primary subflow (Figure 2-13b) had a higher average throughput than the MPTCP connection using Wi-Fi for the primary subflow (Figure 2-13a).

Similarly, Figure 2-14 shows traces collected at a location where Wi-Fi had higher throughput than LTE had. Here, using Wi-Fi as the primary subflow for MPTCP results in higher throughput.

2.2.4.2   MPTCP Throughput as a Function of Flow Size
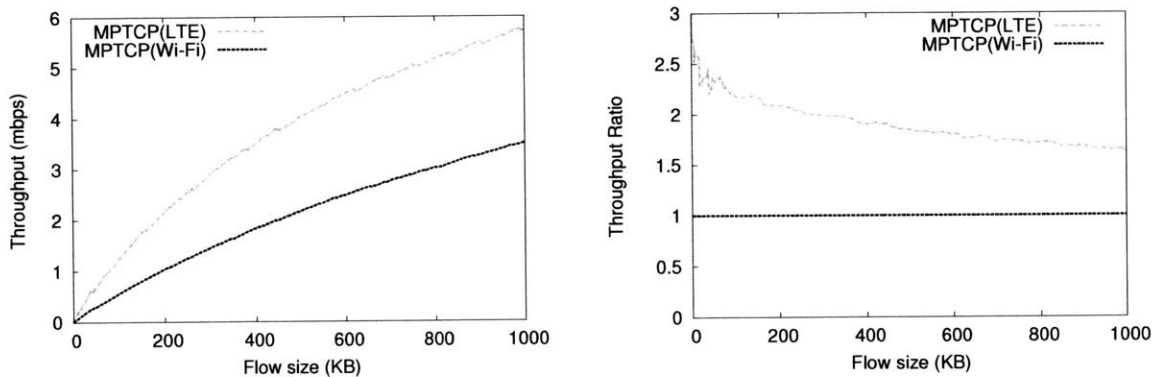
(a) Absolute throughput difference: larger difference between Wi-Fi and LTE for larger flow sizes.

(b) Relative throughput ratio: larger difference between Wi-Fi and LTE for smaller flow sizes.

Figure 2-15: Absolute throughput difference and relative throughput ratio as a function of flow size when LTE has higher throughput than Wi-Fi has.

Figures 2-15a and 2-16a show how MPTCP throughput changes as the flow size increases. The flow size is measured using the cumulative number of bytes acknowledged in each ACK packet received at the MPTCP client. Figures 2-15b and 2-16b show the relative throughput ratio change as flow size increases. The relative throughput ratio is defined as:
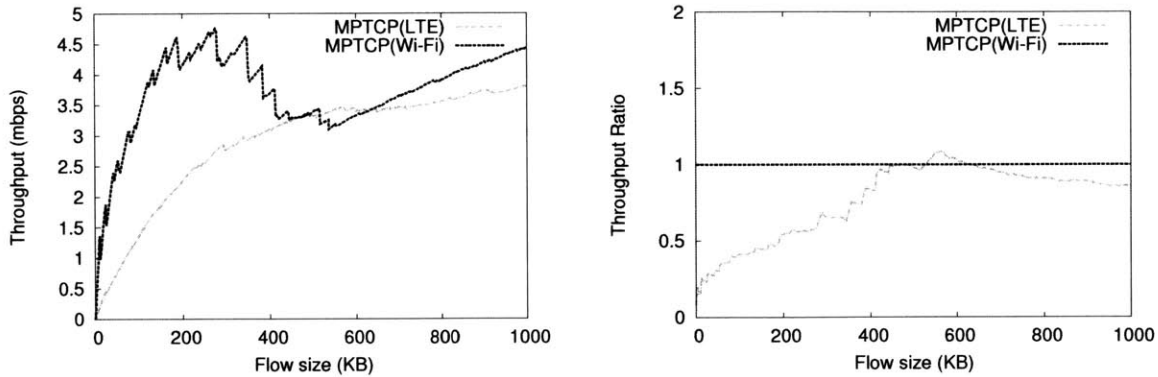
47

(a) Absolute throughput difference: larger difference between Wi-Fi and LTE for larger flow sizes.

(b) Relative throughput ratio: larger difference between Wi-Fi and LTE for smaller flow sizes.

Figure 2-16: Absolute throughput difference and relative throughput ratio as a function of flow size when Wi-Fi has higher throughput than LTE has.

$$\frac{MPTCP_{LTE}}{MPTCP_{Wi-Fi}}.$$

Although the absolute value of the difference in throughputs is smaller for small flow sizes (Figures 2-15a and 2-16a), the relative throughput ratio is larger (Figures 2-15b and 2-16b). Thus, for a connection with a given flow size, using the correct interface for MPTCP primary subflow can reduce the flow completion time, and the relative reduction can be significant for smaller flow sizes. For example, in Figure 2-15a, the absolute throughput difference between LTE and Wi-Fi is 0.5 Mbit/s for a 100-KByte flow, and about 3 Mbit/s for a 1-MByte flow. But in Figure 2-15b, the relative throughput ratio is 2.2× for a 100-KBybte flow, larger than the 1.5× for a 1-MByte flow.

2.2.5   Coupled and Decoupled Congestion Control

To understand how the choice of congestion control algorithm within MPTCP affects its throughput, at 7 of the 20 locations, we measured the following different MPTCP configurations on the Verizon LTE network and each location's dominant Wi-Fi network:

1. LTE for primary subflow, *coupled* congestion control.

2. LTE for primary subflow, *decoupled*[4] congestion control.

---

[4]Here, the decoupled congestion control uses TCP Reno for each subflow.

3. Wi-Fi for primary subflow, *coupled* congestion control.

4. Wi-Fi for primary subflow, *decoupled* congestion control.

At each location, we measured 10 runs for each of the 4 configurations, along both the uplink and the downlink. Thus, each of the four configurations has 140 data points $((10 + 10) \times 7)$.
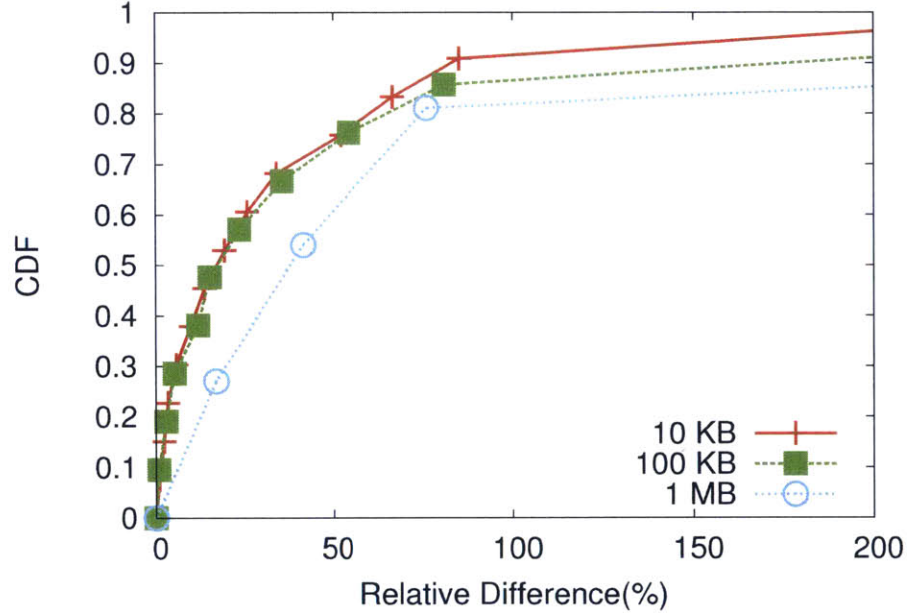
Figure 2-17: CDF of relative difference between $MPTCP_{coupled}$ and $MPTCP_{decoupled}$, for different flow sizes. The median relative difference for each flow size: 16% for 10 KBytes, 16% for 100 KBytes and 34% for 1 MByte. Thus, throughput for larger flow sizes is most affected by the choice of congestion control.

To quantify the throughput difference between configurations, we compute:

$$r_{network} = \frac{|MPTCP_{LTE.coupled} - MPTCP_{Wi-Fi.coupled}|}{MPTCP_{Wi-Fi.coupled}}, \text{ or}$$

$$r_{network} = \frac{|MPTCP_{LTE.decoupled} - MPTCP_{Wi-Fi.decoupled}|}{MPTCP_{Wi-Fi.decoupled}}.$$

Here, $r_{network}$ is the relative throughput difference when using different networks for primary subflow. $MPTCP_{n,c}$ is the throughput measured when using network n for primary subflow and using congestion control algorithm c. We also compute:

$$r_{cwnd} = \frac{|MPTCP_{LTE.decoupled} - MPTCP_{LTE.coupled}|}{MPTCP_{LTE.coupled}}, \text{ or}$$

49

$$r_{cwnd} = \frac{|MPTCP_{Wi-Fi.decoupled} - MPTCP_{Wi-Fi.coupled}|}{MPTCP_{Wi-Fi.coupled}}.$$

Here, r_{cwnd} is the relative throughput difference when using different congestion control algorithms.

(a) 10 KB   (b) 100 KB   (c) 1 MB
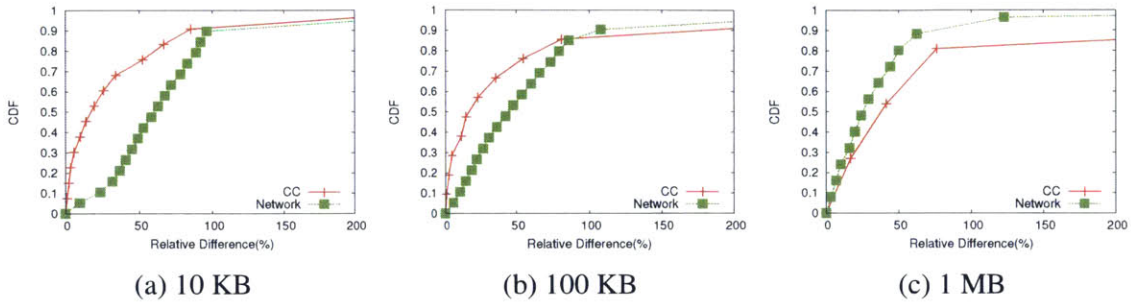
Figure 2-18: CDF of relative difference using different networks for primary subflow (labeled as "Network") vs. using different congestion control algorithms (labeled as "CC"), across 3 flow sizes. Median values for CC curves are: 16% for "10 KB", 16% for "100 KB", and 34% for "1 MB". Thus, using different congestion control algorithms has more impact on larger flows. Median values for Network curves are: 60% for " 10 KB", 43% for "100 KB", and 25% for "1 MB". Thus, using a different network for the primary subflow has greater impact on smaller flows.

Figure 2-17 shows the CDF of the relative throughput difference between using coupled and decoupled congestion control for three flow sizes: 10 KBytes, 100 KBytes, and 1 MByte. The rightmost CDF curve corresponds to the relative difference for 1 MByte, while the left-most one is for 10 KBytes. Thus, using different congestion control algorithms has a greater impact on larger flow sizes. In Figure 2-18, a pair-wise comparison between using different networks (labeled with"Network") and using different congestion control algorithms (labeled with "CC") for each flow size shows the following:

1. For small flow sizes, throughput is more affected by the choice of network for the primary subflow. For example, in Figures 2-18a and 2-18b, "Network" is to the right of "CC".

2. For large flow sizes, throughput is more affected by the choice of congestion control (decoupled or coupled) algorithms. For example: in Figure 2-18c, "CC" is to the right of "Network". However, the choice of network for the primary subflow is also important.

In practice, selecting the best network for the primary subflow is more feasible than changing congestion control algorithms for each MPTCP connection, since the primary flow can be defined solely by the MPTCP endpoint initiating the connection, while the congestion control algorithm requires support at both endpoints.

2.2.6 Full-MPTCP and Backup Modes

In § 2.2.4 and § 2.2.5, all measurements were done using Full-MPTCP mode, since our focus was on how MPTCP's throughput changes under different configurations, when all paths are fully utilized. Backup mode is an MPTCP mode where only a subset of paths are used to save energy, especially on power-constrained mobile devices. In this section, we first show how Backup mode differs from Full-MPTCP at the per-packet level. Then we discuss the energy efficiency of both Full-MPTCP and Backup modes.

2.2.6.1 Packet-Level Behavior of Full-MPTCP and Backup Modes

Figure 2-19 shows the packet-transmission pattern over time for a long flow employing MPTCP, using Full-MPTCP and Backup modes. We use tcpdump at the MPTCP client to log packet transmission and ACK reception times. In Figure 2-19, we plot a vertical line at time t if there is a packet sent or ACK received at time t in the tcpdump trace. $t = 0$ is the time when the first SYN packet is sent. Each sub-figure contains the packet-transmission patterns on both the Wi-Fi and LTE interfaces for one MPTCP flow. Sub-figures on the left column are packet transmission (sending and receiving) patterns captured when using LTE for the primary subflow, while sub-figures on the right are for using Wi-Fi for the primary subflow.

Figures 2-20a and 2-20b show that in Full-MPTCP mode, packets are transferred through both Wi-Fi and LTE during the entire MPTCP connection.

Figures 2-19c and 2-19d illustrate the Backup mode where one network is set to be the backup interface. For example, in Figure 2-19c, when Wi-Fi is set to backup, we see only the SYN and SYN ACK packets transferred during the 3-way handshake procedure at $t = 1$, when the connection establishes a Wi-Fi subflow, as well as FIN and FIN-ACK

51
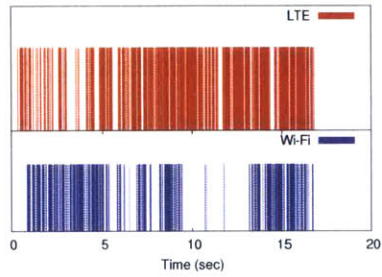
(a) Full-MPTCP, using LTE for primary subflow.
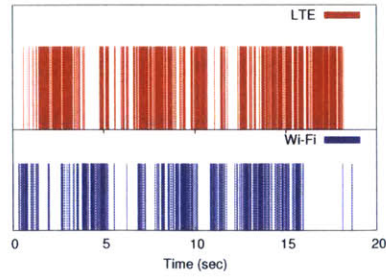
(b) Full-MPTCP, using Wi-Fi for primary subflow.
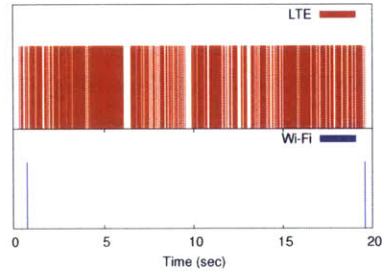
(c) Backup mode, using LTE for primary subflow, Wi-Fi for backup.
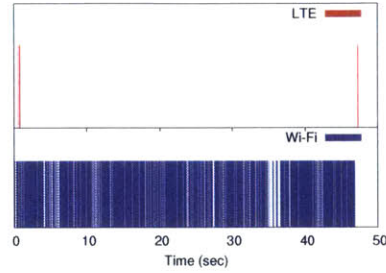
(d) Backup mode, using Wi-Fi for primary subflow, LTE for backup.
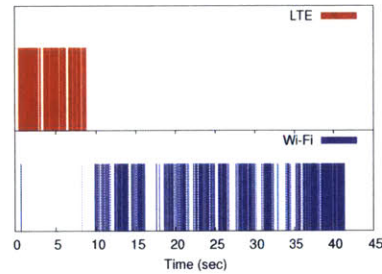
(e) Backup mode, using LTE for primary subflow, Wi-Fi for backup. Then, set LTE to "multipath off" at $t = 9$ sec.
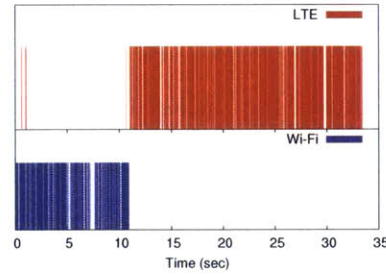
(f) Backup mode, using Wi-Fi for primary subflow, LTE for backup. Then, set Wi-Fi to "multipath off" at $t = 11$ sec.
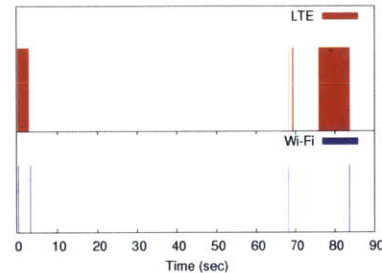
(g) Backup mode, using LTE for primary subflow, Wi-Fi for backup. Unplug LTE at $t = 3$ sec, *but Wi-Fi does not continue transferring the rest of the data.* Plug LTE back in at $t = 68$ sec.
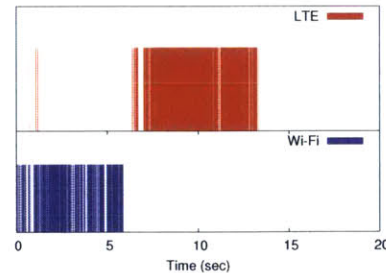
(h) Backup mode, using Wi-Fi for primary subflow, LTE for backup. Unplug Wi-Fi at $t = 6$ sec.

Figure 2-19: Full-MPTCP and Backup modes.

52

packets at $t = 19$, when the connection ends. A similar pattern is shown in Figure 2-19d, when LTE is set to be the backup interface.

Figures 2-19e and 2-19f show packet transmissions in Backup mode when the primary network is disabled mid-flow. We disable the interface by setting the interface to "multipath off" in `iproute`. In Figure 2-19e, Wi-Fi is set to backup. When the connection starts, it transfers data through LTE. At $t = 7$, we disable LTE so no data can be transferred over that interface. We see that the subflow over Wi-Fi is brought up and transfers data until the flow ends. A similar behavior is seen in Figure 2-19f.

In Figures 2-19g and 2-19h, we disable one network by unplugging the USB cable connecting the phone to the laptop instead of disabling it using `iproute`. Interestingly, we observe different behaviors in this experiment. Figure 2-19h shows that when LTE is set to backup, and we unplug Wi-Fi in the middle of the transfer (at $t = 6$), the LTE path is brought up immediately to finish transferring the rest of the data. This behavior is similar to when Wi-Fi was disabled by changing `iproute`. However, in Figure 2-19g, when Wi-Fi is set to backup and we unplug the LTE network in the middle of the transfer (at $t = 3$), the client transfers only one `TCP Window Update` packet to the server through the Wi-Fi subflow and then halts. At $t = 68$, we re-connect the phone with the laptop. Then, the connection resumes, transfers the rest of the data through the LTE subflow, and ends the session by sending FIN packets on both path.

The reason disabling paths by physically disconnecting them can cause different behaviors from disabling them in software is still under investigation.

2.2.6.2 Energy Efficiency in Backup Mode

As shown in Figures 2-19c and 2-19d, if MPTCP is set to Backup mode, the backup interface still transfers SYN and FIN packets when a connection starts and ends. In Figure 2-20, we show that in certain configurations, these SYN/FIN packets can consume excessive amounts of energy on a mobile device. Here, we measure the power level of the tethered phones using a power monitor [43] when each phone serves as the backup or non-backup interface. In all sub-figures of Figure 2-20, the base power consumed is 1 watt. This is the power consumed when the network interfaces are not active. It is the total power consumed
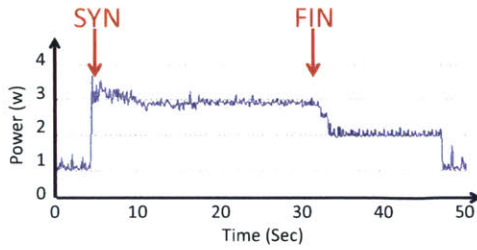
(a) LTE power level when used for non-backup subflow.
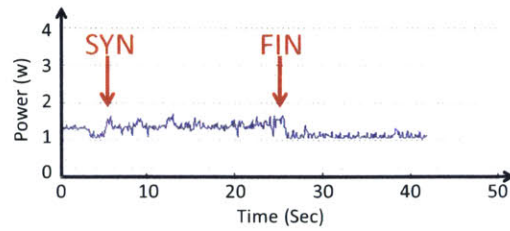
(b) Wi-Fi power level when used for non-backup subflow.
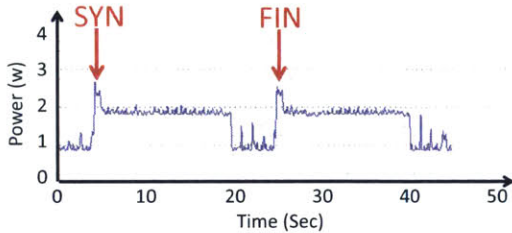
(c) LTE power level when used for backup subflow.
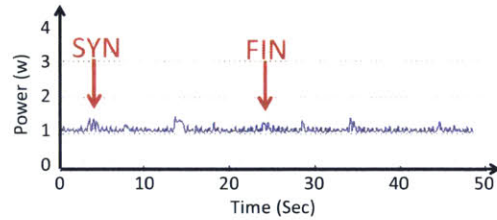
(d) Wi-Fi power level when used for backup subflow.

Figure 2-20: Power level for LTE and Wi-Fi when used as non-backup subflow. LTE has a much higher power level than Wi-Fi in non-backup mode. LTE also consumes an excessive amount of energy even in backup mode.

by the other parts of the phone, such as the screen and the CPU.

Figure 2-20a shows the power level of LTE when it is actively transmitting data, that is, Wi-Fi is set as a backup interface. Similarly, Figure 2-20b shows the power level of Wi-Fi when it is active. We can see that the Wi-Fi power level is much lower than that of LTE. Also, in Figure 2-20a, after the FIN packet is sent, there is a 15-second period in which the LTE power level stays at 2 watts, instead of the 1-watt base power level. The energy consumed in this 15-second period is called the *tail energy* [16, 26].

Figures 2-20c and 2-20d show the power level when Wi-Fi or LTE is set to be the backup interface. In Figure 2-20d, the energy consumed by Wi-Fi is negligible. However, in Figure 2-20c, when a SYN or a FIN packet is transmitted through LTE, the power level stays high for about 15 seconds due to the tail energy effect. Thus, even if only SYN and FIN packets are transferred through LTE, the LTE interface still consumes an excessive amount of energy. For flows shorter than 15 seconds, little energy can be saved if the LTE interface is set to be the backup interface. To actually reduce energy consumption in

this case, *fast dormancy* [31] should be used to quickly put the LTE interface in the low-power mode after a SYN and FIN. Alternatively, the Backup mode should be implemented in a *break-before-make* manner. Prior work [57] has proposed *Single-Path* mode, which establishes a new MPTCP subflow only after the current subflow is inactive, at the expense of two more round-trip times compared with the current Backup mode.

2.3 Mobile App Traffic Patterns

So far, our measurements have looked at the flow-level performance of TCP over Wi-Fi or LTE, and of MPTCP over both Wi-Fi and LTE. We next turn to how the choice of networks for a multi-homed mobile device affects application-level performance as perceived by a mobile app that uses one or more of these networks. To measure performance at the level of a mobile app, we first record (§2.3.1) and analyze traffic (§2.3.2) originating from a mobile app, and then replay it under emulated link conditions (§2.4).

2.3.1 Record-Replay Tool

Mahimahi [53] is a record-and-replay tool that can record and replay client-server interactions over HTTP. Mahimahi's RecordShell is a UNIX shell that records HTTP traffic and stores it as a set of request-response pairs. Later, during replay, Mahimahi's ReplayShell—another modified UNIX shell—matches incoming requests to stored requests, ignoring time-sensitive fields in the request header (e.g., If-Modified-Since) that have likely changed since recording.

Mahimahi also includes shells to emulate network delays and fixed-rate and variable-rate network links using packet-delivery traces. We extend these capabilities and develop a new shell, MpShell, to emulate multiple links along with their associated link delays. This allows us to mimic a multi-homed mobile phone that can use both cellular and Wi-Fi links. We use a trace-driven approach, as Mahimahi does, to emulate both the cellular and Wi-Fi links.

Because Mahimahi is agnostic to the specific client or server that generates the HTTP traffic, we use it to record all HTTP traffic to and from a mobile app running inside an An-

droid emulator. Later, using ReplayShell and MpShell, we run the same mobile app within the Android emulator under appropriately emulated network conditions. This enables us to evaluate how MPTCP—or any other multipath-capable transport—affects application performance of a real mobile app.

2.3.2 Traffic Patterns of Mobile Apps

Figure 2-21 shows typical traffic patterns we observed across different mobile apps run inside RecordShell. We observed that apps tend to initiate multiple TCP connections when launched or in response to a user interaction. Most of these connections transfer only a small amount of data (e.g., connection ID 2 in Figure 2-21c). Some connections, such as connection ID 2 in Figure 2-21a, persist after small data transfers.

A few connections, such as connection ID 30 in Figure 2-21d and connection ID 8 in Figure 2-21f, transfer significant amounts of data, lasting several seconds. The first example (ID 30) occurred when the user clicked a link to play a movie trailer. The app downloaded the entire trailer in one HTTP request. The second example (ID 8) occurred when the user clicked a PDF file in the user's Dropbox folder and the app downloaded the whole file.

In summary, we can categorize app traffic patterns as *short-flow dominated* and *long-flow dominated*. *Short-flow dominated* apps have only short connections or long-lived connections with little data transferred. *Long-flow dominated* apps have one or multiple long-lasting flows transferring large amounts of data.

2.4 Mobile App Replay

We feed the app traffic patterns described in §2.3 into Mahimahi's ReplayShell for subsequent replay. To accurately emulate different network conditions, we use the recorded single-path TCP packet traces on both Wi-Fi and LTE as a proxy for the true packet-delivery trace for Wi-Fi and LTE[5]. We use these TCP traces to emulate the Wi-Fi and LTE links

---

[5]This approach does underestimate the true packet-delivery trace of the underlying network because TCP takes a finite duration to reach the link capacity due to slow start.
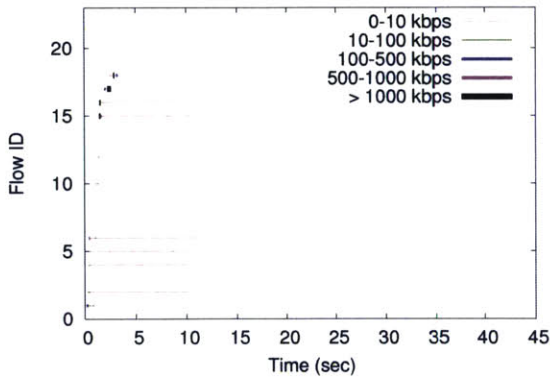
(a) CNN launch.
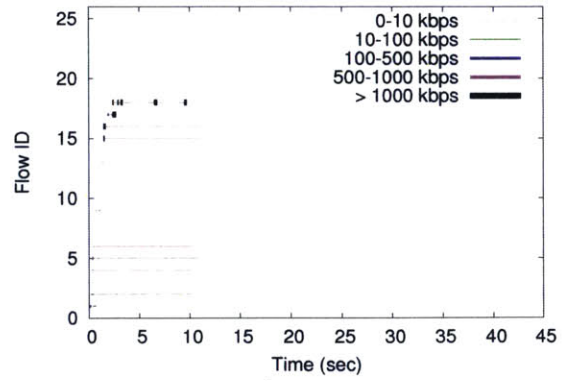
(b) CNN click.
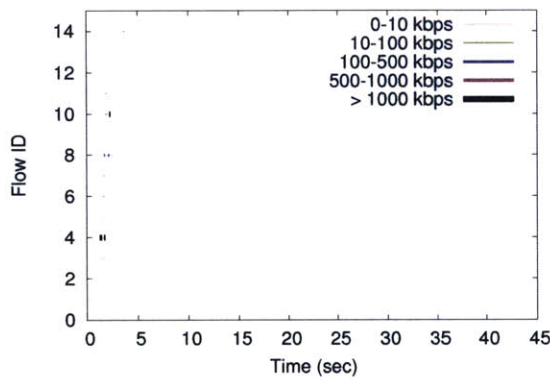
(c) IMDB launch.
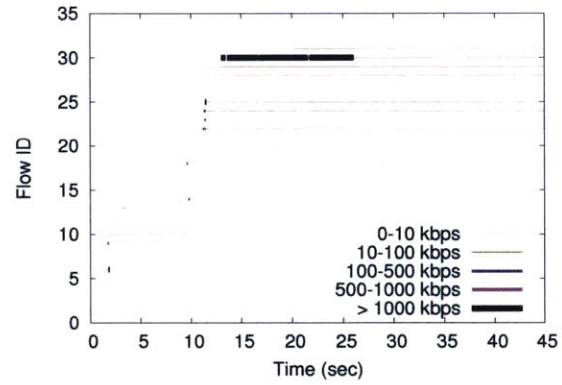
(d) IMDB click.
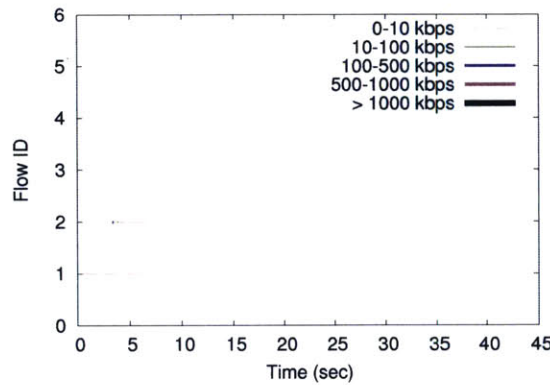
(e) Dropbox launch.
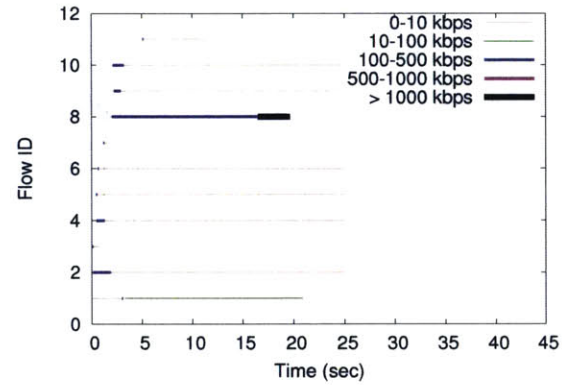
(f) Dropbox click.

Figure 2-21: Traffic patterns for app launching and user interacting. Figures 2-21d and 2-21f show the "long-flow dominated" traffic pattern; the other figures show the "short-flow dominated" pattern.

within MpShell. We emulate 20 distinct network conditions using the Wi-Fi and LTE TCP data previously collected at 20 locations (§4.6.1).

We present results from replaying two traffic patterns. We refer to the first as the *short-*

flow dominated app in which, as shown in Figure 2-21a (CNN launch), an app initiates several connections but transfers only a small amount of data on each connection. We refer to the second as the *long-flow dominated app* in which, as shown in Figure 2-21f (Dropbox user click), an app initiates several connections and transfers a large amount of data for a few seconds over a small subset of the connections. We run each app pattern over the 20 different network conditions (we show only the results from 4 representative conditions due to space limitations). For each network condition, we emulate 6 configurations:

1. Wi-Fi-TCP: Single-path TCP running on Wi-Fi.

2. LTE-TCP: Single-path TCP running on LTE.

3. MPTCP-Coupled-Wi-Fi: MPTCP with coupled congestion control using Wi-Fi for the primary subflow.

4. MPTCP-Coupled-LTE: MPTCP with coupled congestion control using LTE for the primary subflow.

5. MPTCP-Decoupled-Wi-Fi: MPTCP with decoupled congestion control using Wi-Fi for the primary subflow.

6. MPTCP-Decoupled-LTE: MPTCP with decoupled congestion control using LTE for the primary subflow.

Using tcpdump during the emulation, we collect the timestamp at the start and end of each HTTP connection. Then, we calculate the *app response time*: the time between the start of the first HTTP connection and the end of the last HTTP connection[6].

2.4.1 Short-Flow Dominated App Replay

Figure 2-22 shows the app response time for the CNN app launching in different configurations under different network conditions. For clarity, we show only the emulation results for 4 representative network conditions out of the 20 we emulated; results for other conditions are similar.

Network Condition IDs 1 and 2 emulate locations where Wi-Fi has a much higher bulk

---

[6]This metric does not account for computation time that might be spent in the app itself after the last HTTP connection ends, but this is impossible to measure without instrumenting or rewriting existing applications to report these numbers.
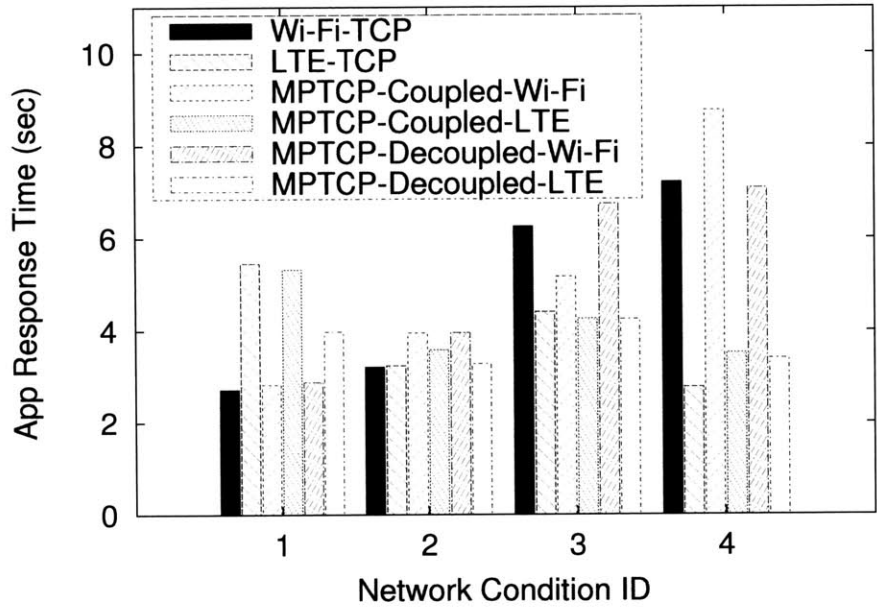
Figure 2-22: CNN app response time under different network conditions.
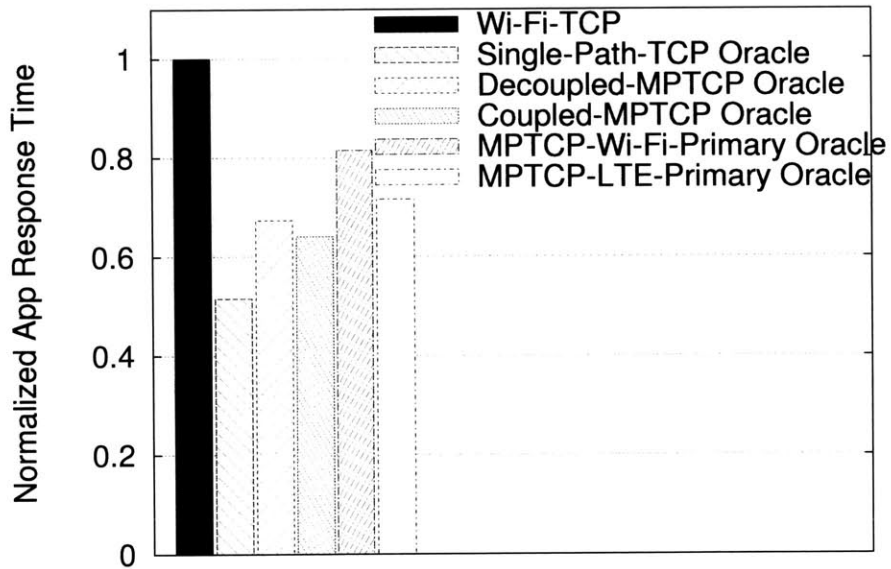
Figure 2-23: CNN normalized app response reduction by different oracle schemes.

TCP throughput than LTE has, and in Network Condition IDs 3 and 4, LTE outperforms Wi-Fi. In Figure 2-22, we observe that:

1. Selecting the proper network to transmit for single-path TCP significantly affects

app response time. For example, in Network Condition 1, the app response time for Wi-Fi-TCP is 2.7 seconds, while LTE-TCP has an app response time of 5.5 seconds, implying that using the proper network for single-path TCP can reduce the app response time by about $2.0\times$. For a network condition in which LTE has better performance, such as Network Condition ID 4, the app response times for TCP over Wi-Fi (shown as "TCP-Wi-Fi" in Figure 2-22) and TCP over LTE (shown as "TCP-LTE" in Figure 2-22) are 7.2 seconds and 2.8 seconds, respectively. In this case, using LTE can reduce the app response time by $2.6\times$.

2. Using MPTCP does not provide much improvement for the *short-flow dominated* app pattern. For instance, in Network Condition 1, MPTCP-Coupled-LTE and MPTCP-Decoupled-LTE have app response times of 5.3 and 4.0, respectively. Compared to TCP over LTE, these MPTCP schemes reduce the app response time by only 4% and 15%, much smaller improvements than the $2\times$ improvement seen when using TCP over Wi-Fi compared to TCP over LTE.

In summary, Figure 2-22 shows that the choice of network for the primary subflow has a strong impact on app response time. This result is consistent with the results we show in §2.2.5.

We also study the extent to which app response times can be reduced if we have access to an optimal network selection algorithm: an oracle that knows the right network to use, given a particular congestion control strategy (coupled vs decoupled) and another oracle that knows the right congestion control strategy to use given a particular choice for the network used by the primary subflow. Figure 2-23 shows the app response time with different oracle schemes, averaged across all 20 network conditions and normalized by the app response time with single-path TCP over Wi-Fi (the default on Android today). The oracle schemes are:

1. Single-Path-TCP Oracle: Uses single-path TCP and knows which network minimizes app response time.

2. Decoupled-MPTCP Oracle: Uses MPTCP decoupled congestion control and knows which network to use for the primary subflow to minimize app response time.

3. Coupled-MPTCP Oracle: Uses MPTCP coupled congestion control and knows which

network to use for the primary subflow to minimize app response time.

4. MPTCP-Wi-Fi-Primary Oracle: Uses MPTCP with Wi-Fi for primary subflow and knows which congestion control algorithm to use to minimize app response time.

5. MPTCP-LTE-Primary Oracle: Uses MPTCP with LTE for primary subflow and knows which congestion control algorithm to use to minimize app response time.

We can see in Figure 2-23 that the 50% reduction in app response time with Single-Path-TCP Oracle is the most substantial, while the reductions with the MPTCP Oracles range from 15% to 35%. This suggests that MPTCP does not reduce app response time as significantly as selecting the right network for single-path TCP does.

2.4.2 Long-flow Dominated App Replay
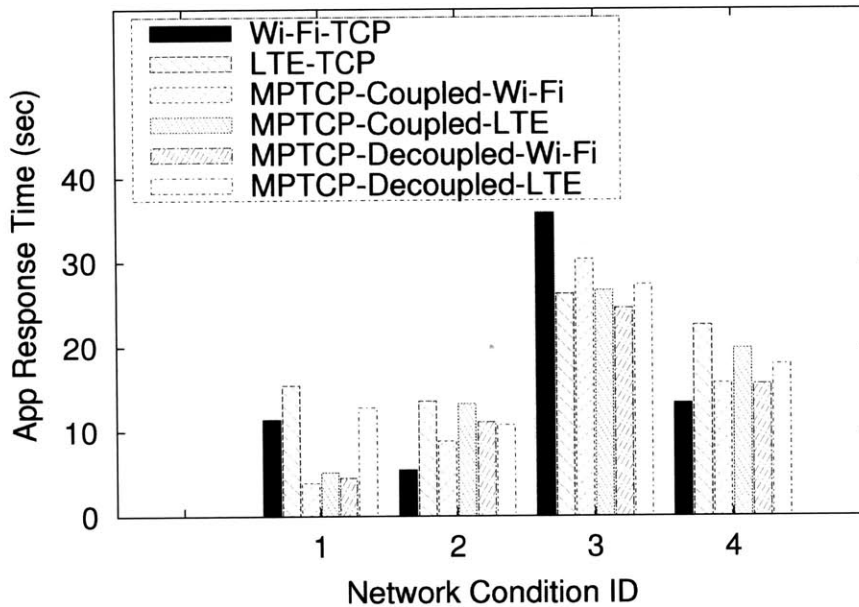
Figure 2-24: Dropbox app-response time under different network conditions.

Figures 2-24 and 2-25 show emulation results for the *long-flow dominated* traffic pattern, using the same data analysis methods and oracles as used in the previous subsection.

In Figure 2-24, Network Condition IDs 1 and 2 emulate places where Wi-Fi has a much higher TCP throughput than LTE has, and Network Condition IDs 3 and 4 represent places where LTE outperforms Wi-Fi. We observe that:
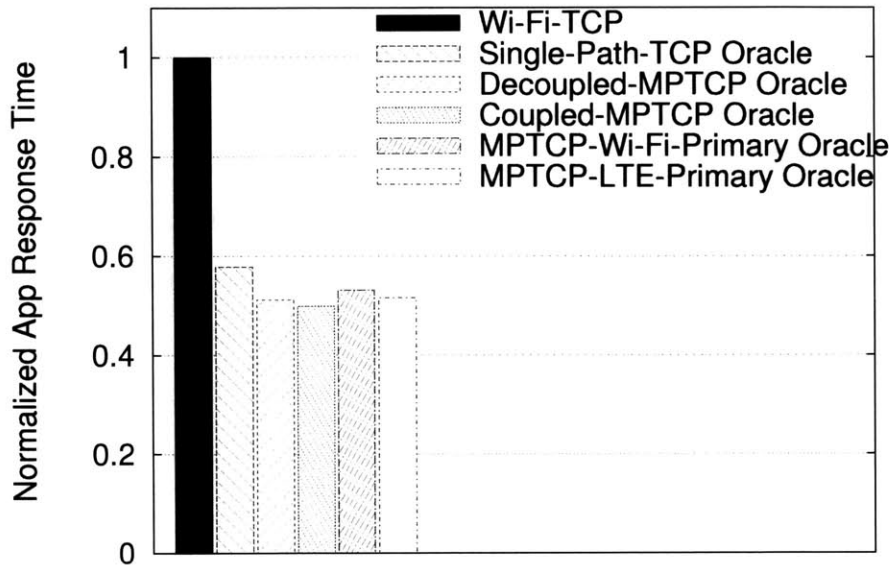
Figure 2-25: Dropbox normalized app-response reduction by different oracle schemes.

1. Using MPTCP helps to reduce app response-time. For example, at Network Condition 1, when using single-path TCP, the app response time is 10 seconds for Wi-Fi and 15 seconds for LTE. When using MPTCP, the app response time is 5 seconds.

2. Selecting the proper network is important; for example, at Network Condition ID 2, the app response time for MPTCP-Coupled-Wi-Fi is 8 seconds, but if LTE is used for the primary flow, response time increases to 14 seconds.

3. Selecting the proper congestion control algorithm also affects app response time. For example, at Network Condition ID 1, when using LTE for the primary subflow, the app response time for coupled congestion control is 4 seconds, while the response time with decoupled congestion control is 13 seconds.

In Figure 2-25, we can see that:

1. MPTCP Oracles reduce the app response time by up to 50%, while the Single-Path-TCP Oracle reduces app response time by only 42%. So, using MPTCP can help improve performance for long-flow dominated apps.

2. For MPTCP Oracles, both selecting the proper network for the primary flow and selecting the appropriate congestion control can reduce the normalized app response

time by about 50%, implying that both mechanisms are almost equally beneficial to long-flow dominated apps.

2.5 Related Work

We discuss related work under two headings: prior work comparing Wi-Fi with cellular network performance and Multi-Path TCP.

2.5.1 Wi-Fi/Cellular Comparison

Several prior papers compare cellular network performance with Wi-Fi. Sommers et al. [71] analyzed crowd-sourced data from `SpeedTest.net`. Each data sample represents one run of a TCP upload/download test triggered by a mobile phone user when the phone is connected to the Internet through either Wi-Fi or a cellular network. We also collected our data in a crowd-sourced manner. However, our mobile app, *Cell vs. Wi-Fi*, measures both Wi-Fi and cellular network performance on the same device at (almost) the same time. Thus, our dataset reflects the performance difference observed from a single device at almost the same time. Deshpande et al. [28] measured both 3G and Wi-Fi performance simultaneously using a single device, but their measurement was focused on a vehicular setting, and they measured only 3G, not LTE. Our dataset focuses on LTE measurements instead. In our app, we used an activity-recognition API provided by Google [6], which shows that most of our measurements happen when users are still. Moreover, our data was collected in a crowd-sourced manner, allowing it to capture a wide diversity of conditions.

2.5.2 Multi-Path TCP

Multipath TCP (MPTCP) [77] and its recent implementation in iOS 7 [49] allow a single TCP connection to use multiple paths. MPTCP provides TCP's reliable, in-order bytestream abstraction while taking advantage of multiple paths for increased throughput and fault tolerance. Previous work has looked at MPTCP in a mobile context. Raiciu et al. studied mobility with MPTCP [67]. Pluntke et al. designed a scheduler that picks radio

interfaces with a view to reduce mobile energy consumption [63]. Paasch et al. proposed different MPTCP modes to be used by mobile devices for mobile/Wi-Fi handover [57]. Barlow-Bignell et al. [18] studied MPTCP performance in the presence of Wi-Fi interference where multiple devices connected to the same AP could interfere with each other if they transmitted packets simultaneously. Closest to our work is the work of Chen et al., who measured MPTCP performance over cellular networks and Wi-Fi [24]. Their measurement focuses on using different numbers of subflows and fine-grained statistics, such as out-of-order delivery and round-trip times. Instead, our focus is on studying the choice of networks for the primary subflow, the choice of congestion-control modes, MPTCP's energy consumption, and MPTCP's effect on higher-level metrics such as flow completion times and app response times.

2.6 Chapter Summary

This chapter describes the measurement study of single-path TCP and MPTCP over LTE and Wi-Fi networks. For single-path TCP, we found that LTE outperforms Wi-Fi 40% of the time—a higher percentage than one might expect at first sight. We also found that MPTCP offers no appreciable benefit over TCP for shorter flows, but it does improve performance for longer flows. For MPTCP, we found that, especially for short flows, it is crucial to select the correct network for the primary subflow. For long flows, it is equally important to select the proper congestion control algorithm. To understand how TCP and MPTCP over LTE and Wi-Fi can affect mobile app performance, we analyzed mobile apps' traffic patterns, and categorized apps as either *short-flow dominated* or *long-flow dominated*. For each category, we emulated app traffic patterns and the results we observed match our MPTCP measurement findings.

Our findings also bring up new research questions: How can we automatically decide when to use single-path TCP and when to use MPTCP? How should we decide which network to use for TCP or which network to use for a subflow with MPTCP? We think these are non-trivial questions due to the high mobility of devices and rapidly changing network conditions. Also, with energy consumption being a major concern for mobile

devices, how can we make the decisions when trying to minimize energy consumption? We will address these problems in the following chapters.

Chapter 3

Delphi: A Controller for Mobile Network Selection

In the previous chapter, our measurement study shows that there is a need for mobile devices to select the best network for applications, adapting to current network conditions as well as traffic shape. In this chapter, we present the design, implementation, and evaluation of *Delphi*, a software module that achieves this goal. Our starting point is from the perspective of users and applications rather than the transport layer or the network. Depending on the *objectives* of interest, Delphi makes different decisions about which network to use and in what order.

We consider three objectives (though the framework handles other objectives as well):

1. minimize the time to complete an application-level transfer (the ratio of transfer size to transfer throughput);

2. minimize the energy per byte of the transfer, which usually (but not always) entails picking one network; and

3. minimize the monetary cost per byte of the transfer.

Delphi provides a framework to optimize these and similar objectives. This problem is challenging because the answer changes with time and depends on location and user movement.
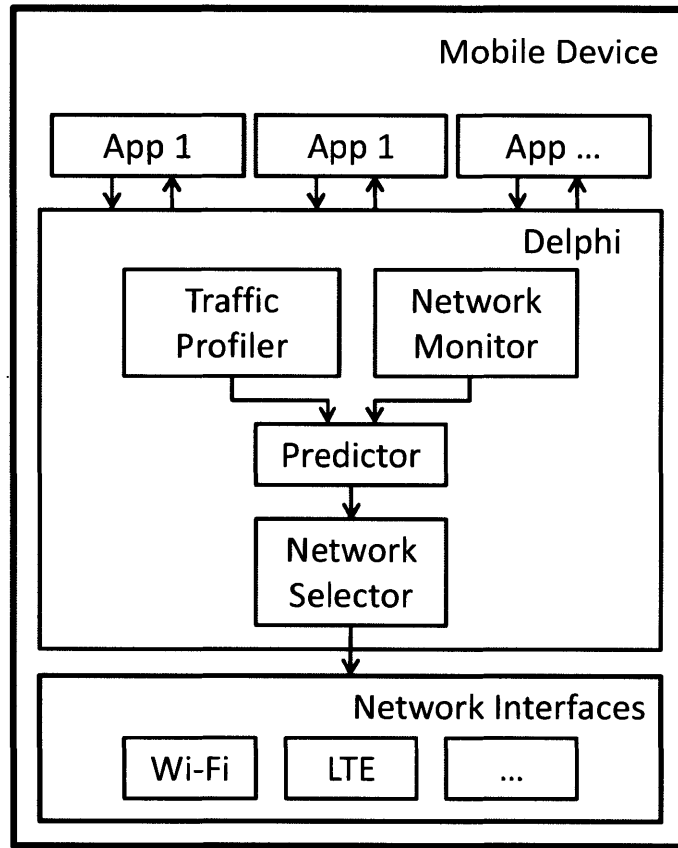
Figure 3-1: Delphi design.

3.1 Overview

Delphi uses three pieces of information to select the network(s) to use for a data transfer:

1. App traffic profile regarding how much data a transfer sends or receives, for example, as part of a HTTP transaction.

2. Network conditions for the wireless interfaces, for example, channel quality, current load in the network, end-to-end delay, etc. This information allows us to estimate higher-layer network performance metrics, such as flow completion time, average burst throughput, etc.

3. The objective function to be optimized, such as the flow completion time, energy per byte, or monetary cost for the transfer.

Figure 3-1 shows the four components in Delphi, which is implemented as a software controller between the application and transport layers. The Traffic Profiler (§3.2) esti-

mates transfer sizes, and the Network Monitor (§3.3) collects data needed for the Predictor to predict current network performance. The Predictor (§3.4) feeds the prediction to the Network Selector (§3.5), which selects the network(s) to optimize the specified objective. Implementing this design requires no modification to applications (§3.6).

3.2 Traffic Profiler

A recent study [25] analyzed 90,000 Android apps and found that 70,000 of them used HTTP or HTTPS, and that among the 70,000, 70% of them used HTTP and not HTTPS. Thus, we designed the Traffic Profiler by first focusing on HTTP.

When a mobile user downloads a file using an HTTP GET, the HTTP GET response header usually contains a "Content-Length" field specifying the length of the response. During uploads, the mobile device issues an HTTP POST whose Content-Length field specifies the transfer size. In both cases, the Content-Length field provides the relevant transfer size information to the Traffic Profiler readily.

	Count	Percentage
HTTP Transactions	59679	100%
Transactions with Content-Length	50865	85%
Predictable Transactions	50613	84%
Chunked-Encoding Transactions	3559	6%

Table 3.1: HTTP transaction data lengths for the Alexa top 500 sites. 84% of the transfer lengths are predictable by the Traffic Profiler.

However, the Content-Length field is not mandatory for HTTP headers; for instance, HTTP transactions often use chunked encoding when the length of data to be transmitted is dynamic. To determine how many HTTP transactions contain the Content-Length header, we use a record-and-replay tool, Mahimahi [53], to record the HTTP requests and responses when loading the homepage of the Alexa top-500 websites [9]. The results are listed in Table 3.1. When each site is loaded once, the total number of HTTP transactions is 59,679. We note that 84% of the transactions are predictable by the Traffic Profiler. Here, *predictable* means the relative difference between the Content-Length value and the actual amount of data transmitted is less than 10%. Thus, using the Content-Length field to pre-

dict the size of the data transfer works for most (84%) HTTP transactions. For HTTPS, the header is encrypted. To be able to look into the headers, we could set up an SSL proxy on the mobile device and make all traffic go through it [73].

Delphi also provides an API for the application to let the Traffic Profiler know how much data it is going to transfer. Compared with the Traffic Profiler monitoring data transmissions on its own, this API allows the Traffic Profiler to unambiguously determine the amount of data the application is going to transfer. As shown in §3.4.2.1, providing accurate transfer length helps Delphi make better network selections. This benefit can incentivize application developers to adopt the API for better performance while providing better security guarantees (for applications using HTTPS).

The Traffic Profiler notifies the Predictor by sending it (`TCP_CONNECTION_ID,` `data_length, direction`) (*direction* means whether the device is downloading or uploading data) when any of the following events occur:

1. an API call occurs from the app;
2. a request to initiate a new TCP connection is observed; or
3. an HTTP request/response is observed.

The Traffic Profiler may not be able to tell how much data is going to be transmitted in Case 2 and sometimes in Case 3 (e.g., chunked encoding). In such cases, the Traffic Profiler will simply return a `data_length` of 3 KBytes. If `chunked encoding` is observed, the profiler updates the predicted transfer size to be 100 KBytes. We chose these numbers because they are the median values of data transmission length observed in the Alexa top 500 sites in US (April, 2014). §3.4.2.1 analyzes how these default data length values affect network selection results.

3.3 Network Monitor

The Network Monitor tracks a set of network-condition indicators for both Wi-Fi and LTE, and notifies the Predictor whenever an indicator value changes.

Category	Wi-Fi Indicators	LTE Indicators
Passive indicators	RSSI, Link Speed,Wi-Fi AP Count	Signal Strength, DBM, RSSNR, CQI,RSRP, RSRQ, Wi-Fi AP Count
Active probing	Max/Min/Mdev Ping RTT, DNS Lookup Time, UDP throughput, UDP loss-rate, UDP packet inter-arrival-time mean/median/90th percentile	

Table 3.2: Network indicators monitored by Delphi.

3.3.1 Network Indicators

Table 3.2 lists the indicators used by Delphi. These indicators are categorized into 2 subgroups: passive measurement and active probing. The passive measurements capture channel quality and contention for the last-hop wireless link, which is often the bottleneck along both the forward and reverse paths between the mobile device and the Internet. However, this last-hop information does not always reflect network conditions along the whole path. For example, for LTE networks, the delay introduced by packet buffering at the cell tower side can be significant [35], but it is not captured by last-hop passive measurements. Wi-Fi access in public areas such as shopping malls, airports, etc. may be subject to bandwidth limits introduced at the gateway to the Internet, and these are not captured by last-hop measurements. To capture these non-last-hop, or end-to-end network performance factors, Delphi also runs active probes between the mobile device and an Internet server (see §3.6).

To quantify how each indicator affects TCP throughput, we analyze data collected from 22 locations. Those locations included shopping malls, Wi-Fi-covered downtown areas, and university campuses, where both Wi-Fi and LTE were available. At each location, the total measurement time is at least 1 hour. We compute the Pearson Correlation [75] between the throughput and each indicator. The correlation is a number between -1 and $+1$, inclusive. A value close to $+1$ or -1 signifies a strong positive or negative correlation. A value close to 0 signifies weak correlation.

Figure 3-2 shows the absolute value for correlation between throughput and each indicator. The bars in each sub-figure are sorted from strongest to weakest correlation. Figures 3-2a and 3-2b show the correlation over the entire dataset. For both Wi-Fi and LTE, among the most correlated indicators, we see both active probing indicators (such as Wi-Fi UDP throughput and LTE Average Ping RTT) and passive indicators. Figures 3-2c and 3-2d

(a) Wi-Fi: All Data

(b) LTE: All Data

(c) Wi-Fi: Location 1
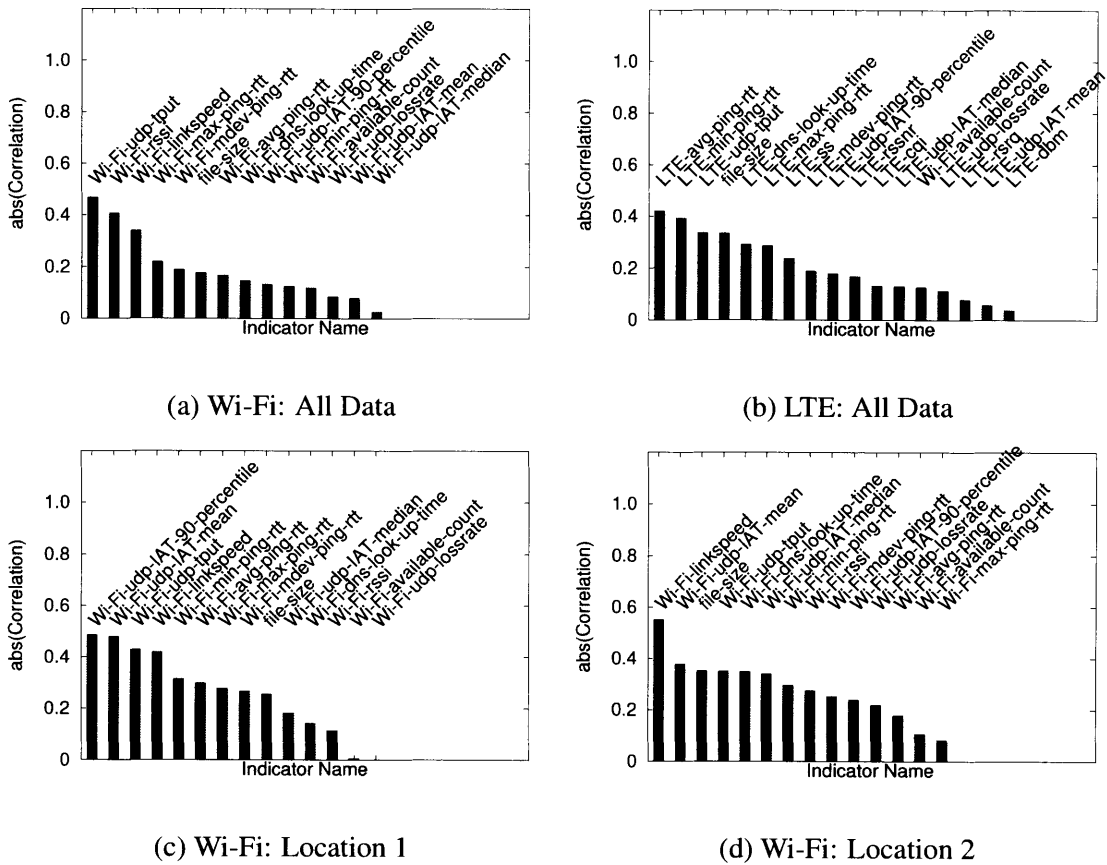
(d) Wi-Fi: Location 2

Figure 3-2: Correlation between Wi-Fi/LTE single path TCP throughput and each indicator.

show the correlation values calculated using data collected at only one location. Compared to Figure 3-2a, at each location, the order of the correlation strength changes. Similar results can be seen in LTE and MPTCP analysis.

3.3.2 Adaptive Probing

As shown in Figure 3-2, actively probing the network can provide important information to estimate network performance. However, active probing can be expensive in terms of energy, bandwidth, and delay. Table 3.3 summarizes the overhead in terms of delay, amount of data transferred, and energy consumption.

To reduce the probing overhead, the Network Monitor probes the network adaptively, *only if* there is a significant change in the passive indicators. Otherwise, it will reuse active probing information collected previously. To further reduce probing overhead, Delphi

Probe Type	DNS Query	10 Pings	UDP
Data Transferred (Bytes)	271	1K	200K
Wi-Fi Median Delay (Sec)	0.64	9.02	0.65
Wi-Fi Energy (mJ)	331	4730	366
Cellular Median Delay (Sec)	0.63	9.01	0.58
Cellular Energy (mJ)	1378	19697	1613

Table 3.3: Overhead for one occurrence of active probing. The delay values are the median value across all measurement data collected at 22 locations. The energy values are measured in an indoor setting. The cellular energy values do not contain tail-energy [26].

adaptively probes only when the mobile device's screen is on, which suggests that the user is currently interacting with the device and is more sensitive to network delays. There are, of course, times when background applications also need low delays (e.g., a cloud-based navigation app), but in the common case, delay is less of a concern in such situations. For background transmissions, Delphi will probe the network only when these two conditions occur: 1) there is a large change in the passive measurements; and 2) there is a data transmission request.

Adaptive probing has two benefits:

1. It is more energy-efficient than with fixed-rate probing.

2. It is proactive compared with probing only on a transmission request, which would delay the request.

To evaluate adaptive probing, we simulate it using our collected data as follows. At each location, we collected data from a series of runs measured back to back. We take the first run's passive and active measurement as input. Then, for the second run, we compare the passive measurement values with the first run. If the passive measurement difference d is less than a certain threshold Th, we keep the first run's active probing values as our measured number and use the second run's active probing values as the ground truth to calculate an error e. If d is greater than Th, we do active probing again.

The definitions of d and e for a run r are:

$$d_r = \sum_{i=1}^{m} \frac{|p_{i,r} - p_{i,r-1}|}{p_{i,max} - p_{i,min}} \tag{3.1}$$
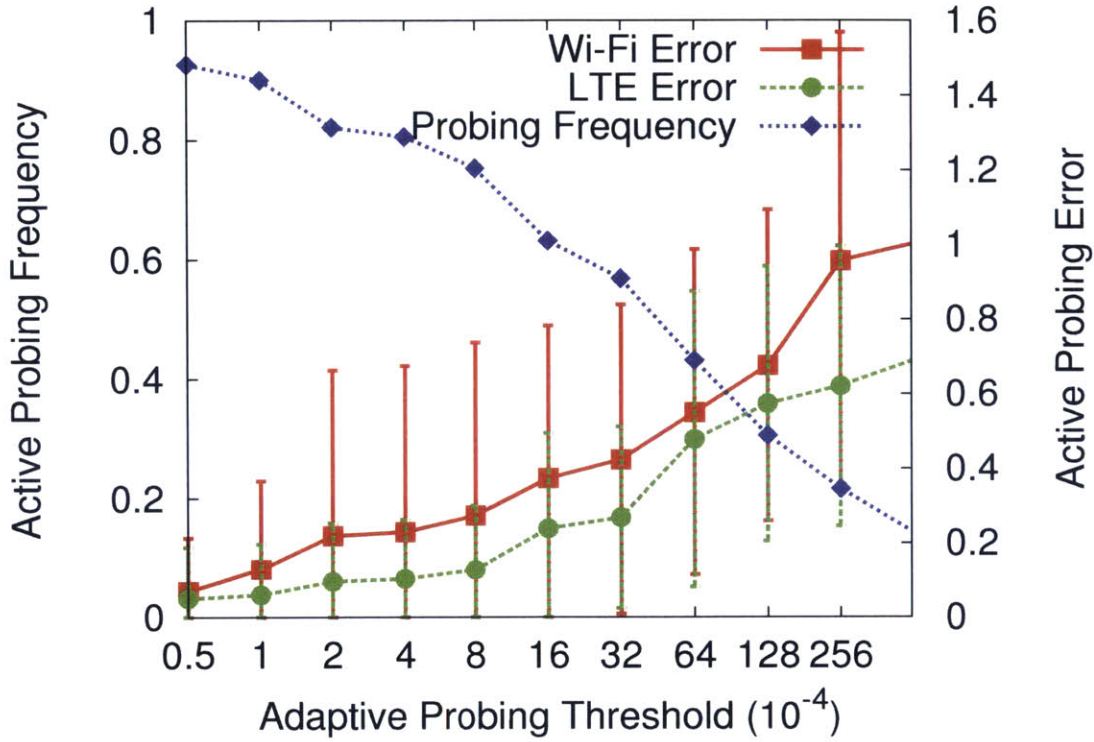
Figure 3-3: As the adaptive probing threshold (x-axis) increases, the number of probing decreases and the probing error increases. Here the left y-axis shows the probing frequency, which is the average number of probing in every five minutes.

$$e_r = \sum_{j=1}^{n} \frac{|\hat{a}_{j,r} - a_{j,r}|}{a_{j,r}} \qquad (3.2)$$

Here, m is the total number of passive indicators; p_i is the value of the passive indicator i; $p_{i,max}$ and $p_{i,min}$ are the max and min values for these indicators; n is the total number of active indicators; $\hat{a}_{j,r}$ is the active probing value for indicator j, and $a_{j,r}$ is the ground truth value in run r.

Figure 3-3 shows that as the probing threshold increases, fewer probes are triggered. Also, as the probing threshold increases, the error of reusing the previous active probing value increases. In §3.4, we will analyze the extent to which the choice of network is affected by this adaptive probing error.

3.4 Predictor

Delphi's Predictor takes the traffic profile and network status as input to estimate network performance. In this section, we focus on how it estimates TCP flow completion time because flow completion time is used in all our objectives mentioned in §3.5. However, similar techniques can be used to estimate other metrics such as average throughput (for streaming applications) or average RTT (for interactive applications).

To predict TCP flow completion time, or related metrics such as the end-to-end throughput for Wi-Fi and LTE networks, previous work either uses historical data from the same flow to predict current throughput [78], or it outputs binary results such as high/low throughput [22]. However, for Delphi, the prediction is more challenging: First, it needs to make its decision just before the connection transfers data, and recent historical data may not always available. Second, it needs to return numerical values instead of binary results to be fed into the Selector.

We use a machine learning model, the regression tree [56], to estimate TCP flow completion time. This learning method matches well with our problem definition, as it takes multi-dimensional vectors as input and produces a real-valued result. In our case, the multi-dimensional input includes data size and network condition indicators. Another advantage of using a regression tree is that by assigning different weight to different indicators when traversing through different branches, per-location differences (Figure 3-2) are captured naturally. Regression trees have been used to solve other network performance estimation problems [78] due to their low memory and computation overhead.

Delphi constructs four regression trees to predict the flow completion time for single-path TCP over Wi-Fi or LTE, and for MPTCP using Wi-Fi or LTE for the primary subflow. We estimate the flow completion time of MPTCP using separate trees instead of deriving it from the flow completion time estimated for single-path TCP because a previous measurement study [27] shows that throughputs of single-path TCP over two networks do not add up to the throughput of MPTCP. Besides, there are cases where MPTCP over both networks gives lower throughput than single-path TCP over a single network does.

The prediction accuracy is affected by two factors:

(a) TCP over Wi-Fi   (b) TCP over LTE
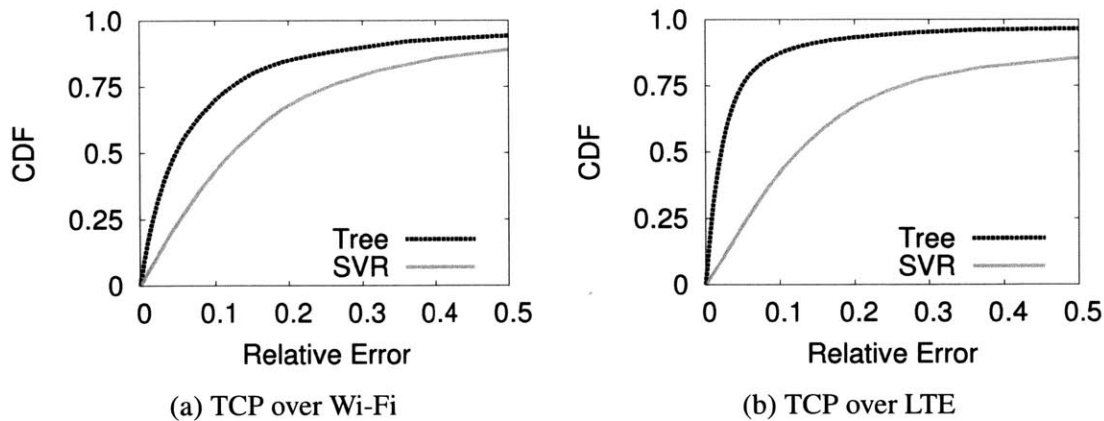
Figure 3-4: Relative error when using the regression tree and support vector regression to learn the flow completion time. The line marked with "Tree" shows the relative error of the regression tree model. The line with "SVR" shows the relative error of the support vector regression model.

1. the predictive power of the machine learning model, that is, whether regression trees are a good model for predicting flow completion time, and

2. the measurement accuracy of the inputs to the machine-learning methods.

3.4.1 Regression Tree Prediction Accuracy

Here, we use our dataset collected from 22 locations to analyze Delphi's prediction accuracy. To train the regression tree model, we randomly select 10% of the total samples from our dataset. We then use the remaining 90% as our testing data. As a comparison, we also train support vector regression (SVR) models with the radio basis kernel [60], which also takes a multi-dimensional vector as input and produces numerical results. The SVR models also consist of four separate models, each for one network configuration. To train each SVR model, we first sort all the indicators from the most correlated to the least correlated with the flow completion time. Here, we compute the correlation across all the data, not just the 10% in the training set, so that the sorting will not be biased by the training set. Then, we train the SVR model using the N most correlated features. As N increases, the testing errors first decrease (because the model improves in predictive power) and then increase (because the model overfits to the training set). For each SVR model, we choose the N that gives the smallest error. Thus, the resulting models are the best that can be achieved

76
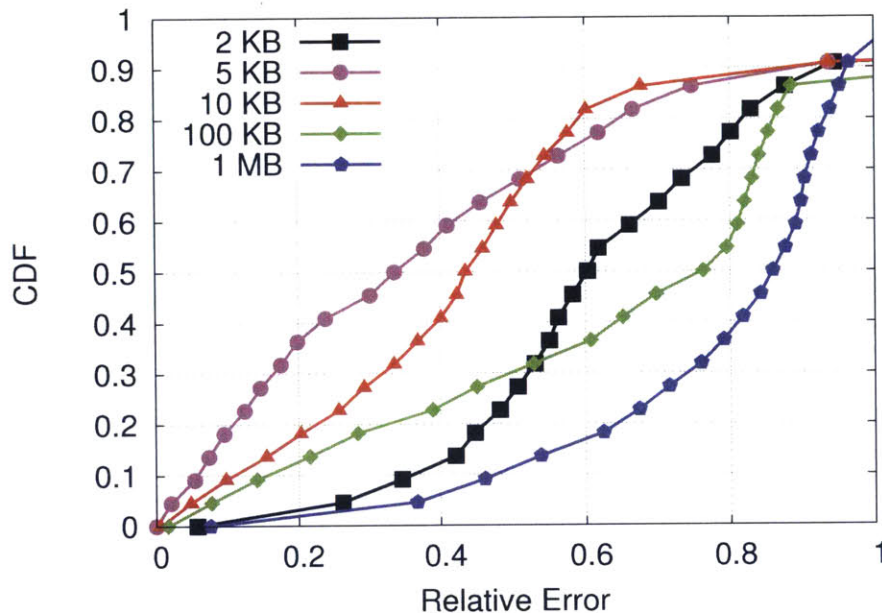
Figure 3-5: Relative error when using an empirical flow size number (3 KBytes) to predict flow completion time. The legends are the actual flow sizes.

using the SVR method given the features that we measure.

We test both models using the same testing set. Figure 3-4 shows the CDF of relative error between the learned result and the ground truth when predicting Wi-Fi and LTE. MPTCP predictions give similar results. Here, the regression tree model predicts the flow completion time with smaller error than the SVR model. Regression tree is more powerful because it is able to traverse through different paths in the tree when predicting different locations.

The median testing error ranges from 2% to 10% across the four regression tree models. Given that the training set consists of only 10% of the data, this shows the TCP flow completion time is predictable using regression trees.

3.4.2   Input Error Analysis

§3.4.1 shows the prediction error when the input feature vectors are accurate. As described earlier, the Traffic Profiler sometimes needs to guess the transfer size, and the Network Monitor may reduce active probing frequency to reduce energy and traffic overhead. Thus, the input to the regression tree is not always perfect. In this section, we investigate what
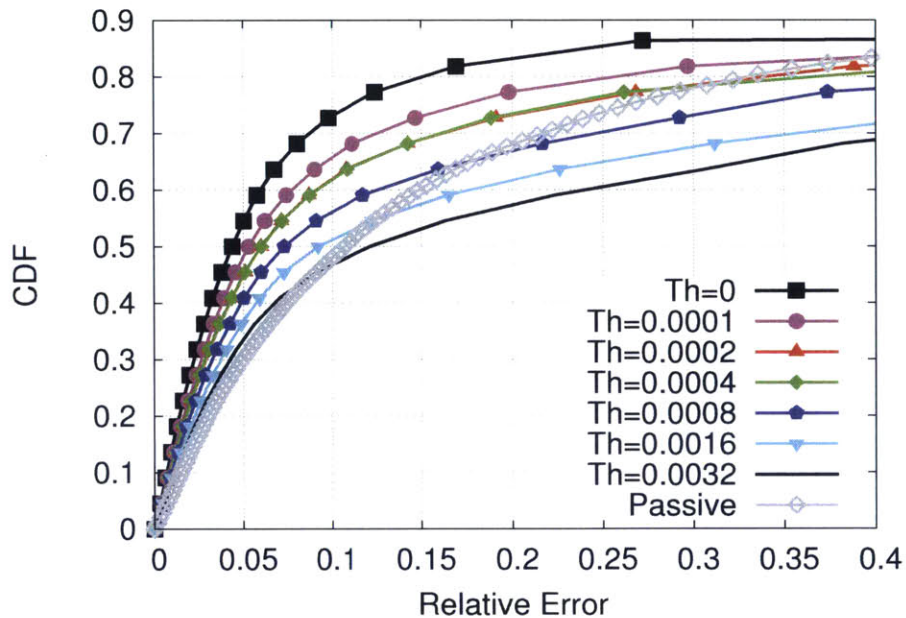
Figure 3-6: Relative error when using adaptive probing to predict flow completion time.

impact these imperfections have.

3.4.2.1 Traffic Profiler Error

As mentioned in §3.2, when there is no Content-Length field specified in a burst of transmission, the Traffic Profiler returns an empirical number of 3 KBytes. Figure 3-5 shows the relative error using an inaccurate transfer size as a regression tree's input (in Figure 3-5, we show only the results for TCP over LTE for clarity, but similar results hold for Wi-Fi and MPTCP). Here, we split the testing dataset into smaller subsets; each subset contains measurement done for a certain transfer size. As the difference between the actual transfer size and 3 KBytes increases, the relative error increases. The prediction error is significantly higher than the previous 2%-10%. Fortunately, however, only less than 15% of transfers are affected by this error, as noted in §3.2.

3.4.2.2 Network Monitor Error

Another source of error is adaptive probing. We run the regression tree testing over different Th values, which is an adaptive probing parameter. Figure 3-6 shows the CDF curves of

relative errors for LTE. Here, as Th increases (i.e., probing less frequently), the prediction error increases. Wi-Fi and MPTCP predictions also gives similar results.

3.5 Network Selector

Delphi's Selector uses network performance predictions, transfer lengths, and the specified objectives for application transfers to determine which network to use. The choice of network depends on three factors: throughput, energy efficiency, and monetary cost.

3.5.1 Objective Functions

Throughput, S: The Selector can estimate the average throughput of the current transfer using the transfer size f that is provided by the Traffic Profiler and the flow completion time t that is provided by the Predictor. Using the subscript i to refer to the choice of the network (either Wi-Fi or LTE or MPTCP with a specified primary subflow), we have:

$$S_i = \frac{f}{t_i} \tag{3.3}$$

Energy per byte, E_i: Knowing the power level p_i of each network choice i, together with the above t_i and f, the energy to transmit one byte is:

$$E_i = \frac{p_i \cdot t_i}{f} \tag{3.4}$$

The energy per byte is a metric that captures both battery consumption and transfer rate. A faster transfer over a network that has a higher power consumption may incur lower energy per byte. As a result, minimizing energy per byte is not always the same as picking the network with the lowest power consumption.

Monetary cost per byte, M_i: The "dollar" cost incurred when transferring each byte of the transfer on network choice i.

By knowing S_i, E_i, and M_i, the Selector chooses the network that maximizes the following objective function:

$$O_i = \frac{S_i{}^{\alpha}}{E_i{}^{\beta} \cdot M_i{}^{\gamma}} \tag{3.5}$$

This objective function prefers networks with high S_i values, meaning in a given second, it wants the device to transfer more bytes. It also prefers networks with low E_i value, meaning when consuming one joule of energy, it wants the device to transfer more bytes. Similarly, it prefers networks with low M_i values, meaning when consuming one dollar, it wants the device to transfer more bytes.

The exponents α, β, $\gamma \in [0, \infty)$ determine the relative importance of throughput, energy efficiency, and monetary cost, respectively. For example, if $\alpha = 1$, $\beta = 0$, and $\gamma = 0$, then $O_i = S_i$, and the Selector will select the network with the highest average throughput. This optimization is realistic if the device has an unlimited data plan and is connected to an AC power source. As another example, if $\alpha = 0$, $\beta = 1$, and $\gamma = 0$, then $O_i = 1/E_i$, and the Selector will select the network that consumes the least amount of energy. This optimization is preferable when the device is about to run out of battery.

In our experiments, we set α, β, γ to different values to experiment with different scenarios. In a more realistic implementation, α, β, and γ can be pre-defined by users or decided by Delphi dynamically according to the phone's current status. For example, β can increase as the battery level decreases. If the mobile device user has a limited monthly data plan for a cellular network, γ can increase as the amount of data plan consumed is approaching the budget, and set at a large number once the cellular usage exceeds the budget. Picking different values of α, β, and γ makes the objective function expressive enough to handle a range of preferences.

3.5.2 Energy Model

An energy model is required to estimate E_i. We measured the power level of both Wi-Fi and LTE on a Galaxy Nexus phone by connecting it to a power monitor [43]. We measured the power level during both TCP uploads and downloads using Wi-Fi and LTE. We also measured the power level across different transmission rates for both Wi-Fi and LTE, by changing the underneath channel quality. To do so, for Wi-Fi, we change the distance

Interface	LTE	Wi-Fi
Send Tput (mbps)	2.3~4.4	7.4~9.4
Send Power (mW)	2778±56	536±23
Recv Tput (mbps)	0.1~1.5	7.3~9.5
Recv Power (mW)	1674±95	428±58

Table 3.4: Power level measurement for Wi-Fi and LTE in a indoor setting. The Wi-Fi power is measured when the mobile device is associated with an AP deployed inside the building. The LTE power is measured when the mobile device is connected to Verizon LTE network.

between the phone and the access point. For LTE, we change the channel quality by moving into and out of buildings.

Table 3.4 shows the results. For each network, both while uploading and downloading data, the power level stays the same regardless of the data rate. Hence, we model the power p_i for each network using two constant numbers (one for upload and one for download). However, for LTE, there is an additional tail energy [26] component that is consumed after a transfer finishes, which we treat as a constant number. As a result, when estimating the energy consumed for LTE, Delphi adds this tail energy to the total energy consumed.

3.5.3   Selector Performance

To quantify the Selector's performance, we run simulations using data that we collected from 22 locations. We wrote a simulator that operates on this data set as described below. The dataset collected earlier maps a feature vector (made up of all the features listed in Table 3.2) to a tcpdump trace captured when running standard TCP on Wi-Fi and LTE and a tcpdump trace for MPTCP in striped mode using Wi-Fi as the primary subflow and using LTE as the primary subflow.

When evaluating any scheme, we assume all the features required by Delphi are available at the beginning of each run. We run Delphi's selection algorithms, described earlier, using the features collected at the beginning of the run along with flow size as input. We then pick the network interface that maximizes the objective function described above and look at the previously collected tcpdump trace to determine the duration from the beginning of the trace until a transfer size worth of bytes are transferred. We repeat the same

81
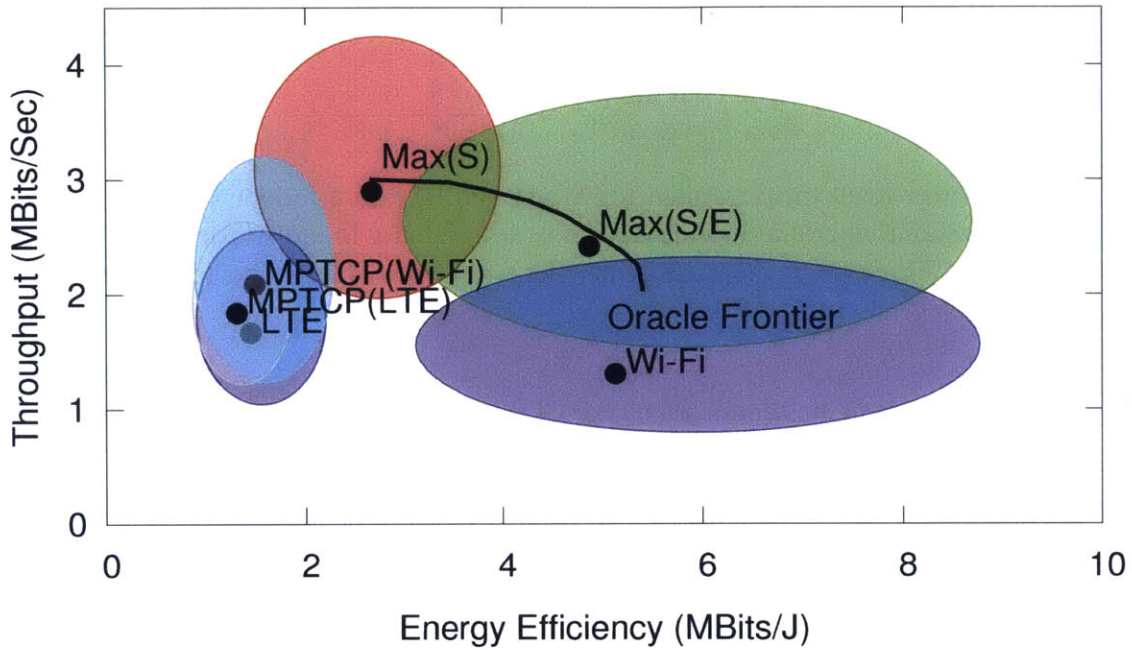
Figure 3-7: Megabits per joule and throughput values for different schemes. The black line shows a frontier of the best median values that can be achieved when setting $\alpha = 1$, $\gamma = 0$ and changing β from 0 to 5. For each scheme, the black dot shows the median value and the ellipse shows the 30th and 70th percentiles.

procedure, without any prediction, for the other policies for every run at each location.

In these simulations, we set $\gamma = 0$, meaning we do not consider monetary cost. Figure 3-7 shows the simulation results. The x-axis of the figure shows the number of bits that can be transmitted when consuming one joule. The y-axis shows the throughput. We first draw a frontier line by changing β from 0 to 5. When computing the frontier, we also use the ground-truth value of each flow's completion time so that the frontier represents the best that can be achieved if we have a perfect predictor. We call this line "Oracle Frontier".

In Figure 3-7, Wi-Fi, LTE, MPTCP(Wi-Fi), and MPTCP(LTE) are four fixed schemes where the same network is used across all locations. Here, Wi-Fi and LTE refer to transmitting data using single-path TCP over Wi-Fi or LTE. MPTCP(Wi-Fi) and MPTCP(LTE) refer to transmitting data over MPTCP, while using Wi-Fi or LTE for primary subflow. "Max(S)" and "Max(S/E)" are two schemes run by the Selector. In Figure 3-7, the two Delphi schemes, Max(S) and Max(S/E), fall close to the frontier line. In Max(S), the Selector set $\beta = 0$, meaning it is simply trying to maximize throughput. In Max(S/E), $\beta = 1$,
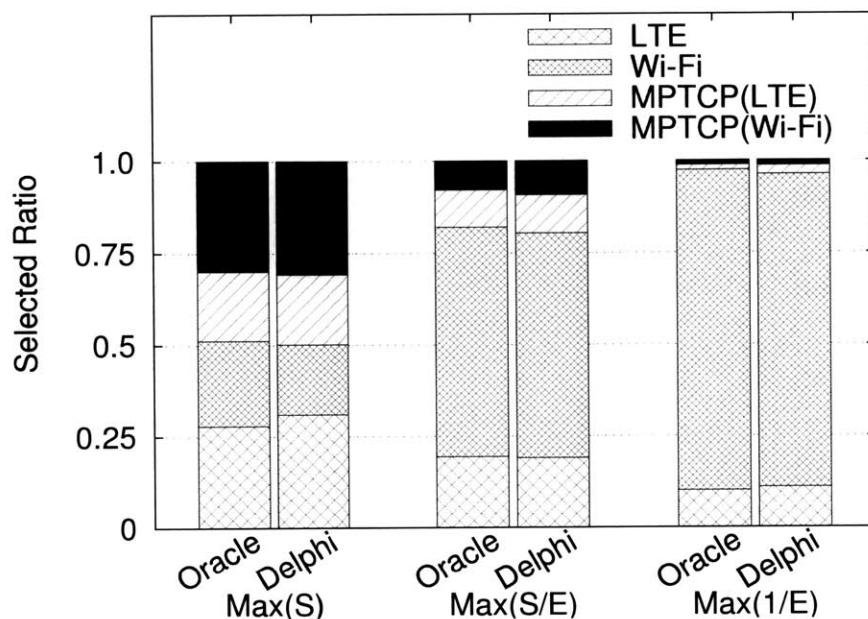
Figure 3-8: Percentage of each network(s) is selected when using different objective functions.

meaning it tries to select networks with high throughput but without consuming too much energy. We can see that Max(S) and Max(S/E) are much closer to the Oracle Frontier line than any other schemes are.

Objective	Max(S)	Max(S/E)	Wi-Fi
Throughput (Mbits/Sec)	3.0	2.6	1.4
Energy Efficiency (Mbits/J)	2.8	4.9	5.2

Table 3.5: Median values for Max(S), Max(S/E) and Wi-Fi as shown in Figure 3-7.

Table 3.5 lists the *x* and *y*-axis median values for Max(S) and Max(S/E), together with the median value for the fixed scheme that always uses Wi-Fi for comparison. Here, Max(S) gives the highest median throughput of 3.0 Mbit/s, which is a 2.1× gain over Wi-Fi's 1.4 Mbit/s. Max(S/E) tries to achieve high throughput with high energy efficiency. Its median energy efficiency is 4.9 Mbit/J, 6% worse than always using Wi-Fi, but it achieves a median throughput of 2.6 Mbit/s, a 1.9× gain over Wi-Fi.

We now take a closer look at each scheme. When an objective function is defined, how many times is each available choice selected? Figure 3-8 shows the percentage of time that each network choice is selected when trying to optimize different objectives. First, we can
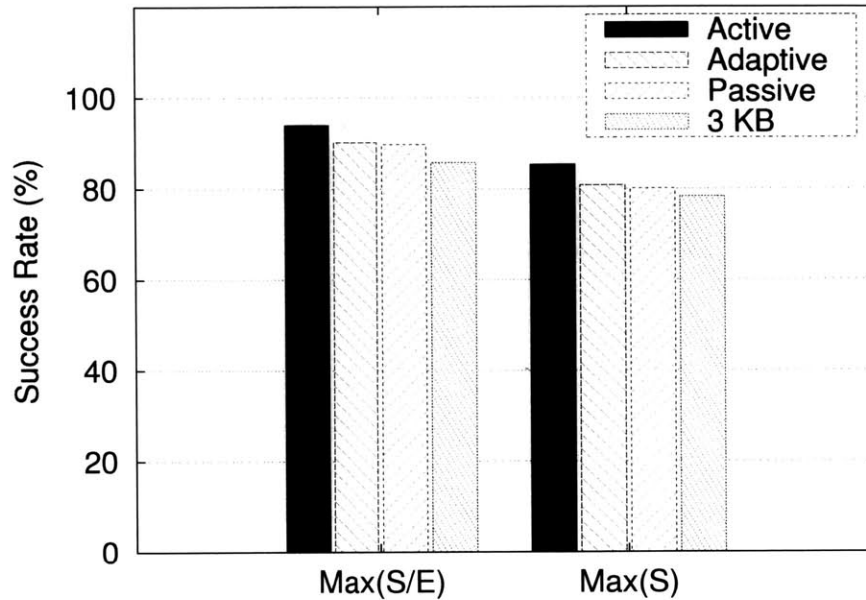
Figure 3-9: Success rate for different schemes.

see that Delphi makes very similar decisions compared with an omniscient oracle. However, for each specific objective function, Delphi chooses different networks. For example, when maximizing throughput, Delphi selects LTE more often than Wi-Fi or any other MPTCP-based scheme because LTE provides the highest throughput in a large number of cases in our dataset. For Max(S/E) (maximizing throughput over energy) or for Max(1/E) (minimizing energy consumption), Delphi tends to choose Wi-Fi much more often, since Wi-Fi is generally more energy-efficient. However, both the oracle and Delphi still select other network(s) because there are cases where Wi-Fi gives really low throughput, lengthening the transfer and consuming significant energy in the process.

To understand these errors in more detail, we compare the decision made by the oracle and by Delphi. We say that Delphi makes a successful decision if it selects the same network(s) as the oracle. Figure 3-9 shows the ratio of successful decisions affected by different error sources. Here, "Active" refers to using active probing information for flow-completion time prediction. "Adaptive" refers to our adaptive probing technique described earlier. "3 KB" refers to using active probing, in which the Traffic Profiler outputs 3 KBytes in 16% of the total outputs. We selected 16% because we found that in 16% of the total network transactions data size is not predictable (Table 3.1 in §3.2).

84

We can see that Active gives the highest success ratio (93% for Max(S/E) and 85% for Max(S)). As we add error to the network measurement input, or Adaptive, the success ratio is lower (90% and 81%, respectively). Finally, inaccurate transfer size information gives us the lowest success rate (86% and 78%, respectively). These results show that we can achieve high success rates by adding active probing overhead. If the overhead is a concern, removing active probing can still give reasonable results. However, being able to predict the size of the burst of traffic is more important.

3.5.4 System Generalization

Model Type	Obj.	Throughput (Mbits/Sec)	Energy Efficiency (Mbits/J)
SVR	Max(S)	2.3	1.6
Reg. Tree	Max(S)	2.1	2.0
Wi-Fi Only	-	1.4	5.6
LTE Only	-	1.7	1.5
SVR	Max(S/E)	1.4	5.6
Reg. Tree	Max(S/E)	1.9	2.7

Table 3.6: Median values for throughput and energy efficiency when testing different models at new locations.

In our above analysis, both our training and testing datasets are generated from the 22 locations we measured. These results show the improvement when we have prior knowledge of the network condition of each location. In this section, we show the results in a more challenging condition: we test Delphi's performance when there is no prior knowledge. This corresponds to the real use case when a smartphone user enters a new location that he or she has never been to.

We trained Delphi using data collected from 21 out of the 22 locations and tested it on the last location. We repeated this process 22 times by using each location to be the testing set. Table 3.6 shows that when maximizing throughput, Delphi achieves up to $1.6\times$ improvement (when using the SVR model) over Wi-Fi. When maximizing throughput over energy consumption, Delphi behaves as well as Wi-Fi and better than using LTE only. These results show that 1) when there is no prior knowledge, the improvement decreases, and 2) the SVR model achieves higher improvement than the regression tree does. This is

85

because the regression tree is powerful when it characterizes data in a training set, which means it tends to overfit, and is less powerful when predicting new data. Thus, Delphi can use the SVR model to make decisions when entering new locations, or crowd-sourcing measurement techniques [68] can be used to feed the smartphone with prior knowledge of new locations to further improve performance.

3.6 Implementation

We implemented Delphi on a laptop (2.4GHz Dual Core with 4GB RAM, comparable to a smartphone) running MPTCP (Ubuntu Linux 13.10 with Kernel version 3.11.0, with the MPTCP Kernel implementation version v0.88 [51]). We tethered two smartphones to the laptop, one in airplane mode with Wi-Fi enabled and the other with Wi-Fi disabled but connected to the Verizon LTE network. The reason we implemented Delphi on a laptop instead of a smartphone is to utilize existing machine learning libraries. We also enabled MPTCP on a Galaxy Nexus phone running Android 4.1 [48] to validate that all the following functionality is feasible on smartphones. All the measurement data used for simulation in the previous settings are also collected under the same setting.

The current implementation of Delphi is a user-level application implemented in Python. One thread of Delphi serves as the Network Monitor; it continuously polls passive indicator values from both phones over the USB interface every 500 milliseconds.

Switch Type	Send Delay (ms)	Recv Delay (ms)
LTE switch on	494± 1	507 ± 13
Wi-Fi switch on	495 ± 2	782 ± 47

Table 3.7: Switching delay, averaged across 10 measurements. The switching delay is defined as the time between an `iptable` rule-changing command being issued and a packet transfer occurring on the newly brought-up interface. The send delay is the delay for the first out-going packet showing up, and the receive delay is for the first ACK packet coming from the server.

The other thread serves as the Traffic Profiler, Predictor, and Selector. It runs `tcpdump` to monitor packet transmissions in real time. Once it sees that a network transfer has been initiated, it looks for an HTTP request or response header and reads the Content-Length

information from the header. It then calls the Predictor function to predict the transfer completion time and then calls the Selector function to select a single network by changing `iptable` rules [50]. This procedure of turning an interface off allows MPTCP to migrate to the new connection because it supports break-before-make semantics. When the network is idle, this thread also reads the passive indicator values periodically (every 5 seconds), and uses a default value of 3 KBytes as transfer length when calling the Predictor and Selector functions so that the network can be pre-selected before a new TCP connection starts. When a connection is actively transmitting, Delphi also periodically (every 500 milliseconds) reads the passive indicator values so that it can detect significant network environment changes in case the mobile device is moving. This allows Delphi to dynamically select networks during long-running transfers. Once the Selector decides an interface switching is required, it achieves the switch by changing `iptable` entries for that specific TCP connection. Table 3.7 shows the interface switching delay measured in an indoor setting. Each number is an average across 10 measurements. The switching delay is defined as the time between an `iptable` rule-changing command being issued and a packet transfer occurring on the newly brought-up interface. In our current implementation, the out-going delay is 500 ms. During this 500 ms, the transfer does not pause but continues on the pre-selected network. Notice that not all connections will experience this delay because Delphi can pre-select the network configurations as it observes a network condition change. This switch delay will happen only when 1) the network condition changes during a transfer or 2) the network selection result based on the actual transfer size is different from the result based on the default 3 KBytes value. In our experiments (§3.7.2), 18% of HTTP transactions incur a network switch during data transfer.

We configured the laptop to pass all its HTTP traffic through an MPTCP-enabled proxy server. Because current app servers do not always support MPTCP, the proxy server allows our client to run apps over MPTCP while talking to the apps' original server.

(a) Web Browsing

(b) Video Streaming
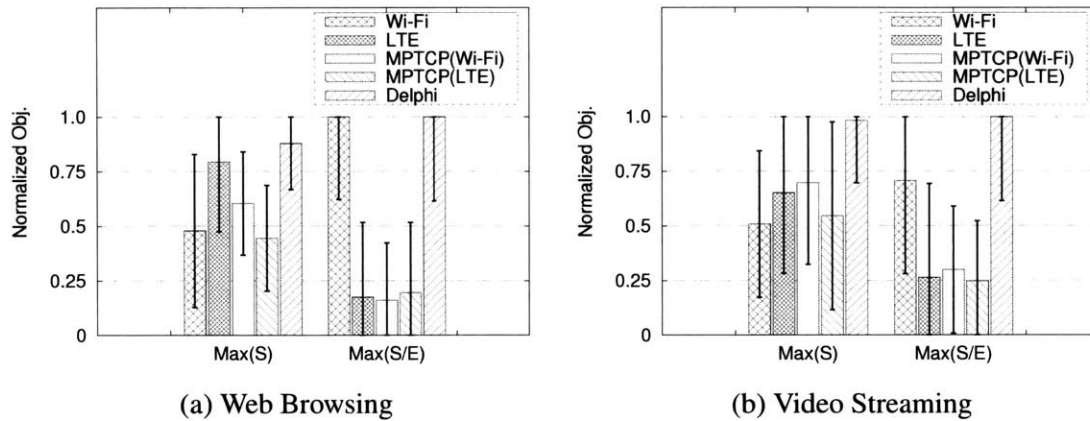
Figure 3-10: Objective function value normalized by oracle. The histogram shows the median value; the error bar shows 20th and 80th percentiles.

3.7 Evaluation

In previous sections, we analyzed the performance of each module using a trace-driven approach. This serves as a micro-benchmark evaluation of Delphi. In this section, we focus on macro-benchmark evaluation done by emulation and real-world experiments.

3.7.1 Delphi Over Emulated Networks

To understand Delphi's performance under real application workloads, we used Mahimahi, a record-and-replay tool that can record and replay client-server interactions over HTTP [53]. In our experiment, we recorded client-server interactions when the client ran two applications: web browsing and video streaming. During replay, Mahimahi replays the recorded interactions on top of an emulated network. Mahimahi can emulate network delays and variable-rate links using packet-delivery traces. In our experiment, we used the tcpdump traces captured during our measurement at 22 locations as packet-delivery traces for network emulation. During the tcpdump measurements, we also measured passive indicator values, which were fed into Delphi during our emulation as inputs to the Network Monitor. This emulation setup enabled us to compare different network selection schemes when running exactly the same application traffic and under the same network conditions.

We used Delphi to optimize two different objective functions, 1) $Max(S)$: maximizing average throughput (i.e. minimizing transfer completion time) and 2) $Max(S/E)$: max-

(a) Breakdown by locations   (b) Breakdown by transfer sizes
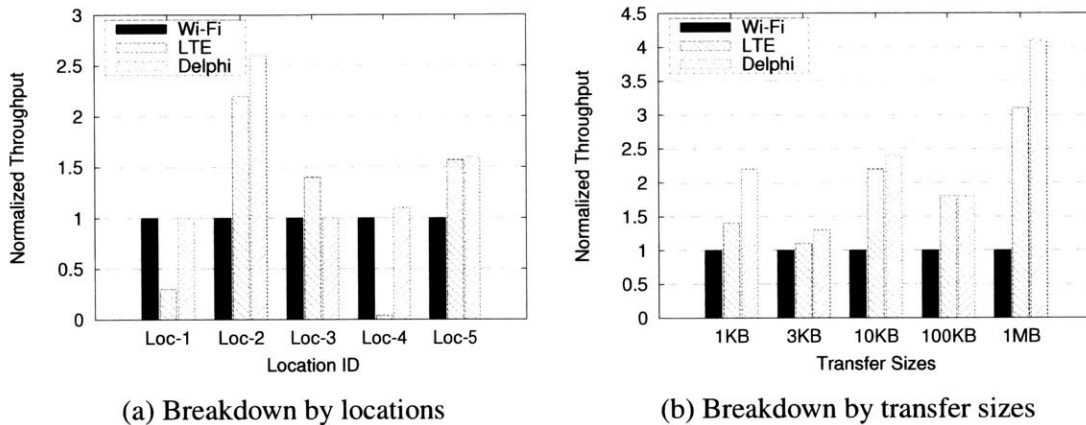
Figure 3-11: Objective function value normalized by oracle. The histogram shows the median value; the error bar shows one standard deviation.

imizing average throughput over energy per byte. In each experiment, we recorded the actual value of S and S/E achieved by Delphi and by using different fixed choices. After running Delphi and the fixed network(s) schemes at one location, we could determine which network choices give the highest values of S and S/E. We call this highest value the *oracle value*. We use the oracle value to normalize the predictions of all schemes that we consider.

Figure 3-10 shows the median normalized value for each scheme across all locations. Figure 3-10a shows the results for web browsing. For $Max(S)$, Delphi gives the highest throughput over all the other fixed schemes. When compared with Wi-Fi, which is the default network selection on most mobile devices, our throughput improvement is 83%, which corresponds to a 46% reduction in transfer time. For $Max(S/E)$ Delphi improves the median normalized throughput over energy per byte by 0% (over Wi-Fi since Wi-Fi tends to be much more energy efficient than other schemes) to $6\times$ (over MPTCP(Wi-Fi)). In Figure 3-10b, for video-streaming applications, for $Max(S)$ Delphi improves the throughput by 93% over Wi-Fi, corresponding to a 49% reduction in transfer time. For $Max(S/E)$, Delphi's improvement ranges from 41% (over Wi-Fi) to $3.9\times$ (over MPTCP(LTE)).

3.7.2 Experiments

To understand how Delphi behaves in the real world, we first trained Delphi's predictor using data we collected at the 22 locations. The model training was done using a desktop (Intel Xeon(R) CPU, 3.30GHz Quad Core, 16 GB RAM). The total training process took five minutes. Then, among the 22 locations, we visited five close to our campus. On our Delphi-enabled laptop, we ran `wget` to download files with various sizes (1 KByte, 3 KBytes, 10 KBytes, 100 KBytes, and 1000 KBytes) from a remote server. For comparison, we also ran the same `wget` with only Wi-Fi or LTE enabled before or after we ran Delphi. We randomized the sequence of configurations (file sizes, network measured). For each configuration, we ran it five times.

Figure 3-11 shows the average improvement of Delphi over Wi-Fi and LTE, when Delphi's objective is set to maximize throughput. Due to high variation of the actual throughput across different configurations, here we show the throughput normalized by Wi-Fi's throughput. Figure 3-11a shows Delphi's performance at each location. We can see that Delphi does not perform perfectly. At Location 3, the LTE had a higher average throughput than Wi-Fi, but Delphi still selected Wi-Fi. However, at other locations, Delphi performed better than always using Wi-Fi or LTE. At Locations 2, 4, and 5, Delphi performed better than both Wi-Fi and LTE, because it used MPTCP running over both networks. In Figure 3-11b, we can see that Delphi achieves improvement for small (1 KByte, 3 KBytes, and 10 KBytes) and large (100 KBytes) transfers. A deeper investigation reveals that the middle-sized (1 MByte) transfers are affected by the switching delay (explained in §3.6) the most: Most of the transfers go through the sub-optimal network(s). However, for large transfers, although it also transfers on the sub-optimal network(s) for some time, most of the transfers happen after the network switch. Thus, Delphi performs well for large transfers. In summary, Delphi increases average throughput by up to 4× compared with Android's default policy that always uses Wi-Fi when it is available.

90
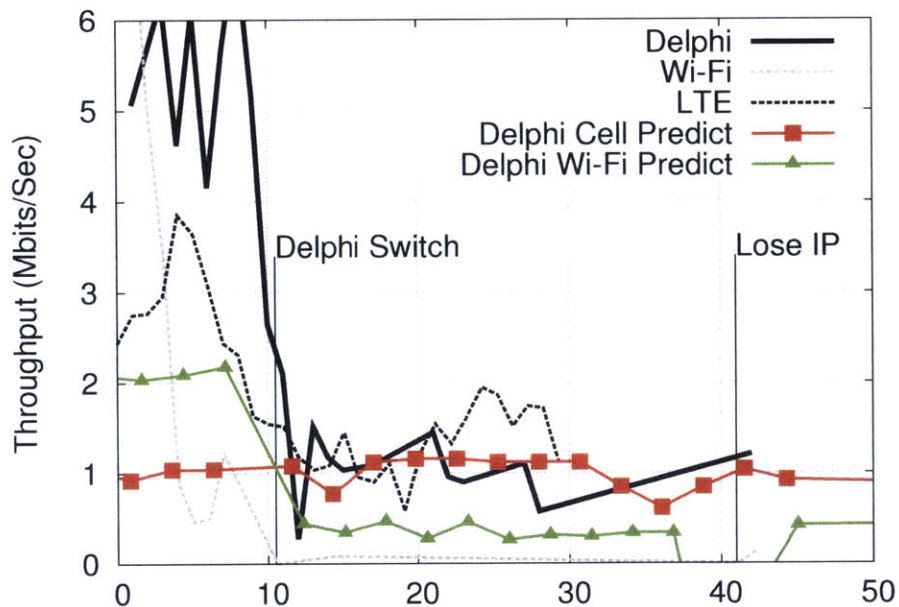
Figure 3-12: When the mobile device is moving away from an access point, Delphi predicts that Wi-Fi can be worse than LTE, then it switches to LTE at time 10.5 seconds. MPTCP handover mode switches to LTE when it sees Wi-Fi loses the IP, which happens at time 41 seconds.

3.7.3 Handling User Mobility

Another benefit of using Delphi is that by continuously monitoring the network conditions using the Network Monitor, Delphi can tell whether the network performance is getting worse and trigger handover proactively. This is best demonstrated when the mobile device is moving. In this experiment, we kept Delphi running on the laptop while moving it from inside a building to outside a building. The tethered Wi-Fi phone was initially connected to the Wi-Fi AP inside the building. As we walked outside the building, the Wi-Fi signal kept decreasing until the phone could not associate with the AP. We ran wget on the laptop to download a large file from our proxy server. In this experiment, we configured Delphi to $Max(S)$ and to select only between Wi-Fi and LTE, not the MPTCP choices, to study the handover behavior. In our experiment, We first ran wget without running Delphi, and with only one interface at a time, to measure the throughput of Wi-Fi and LTE as the laptop moved, shown as "Wi-Fi" and "LTE" in Figure 3-12. Then we ran Delphi while moving the laptop along the same path. In Figure 3-12, we can see that at time 10.5, Delphi predicted
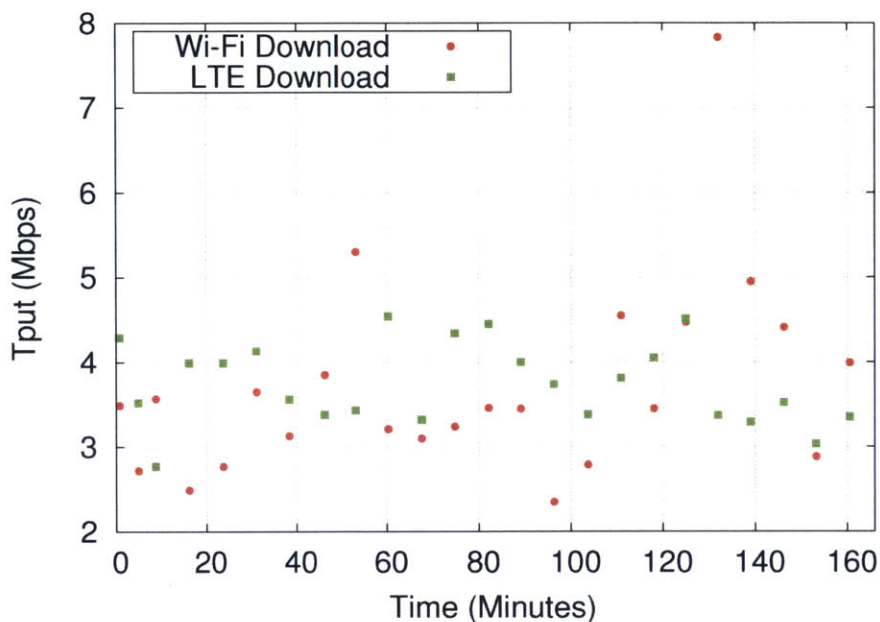
Figure 3-13: Wi-Fi and LTE download throughput at the same location over 2.5 hours.

that Wi-Fi was worse than LTE and consequently triggered a switch, and the throughput dropped but soon recovered to LTE's throughput. In Figure 3-12, we also marked the time when the phone lost its Wi-Fi IP address; this is when a handover will happen according to Multi-Path TCP Handover-Mode proposed in [57]. However, we can see that in this case, Wi-Fi throughput had already dropped to zero before it lost the IP address. Compared with this scheme, Delphi triggers LTE/Wi-Fi handover earlier so that the application sees constantly high throughput.

3.8 Discussion

In this section, we discuss two alternative network selection schemes and compare them with Delphi.

3.8.1 Purely Location-Based Algorithm

The first alternative algorithm is to use location information to make network selection decisions. The assumption is that at certain locations, a mobile device tends to use a certain

92
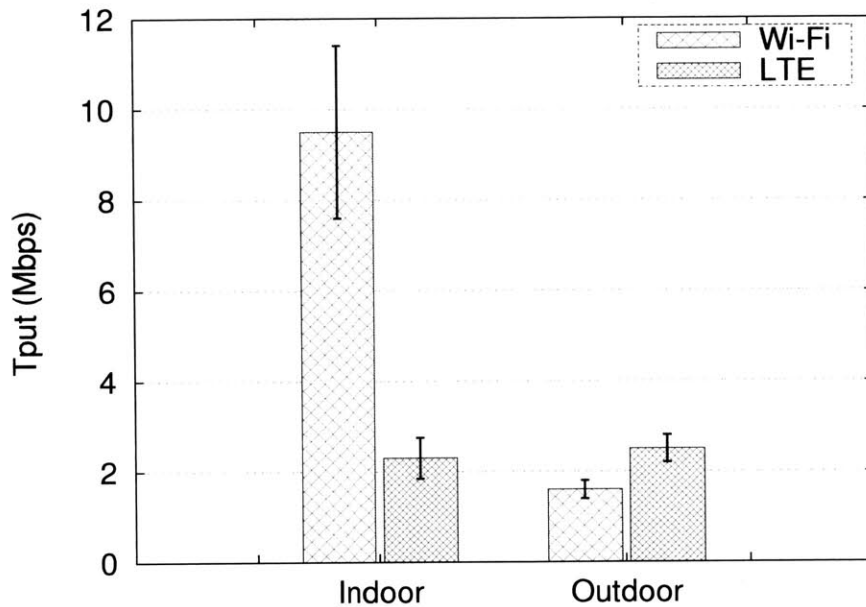
Figure 3-14: Wi-Fi and LTE download throughput measured indoors and outdoors. The bar shows the average throughput over 10 measurements; the error bar shows the standard deviation.

network combination. However, we argue that network location is not the only dominant factor. Figure 3-13 shows the measured Wi-Fi and LTE throughput at one location over a period of 2.5 hours. We can see that both Wi-Fi and LTE throughput varies significantly during this period of time. Wi-Fi has higher throughput than LTE does at certain time points, while LTE has higher throughput than Wi-Fi has at other times. Thus, if the goal is to select the network with the highest throughput, a purely location-based method is not guaranteed to make the correct choice all the time.

Another challenge for using location as the network selection signature is to select a proper granularity of location. Figure 3-14 shows the TCP throughput for Wi-Fi and LTE measured at two nearby locations, one inside a building and one outside the building. The distance between the two locations is about 20 meters. We can see that the throughput changes dramatically between these two locations; thus, the network selection for maximizing throughput will also change. Moreover, as shown in the previous section, when moving from indoors to outdoors, Delphi can detect the network condition change and switch between networks accordingly. To make a location-based approach have similar

93
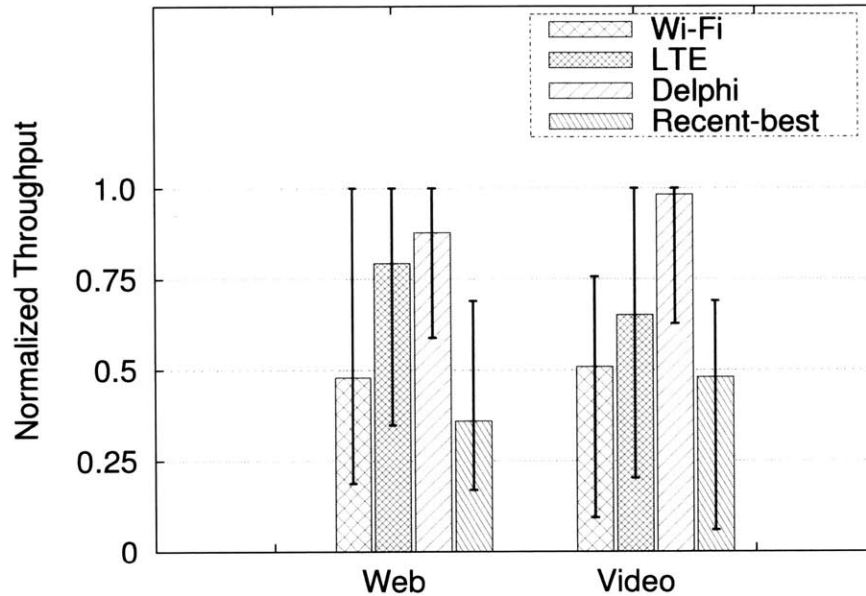
Figure 3-15: Throughput normalized by oracle. The histogram shows the median value; the error bar shows the 20th and 80th percentiles. The bars labeled "Recent-best" show the results for picking-the-recent-best.

capability, it needs to have location and network performance mappings within the granularity of 20 meters or less. This requires intensive measurement done beforehand as well as mobile devices having accurate localization capabilities both indoors and outdoors, which can bring extra computational and energy overhead for the devices.

3.8.2 Picking the Recent-Best Choice

Another idea is to send traffic on each networks or network combinations then select the one that gives the best performance for the rest of the data transfers. We applied this approach to web traffic. A typical web page load consists of many small transfers (HTTP transactions); thus, the first few transfers can be transferred on all available network combinations, and then the rest of the transfers will be assigned to the best one according to the observed performance. We compared this approach with Delphi. Figure 3-15 shows the results when running both schemes to select the network with the highest average throughput. We find that this picking-the-recent-best approach performs worse than Delphi does and even worse than static approaches, in both web page loading and video streaming.

To understand why this picking-the-recent-best scheme performs poorly, we take a deeper look into the results and find that for web page loading, whose traffic consists of many short transfers, the total page load time is dominated by the probing phase to pick the best choice because some data has to be transmitted on the slow network choices.

The video streaming traffic contains a few short transfers at the beginning, which are used for probing. However, because different transfer sizes may result in different network performances, a fast network for short transfers may not be a fast network for long transfers. This probing-while-transferring approach ends up using a slower network for the main video file downloading. In our experiment, for video streaming the success rate (selecting the same network as oracle) for Delphi is 60%, and it decreases to 50% for picking-the-recent-best.

3.9 Related Work

We discuss related work on mobile network selection policies, MPTCP, scheduling algorithms that generalize processor sharing [59] to multiple interfaces, roaming mechanisms to seamlessly migrate between interfaces, and systems and APIs that allow applications to benefit from multiple interfaces.

3.9.1 Mobile Network Selection

Zhao et al. [84] present a system that picks from one of three choices for every flow: regular IP, mobile IP [62] with triangle routing, and mobile IP with bidirectional tunneling. Instead of selecting an entire path within the Internet, as Zhao et al. do, Delphi picks either an LTE link or a Wi-Fi link for the last hop alone. CoolSpots [61] and SwitchR [7] address the question of network selection between Wi-Fi and Bluetooth networks available on the phone. In contrast, Delphi chooses between Wi-Fi and LTE on the last hop using different techniques. MultiNets [54] proposes a mechanism to allow smartphones to use multiple networks based on certain policies, such as energy saving, data offloading, and performance. However, MultiNets explicitly assumes that Wi-Fi is faster than the cellular link is, which no longer holds true [27]. ATOM [42] is a traffic management system allocat-

ing mobile devices' traffic between LTE and Wi-Fi networks operated by the same service provider. ATOM's selection decision was made at the service provider side in a centralized way. However, Delphi is able to make selections across different Wi-Fi and LTE providers, in a distributed approach, in which the mobile devices make the decision.

Theoretical work on this problem includes multi-attribute decision making [17], game theory and reinforcement learning [55], and analytic hierarchy processes [72]. These are primarily evaluated in simulation using simplified models of the network and workloads. In contrast, our evaluation consists of trace-driven simulations and real-world experiments with traffic from unmodified applications.

3.9.2 Multi-Path TCP

Multi-Path TCP (MPTCP) [77], and its recent implementation in iOS 7 [49] allow a single TCP connection to use multiple paths. MPTCP does not specify if interfaces should be used simultaneously or in master-backup mode. The iOS implementation operates in master-backup mode using Wi-Fi as the primary path, falling back to a cellular path only if Wi-Fi is unavailable. Other implementations, such as the default mode in Linux, use all available interfaces in "striped" mode.[1] Delphi can be viewed as specifying an MPTCP network-selection policy when operating on mobile networks. The choice between a cellular link and Wi-Fi is necessarily dynamic in such cases, and a static policy such as the one in Android (use Wi-Fi if it is available) does not suffice.

3.9.3 Processor Sharing for Multiple Interfaces

Recent work [80] extends generalized processor sharing [59] to multiple interfaces. In follow-up work [79], the authors also propose scheduling packets over multiple interfaces while respecting relative preferences (e.g., Netflix should get twice the throughput of Drop-box) and absolute preferences (e.g., give YouTube at least 5 Mbps). These algorithms operate on every packet, while Delphi operates on flow level.

---

[1] Striped mode denotes that packets are striped across both interfaces with one being a primary interface and is the mode in which we use MPTCP for this dissertation.

3.9.4 Roaming Mechanisms

Mobile IP [62] and end-to-end alternatives [70, 76] allow a mobile device to freely roam between networks without disconnecting connections. Multi-Path TCP [77] supports break-before-make semantics as well: an MPTCP connection can have no active subflows for a short duration before a new subflow is created and attached to the connection. These mechanisms are complementary to Delphi, and Delphi can determine the network-selection policy while retaining the roaming mechanisms of the underlying transport protocol.

3.9.5 Systems and APIs to Exploit Multiple Interfaces

The idea of using multiple networks for increased capacity and fault tolerance has attracted significant attention from researchers over the past decade. Early work [13] shows the benefits of combining multiple networks and use cases where selecting the right network can reduce energy consumption, enhance network capacity, and manage mobility.

FatVAP [36] and MultiNet [23] improve throughput by allowing a single Wi-Fi card to connect to multiple APs. COMBINE [10] improves individual device throughput by leveraging the wireless wide area network of neighboring devices. Blue-Fi [11] is a system that uses Bluetooth and cellular tower information to predict whether Wi-Fi is available to reduce the Wi-Fi duty cycle. Airdrop [8], a feature of Apple OS X, allows users to share files over both Wi-Fi and Bluetooth. However, it is designed explicitly for the purpose of file sharing (a long-running flow), while our system focuses on the more common case of both short and long flows on mobile devices today.

Contact Networking [21] provides localized network communication between devices with multiple networks and focuses on designing mechanisms that enable lightweight neighbor discovery, name resolution, and routing. Intentional Networking [33] provides APIs that allow apps to label their network flows. The labels include *background* or *foreground* to specify whether the flow is delay tolerant and `large` or `small` to specify the amount of data to be transmitted. Intentional Networking uses a connection scout that probes network conditions periodically, an overhead Delphi can avoid by using passive measurement only. We consider these abstractions orthogonal because Delphi's network selection pol-

icy is agnostic to the API exposed by the system to applications. Delphi can be used as a decision-making module to select network interfaces within these systems.

3.10 Chapter Summary

We presented Delphi, a software controller to help mobile applications select the best network among multiple choices for their data transfers. Delphi's selection schemes are able to handle trade-offs between high throughput and energy efficiency. Thus it outperforms static schemes such as using Wi-Fi by default (the policy on Android today), or using LTE by default, or always using both, since neither Wi-Fi nor LTE is unequivocally better than the other.

Applications could care about other metrics such as average per-packet delay and tail per-packet delay, or more app-centric metrics such as page-load time for web pages or minimizing the risk of a stall for streaming video. We view Delphi as a first step in answering these questions. One direction of our future work is to provide expressive APIs for applications to express their specific needs to Delphi.

In our work, we use machine learning as a tool to make decisions where a static policy does not suffice. Another direction can be explored in the future is to enhance Delphi's learning capability by using online learning or crowd-sourced learning mechanisms. This would allow mobile devices to make better network selection decisions when they enter locations for the first time.

Chapter 4

Energy Consumption for LTE and 3G

4.1 Introduction

Smartphones and tablets with wide-area cellular connectivity have become a significant, and in many cases, dominant, mode of network access. Improvements in the quality of such network connectivity suggest that mobile Internet access will soon overtake desktop access, especially with the continued proliferation of 3G networks and the emergence of LTE and 4G.

Wide-area cellular wireless protocols need to balance a number of conflicting goals: high throughput, low latency, low signaling overhead (signaling is caused by mobility and changes in the mobile device's state), and low battery drain. The 3GPP and 3GPP2 standards (used in 3G and LTE) provide some mechanisms for the cellular network operator and the mobile device to optimize these metrics [82, 5], but to date, deployed methods to minimize energy consumption have left a lot to be desired.

The 3G/LTE radio consumes significant amounts of energy; on the iPhone 6 Plus, for example, the stated internet-use time is "up to 12 hours on 3G or LTE" (i.e., when the 3G radio is on and in "typical" use) and the talk-time is "up to 24 hours".[1] On the Nexus 5, the equivalent numbers are "up to 7 hours on LTE for internet-use" and "up to 17 hours for

---

[1] http://www.apple.com/iphone-6/specs/

99

talk time"[2]. The fact that the 3G/LTE interface is a battery hog is well-known to most users anecdotally and from experience, and much advice on the web and on blogs is available on how to extend the battery life of your mobile device.[3] Unfortunately, essentially all such advice says to "disable your 3G data radio" and "change your fetch data settings to reduce network usage". Such advice largely defeats the purpose of having an "always on" broadband-speed wireless device, but it appears to be the best one can do in current deployments.

We show the measured values of 3G energy consumption for multiple Android applications in Figure 4-1.[4] This bar graph shows the percentage of energy consumed by different 3G radio states. For most of these applications (which are all background applications that can generate traffic without user input, except for Facebook), less than 30% of the energy consumed was during the actual transmission or reception of data. Previous research arrived at a similar conclusion [15]: About 60% of the energy consumed by the 3G interface is spent when the radio is not transmitting or receiving data.

In principle, one might imagine that simply turning the radio off or switching it to a low-power idle state is all it takes to reduce energy consumption. This approach does not work for three reasons. First, switching between the active and the different idle states takes a few seconds because it involves communication with the base station, so it should be done only if there is good reason to believe that making the transition is useful for a reasonable duration of time in the future. Second, switching states consumes energy, which means that if done without care, overall energy consumption will increase compared to not doing anything at all. Third, the switching incurs signaling overhead on the wireless network, which means that it should be done only if the benefits are substantial relative to the cost on the network.

This chapter tackles these challenges and develops a solution to reduce 3G/LTE energy consumption without appreciably degrading application performance or introducing a significant amount of signaling overhead on the network. Unlike currently deployed methods

---

[2]https://support.google.com/nexus/answer/3467463?hl=en&ref_topic=3415523

[3]http://www.intomobile.com/2008/07/23/extend-your-iphone-3gs-battery-life/

[4]An HTC G1 phone connected to a power monitor [43], with only one application running, at one indoor location.
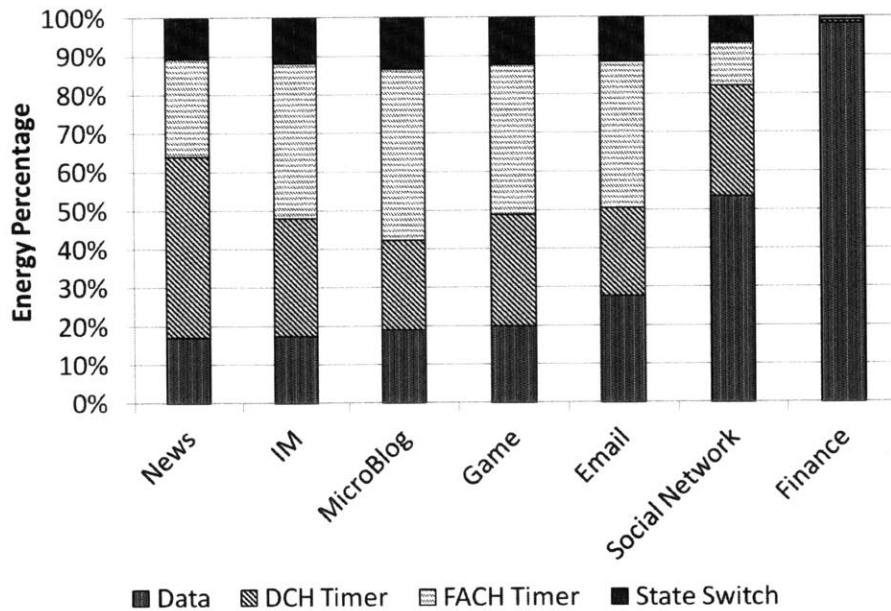
Figure 4-1: Energy consumed by the 3G interface. "Data" corresponds to a data transmission; "DCH Timer" and "FACH Timer" are each the energy consumed with the radio in the idle states specified by the two timers, and "State Switch" is the energy consumed in switching states. These timers and state switches are described in §4.2.

that simply switch between radio states after fixed time intervals—an approach known to be rather crude and sub-optimal [81, 15, 40, 66])— our approach is to observe network traffic activity on the mobile device and switch between the different radio states by adapting to the workload.

The key idea is that by observing network traffic activity, a *control module* on the mobile device can adapt the 3G/LTE radio state transitions to the workload. We apply statistical machine learning techniques to predict network activity and make transitions that are suggested by the statistical models. This approach is well-suited to the emerging *fast dormancy* mechanism [3, 4] that allows a radio to rapidly move between the Active and Idle states and vice versa. Our goal is to reduce the energy consumed by networked background applications on mobile devices.

4.2 Background

This section describes the 3G/LTE state machine and its energy consumption.

4.2.1 3G/LTE State Machine

The Radio Resource Control (RRC) protocol, which is part of the 3GPP standard, incorporates the state machine for energy management shown in Figure 4-2.

(a) 3G RRC.   (b) LTE RRC.
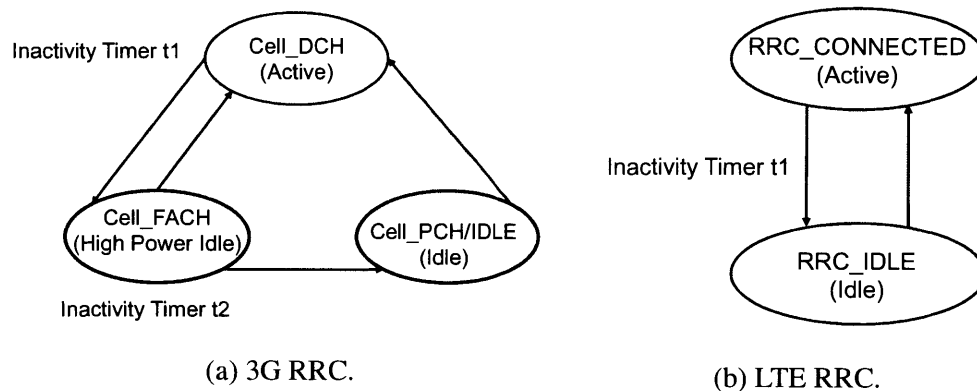
Figure 4-2: Radio Resource Control (RRC) State Machine.

The base station maintains two inactivity timers, t_1 and t_2, for each mobile device. For a device maintaining a dedicated channel in the "Active" (Cell_DCH) state with the base station, if the base station sees no data activity to or from the device for t_1 seconds, it will switch the device from the dedicated channel to a shared low-speed channel, transitioning the device to the "High-power Idle" (Cell_FACH) state. This state consumes less power than Active does but still consumes a non-negligible amount of power. If there is no further data activity between the device and base station for another t_2 seconds, the base station will turn the device to either the Cell_PCH or IDLE state. We refer to the Cell_PCH and IDLE states together as the "Idle" state because the device consumes essentially no power in either state. For LTE networks (Figure 4-2b), there are only two states: RRC_CONNECTED and RRC_IDLE (there are substates in RRC_CONNECTED [34], which we do not discuss here because they are not relevant), and one inactivity timer, shown as t_1.

The inactivity timers (t_1 and t_2) are useful because a state transition from Idle to Active

(Cell_DCH) incurs significant delays. For example, in our measurements in the Boston area (measured in September 2011), these values are $\approx$ 1.4 seconds on AT&T's 3G network, $\approx$ 3.6 seconds on T-Mobile's 3G network, $\approx$ 2.0 seconds on Sprint's 3G network, $\approx$ 1.0 second on Sprint's LTE network, $\approx$ 1.2 seconds on Verizon's 3G network, and $\approx$ 0.6 seconds on Verizon's LTE network (these numbers may vary across different regions). Each state transition also consumes energy on the device and incurs signaling overhead for the base station to allocate a dedicated channel to the device. The inactivity timers also prevent the base station from frequently releasing and re-allocating channels to devices, which causes per-packet delay for the device to be high.

The description given above captures the salient features of the 3GPP standard. Another popular 3G standard is 3GPP2 [5]. Although 3GPP2 networks use different techniques, from the perspective of energy consumption, they are essentially identical to 3GPP [81]; like 3GPP, 3GPP2 networks also have different power levels for different states on the device side and use similar inactivity timers for state transitions. For concreteness, in this paper, we focus on 3GPP networks.

4.2.2 Energy Consumption

We measured the power consumption and inactivity timer values using the Monsoon Power Monitor [43]. Figure 4-3 shows graphs of our measurements during a radio state switches cycle on an HTC Vivid smartphone in AT&T's 3G network and on a Galaxy Nexus smartphone in Verizon's LTE network. (We show results for other carriers in §4.6.) During the High-power Idle (FACH for AT&T) and part of Active (DCH for AT&T, RRC_CONNECTED for Verizon) states, there is no data transmission. The RRC state machine keeps the radio on here in case a new transmission or reception occurs in the near future. Consistent with previous work [15], we use the term *tail* to refer to this duration when the radio is on but there is no data transmission.

We measured the inactivity timer values in AT&T's 3G network in the Boston area to be $t_1 \approx$ 6.2 seconds and $t_2 \approx$ 10.4 seconds. The energy consumed at the end of a data transfer when the radio is in one of the two Idle states before turning off is termed the *tail energy*;
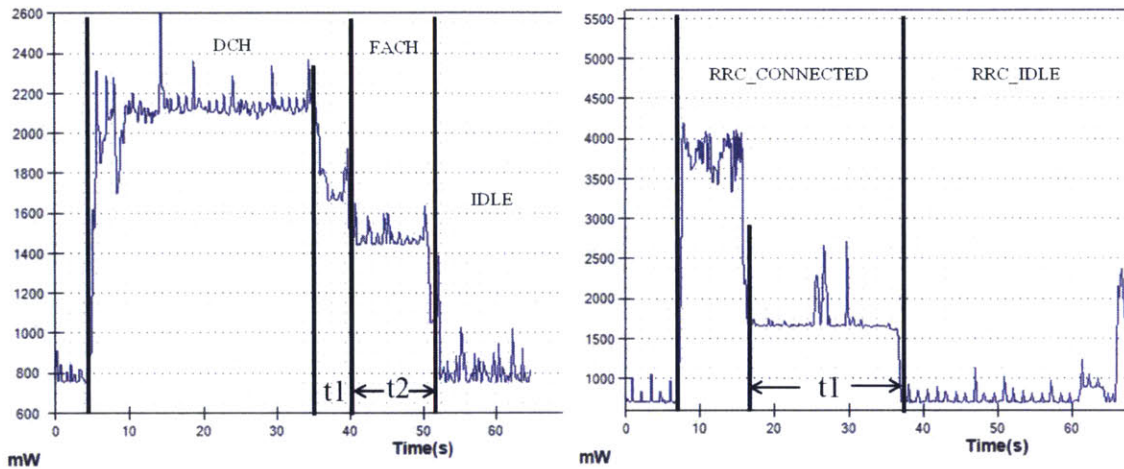
(a) HTC Vivid in AT&T 3G Network.
(b) Galaxy Nexus in Verizon LTE Network.

Figure 4-3: The measured power consumption of the different RRC states. Exact values can be found in Table 4.2. In these figures the power level for IDLE/RRC_IDLE is non-zero because of the CPU and LED screen power consumption.

this energy can be 60% or more of the total energy consumption of 3G [15].

3GPP Release 7 [3] proposed a feature called *fast dormancy*, which allows the device to actively release the channel by itself before the inactivity timer times out on the base station. One of the issues that then arises is that the base station loses control over the connection when mobile devices are able to disconnect by themselves. In 3GPP Release 8 [4], fast dormancy was changed: The mobile device first sends a fast dormancy request, and the base station will decide to release the channel or not. In Europe, Nokia Siemens Networks has applied Network Controlled Fast Dormancy based on 3GPP Release 8 [30]. Because it is not entirely clear what policy any given network carrier will use to decide whether to release the channel upon receiving a request at a base station, in our simplified model, we assume that if the base station is running 3GPP Release 8, whenever the phone sends a fast dormancy request to the base station, the base station will accept and release the channel. Our goal is to evaluate the network signaling overhead of such a strategy as a way to help inform network-carrier policy.

104

4.3 Design

The key insight in our approach to reduce 3G energy consumption is that by observing and adapting to network activity, a *control module* can predict when to put the radio into its Idle state and when to move from Idle to Active state. These state transitions take a nontrivial amount of time—between 1 and 3 seconds—and also add signaling overhead because each transition is accompanied by a few messages between the device and the base station. Hence, the intuition in our approach is to predict the occurrence of *bursts* of network activity so that the control module can put the radio into the Idle mode when it believes a burst has ended, which means there will not be any more traffic in the future for a relatively long period of time. Conversely, the idea is to put the radio in active mode when "enough" bursts of traffic accumulate.

To achieve the prediction, our approach needs to observe network activity and be able to pause data transmissions. To make our approach work with existing applications, we should not require any change to the application code. To achieve these goals, we modified the socket layer and added a control module inside the Android OS source code.

Our system has two software modules: one that modifies the library used by applications to communicate with the socket layer and another that implements the control module, as shown in Figure 4-4. The first module informs the control module of all socket calls; in response, the control module configures the state of the radio. The fast dormancy interface is shown as a dashed module because our system uses it if it is available.

The control module implements two different methods. The first method, called MakeIdle, runs when the radio is in the Active state (Cell_DCH or RRC_CONNECTED) and determines when the radio should be put into the Idle (IDLE or Cell_PCH or RRC_IDLE) state. The second method, called MakeActive, runs when the radio is in the Idle state. In this state, it cannot send any packets without first moving to the Active state; MakeActive determines how long the radio should be idle before moving to the Active state.
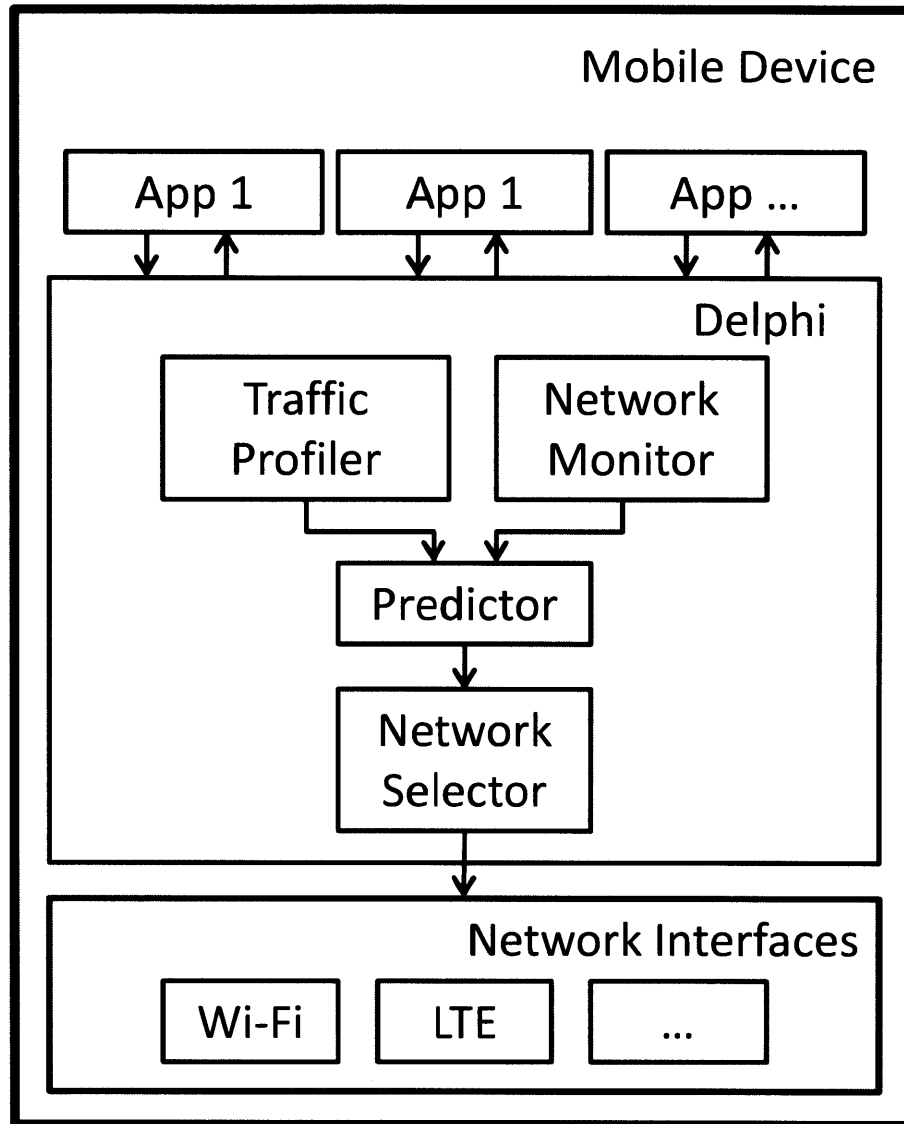
Figure 4-4: System design.

4.4 MakeIdle Algorithm

Instead of using a fixed inactivity timer, the MakeIdle method dynamically decides when to put the radio into Idle mode after each packet transmission or reception. We first show in §4.4.1 how to compute the optimal decision *given* complete knowledge of a packet trace. The result is that the radio should be turned to Idle if there is a gap of more than a certain threshold amount of time in the trace, which depends on measurable parameters. Then, in §4.4.2, we develop an online method to predict idle durations that will exceed this threshold

by modeling the idle time using a conditional probability distribution.

4.4.1   Optimal Decision From Offline Trace Analysis

Suppose we are given a packet trace containing the timestamps of packets sent and received on a mobile device. Our goal is to determine offline when to turn the radio to the Idle state to minimize the energy consumed.
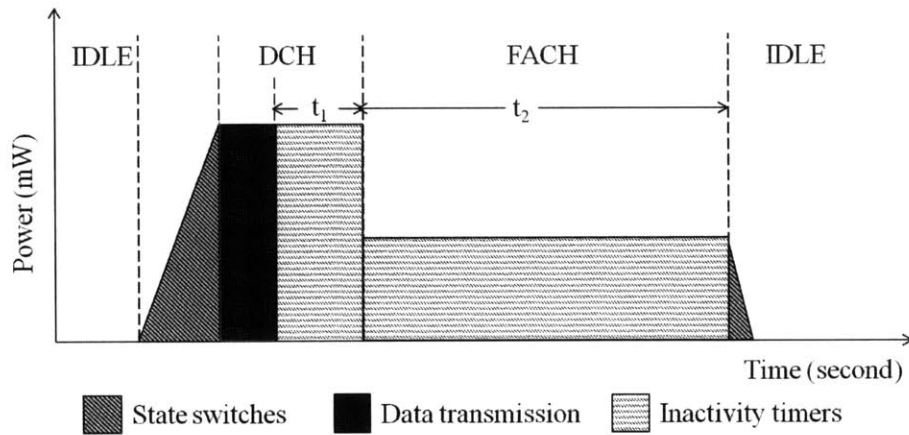
Figure 4-5:   Simplified power model for 3G energy consumption (for an LTE model, t_2 equals to zero).

Figure 4-5 shows a simplified power model we use to calculate tail energy. If the inter-arrival time between two adjacent packets is t seconds, then $E(t)$, the energy consumed by the current RRC protocol with inactivity timer values t_1 and t_2 (see Figure 4-2), is

$$E(t) = \begin{cases} t \cdot P_{t_1} & 0 < t \leq t_1 \\ t_1 \cdot P_{t_1} + (t - t_1) \cdot P_{t_2} & t_1 < t \leq t_1 + t_2 \\ t_1 \cdot P_{t_1} + t_2 \cdot P_{t_2} + E_{switch} & t > t_1 + t_2 \end{cases}$$

Here, P_{t_1} and P_{t_2} are the power values for the Active state and High-power Idle state, respectively; the power consumed in the Low-power Idle state is negligible. E_{switch} is the energy consumed by switching the radio to Idle mode after the first packet transmission and then switching it back to Active for the second packet transmission. It is a fixed value for a given type of mobile device and is easy to measure. On the other hand, if the radio

switches to Idle mode immediately after the first packet transmission finishes, the energy consumed is just E_{switch}.
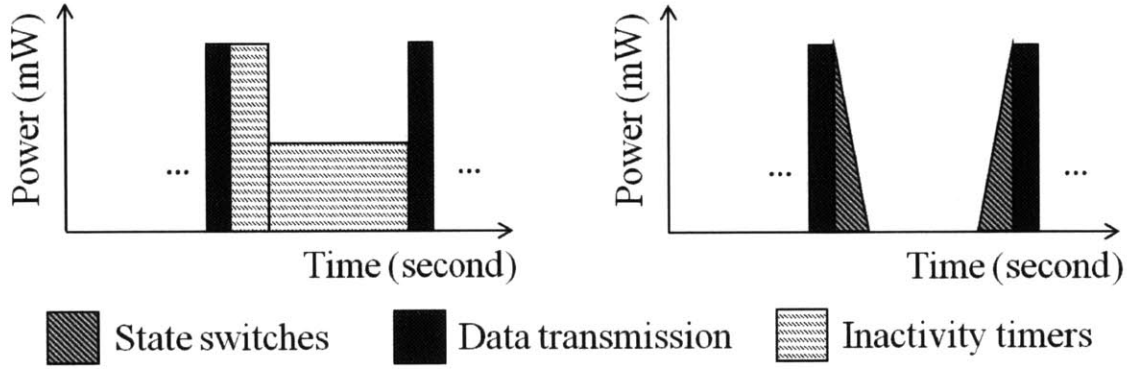
Figure 4-6: If the energy consumed by the picture on the right is less than the one on the left, then turning the radio to Idle soon after the first transmission will consume less energy than leaving it on. The energy is easily calculated by integrating the power profiles over time.

To minimize the energy consumed between packets, the radio should switch to Idle mode after a packet transmission if, and only if, $E_{switch} < E(t)$. Notice that because $E(t)$ is a monotonically non-decreasing function of t, there exists a value for t, which we call $t_{threshold}$, for which $E_{switch} < E(t)$ if and only if $t > t_{threshold}$. This expression quantifies the intuitive idea that after each packet, the radio should switch to Idle mode only if we know that next packet will not arrive soon: concretely, not arrive in the following $t_{threshold}$ seconds. For example, on an HTC Vivid phone in the AT&T 3G network deployed in the Boston area, $t_{threshold}$ works out to be 1.2 seconds.

4.4.2 Online Prediction

To minimize energy consumption in practice, we need to predict whether the next packet will arrive (to be received or to be sent) within $t_{threshold}$ seconds. Of course, we would like to make this prediction as quickly as possible, because we would then be able to switch the radio to Idle mode promptly. We make this prediction by assuming that the packet inter-arrival distribution observed in the recent past will hold in the near future. After each packet, the method waits for a short period of time and sees whether any more packets

arrive. If a packet arrives, the method resets and waits, but if not, it means a transfer may be finished and the radio should switch to Idle mode.

The strategy works as follows:

1. Without loss of generality, suppose the current time is $t = 0$. Compute the conditional probability that no packet will arrive within $t_{wait} + t_{threshold}$ seconds, *given that* no packet has arrived in t_{wait} seconds.

$$P(t_{wait}) = \mathbb{P}(\text{no packet in } t_{wait} + t_{threshold} | \text{no packet in } t_{wait})$$

This conditional distribution is easy to compute given observations of the packet arrival times of the last several packets.

From the traces we collected, we observed that $P(t_{wait})$ increases as t_{wait} increases, when t_{wait} is in the range of $[0, t_{threshold}]$ (if t_{wait} is greater than $t_{threshold}$, it means the radio has been idle for too long a time after the packet transmission, and there is not much room for energy saving). This property implies that the longer the radio waits and sees no packet, the higher the likelihood that no packet will arrive soon.

2. Now we need to find t_{wait} in order to make the likelihood "high enough". During t_{wait}, the radio consumes energy, so to decide how much is high enough, we should take energy consumption into account. Our answer is: $P(t_{wait})$ *is high enough if the expected energy consumption of waiting for t_{wait} and then switching states is less than the expected consumption of waiting for the inactivity timer to time out in the next t_{wait} seconds.*

The method determines t_{wait} by *minimizing* the expected energy consumption across all possible values of t_{wait} and taking the value that minimizes the consumption. We explain how below.

The expected energy consumption of waiting for t_{wait} and then switching states is:

$$\mathbb{E}[E_{wait\_switch}] = [E_{switch} + E(t_{wait})]$$

Here, $E(t_{wait})$ is the energy consumed by waiting for t_{wait} seconds, and E_{switch} is the

109

energy consumed by state switches.

The expected energy consumption of waiting for the inactivity timer to time out is:

$$\mathbb{E}[E_{no\_switch}] = \int_{t=0}^{t_1+t_2} \mathbb{P}(inter\_arrival\_time = t)\frac{dE(t)}{dt}dt$$

(4.1)

The following expression now is a function of t_{wait}:

$$f(t_{wait}) = \mathbb{E}[E_{no\_switch}] - \mathbb{E}[E_{wait\_switch}].$$

(4.2)

The best t_{wait} is the one that maximize $f(t_{wait})$, which means that the corresponding value for t_{wait} gives us the highest expected gains over the current RRC protocol.

In implementing this algorithm, we take the latest n packets (we discuss how to choose n in § 4.6.3) that the control module has seen to construct the inter-arrival distribution. As new packets are seen, the "window" of the n packet slides forward, and the distribution is adjusted accordingly.

4.5 MakeActive Algorithm

MakeIdle reduces the 3G wireless energy consumption by switching the radio to Idle mode frequently. Figure 4-7 (top) shows that MakeIdle may bring more state switches from Idle to Active and from Active to Idle. These switches cause signaling overhead at the base station. One idea to reduce the signaling overhead is to "shift" the traffic bursts in order to combine several traffic bursts together [66, 15], as shown in Figure 4-7(middle and bottom chart). The longer earlier bursts are delayed, the more bursts we can accumulate, and the fewer state switches occur.

In this section, we consider only those background applications for which one can delay the traffic for a few seconds without appreciably degrading the user's experience, not interactive applications where delaying by a few seconds is unacceptable. Our approach differs from previous work [66, 15], where the authors aim to reduce energy consumption

110
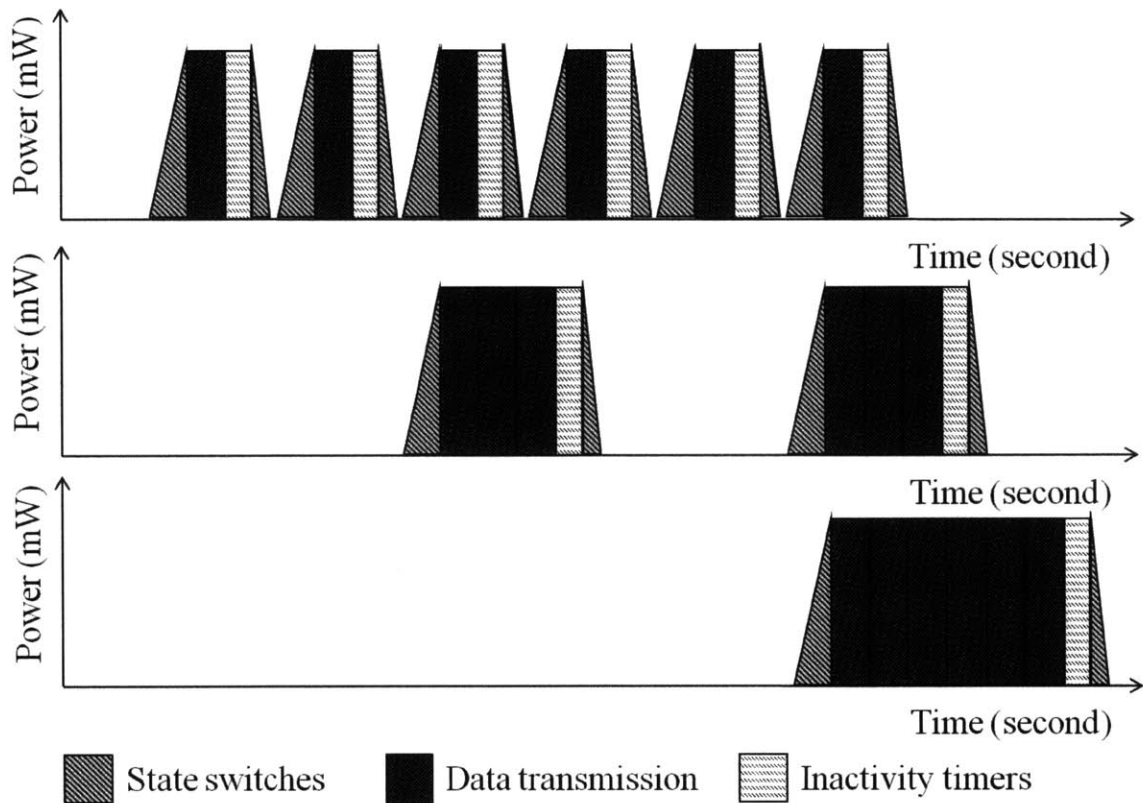
Figure 4-7: "Shift" traffic to reduce number of state switches.

by batching bursts of traffic together so that they can share the tail energy. By contrast, because the MakeIdle algorithm already reduces energy by turning the radio to the Idle mode, MakeActive focuses on reducing the number of state switches to a level comparable to the status quo. As a result, the amount of delay introduced by this method should be much smaller than in previous work.

We first consider a relatively straightforward scheme in which the start of a session (i.e., a burst of packets) can be delayed by at most a certain maximum delay bound, T_{fix_delay}. We then apply a machine learning algorithm, which induces the same number of state switches as the fixed delay bound method but in addition reduces the delay for each traffic burst. Our contribution lies in the application of this algorithm to learn idle durations for the radio, balancing signaling overhead and increased traffic latency.

4.5.1 Fixed Delay Bound

A simple strawman is to set a fixed delay bound, T_{fix_delay}. When the radio is in Idle state, and a socket tries to start a new session at current time t, and no other such requests are pending, the control module decides to delay turning the radio to Active mode until $t + T_{fix\_delay}$ so that other new sessions that might come between time t and $t + T_{fix\_delay}$ will all get buffered and will start together at time $t + T_{fix\_delay}$. There is a trade-off between the delay bound and the number of sessions that can be buffered. Note that once a session begins, its packets do not get further delayed, which means that TCP dynamics should not be affected by this method.

In the current RRC protocol, the inactivity timers t_1 and t_2 guarantee that after each traffic burst, any new burst that comes within $t_1 + t_2$ will not introduce extra state switches between Idle and Active. So in our implementation, we make $T_{fix\_delay} = k \times (t_1 + t_2)$ where k is the average number of bursts during each of the radio's active periods.

4.5.2 Learning Algorithm

The problem with a fixed delay bound is that it does not adapt to the traffic pattern. Every time the delay is triggered, the first transmission may incur a delay of as long as T_{fix_delay}. We show in the evaluation that a large portion of the traffic bursts get delayed by T_{fix_delay}. However, waiting as long as T_{fix_delay} may be overkill; as data accumulates (especially from different sessions), there comes a point when the radio should switch to Active and send data before this delay elapses, which will reduce the expected session delay while still saving energy.

We apply the *bank of experts* machine learning algorithm [44, 47]. Each "expert" proposes a *fixed* value for the session delay. In each iteration (each time the radio is in Idle mode and a transmission occurs), we computed a weighted average value from the experts and updated the weights according to a *loss function*. The process to update each expert's weight is a standard machine learning process, detailed in the Appendix.

The loss function is a crucial component of the scheme and depends on the details of the problem to which the learning is applied. Because our goal is to reduce number of state

switches by batching, in addition to the delay, the loss function should express the trade-off between the total time delayed for all the buffered sessions and the number of sessions buffered. The following equation captures this tradeoff:

$$L(i) = \gamma Delay(T_i) + \frac{1}{b}, \gamma > 0$$

Here, γ is a constant scaling parameter between the two parts of the loss function (we chose 0.008 in our implementation because it gave the best energy-saving results among the values we tried). $Delay(T_i)$ is the aggregate time delayed over b sessions, if we choose expert i; b is the number of sessions currently buffered, which is equivalent to the number of state switches avoided. The $1/b$ term ensures that as the number of buffered sessions increases, the value of this part of the loss function reduces, while the other term $\gamma Delay(T_i)$ may increase.

Let t_j be the arrival time of the jth session. Then,

$$Delay(T_i) = \sum_{j=1}^{b} T_i - t_j.$$

4.6 Evaluation

We evaluate MakeActive and MakeIdle using trace-driven simulation. We first describe the simulation setup. Then, we evaluate the two methods using traces collected from popular applications run by a few real users. Finally, we compare these methods across different cellular networks.

4.6.1 Simulation Setup

Energy model. One challenge in our simulations is to accurately estimate the energy consumed given a packet trace containing packet arrival times and packet lengths. Previous work [34] showed that for 3G/LTE, the value of the energy consumed per bit changes as the size of traffic bursts changes. Because our methods may change the size of the traffic bursts (e.g., MakeIdle may decide to switch the radio to Idle mode within a burst), we built

113

our energy model using the energy consumed per second, which is the power for sending or receiving data.

Network	Sending Power (mW)	Receiving Power (mW)
AT&T 3G	2,043	1,177
Verizon LTE	2,928	1,737

Table 4.1: Average power in mW measured on Galaxy Nexus in Verizon network. The energy consumed by CPU and screen is subtracted.

Table 4.1 shows the average power consumed when the phone is sending or receiving bulk data using UDP. Based on this value, we estimate the energy consumed within a traffic burst using the packet inter-arrival time and the packet direction (incoming/outgoing): For each packet reception, the energy consumed is the inter-arrival time multiplied by the average receive power, and similarly for each packet transmission.
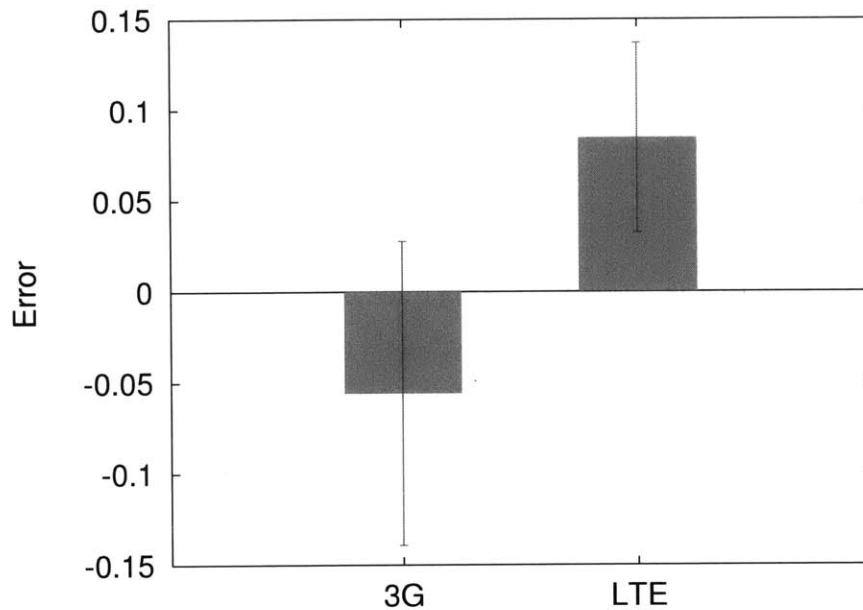
Figure 4-8: Simulation energy error for Verizon 3G and LTE networks.

To justify this method, we measured the smartphone's energy consumption when it was sending and receiving TCP bulk transfers of different lengths. Each experiment contains five runs. In each run, the phone sends and receives TCP bulk transfers of three lengths

(10 KBytes, 100 KBytes and 1000 KBytes) one after another, with a long-enough idle period between each transfer. We found that, on average, the error in the estimated energy consumption is within 10% or less of the true measured value.

One caveat in our energy model is that because fast dormancy is not yet supported on US 3G/LTE networks when we conducted this measurement, we were unable to accurately measure the delay to turn the radio from Active to Idle and the energy consumed. We believe, however, that one can approximate this value by measuring the delay and energy consumed in turning the data connection off on the phone. In practice, we expect the delay and energy of fast dormancy switching to be lower, so we model the turn-off energy and delay for fast dormancy to be 50% of the values measured while turning the radio off. We also evaluated our methods for reasonable fractions (10%, 20%, 40%) other than 50%, and found that the results did not change appreciably; hence, we believe that our conclusions are likely to hold if one were to implement the methods on a device that supports fast dormancy.

Trace data sets. We collected tcpdump traces on an HTC G1 phone running Android 2.2 for the seven different categories of applications listed below. For each category, we chose a popular application in the Android market. Each collected trace was 2 hours long. Most of these applications have the "always on" property in that they usually send or receive data over the network whenever they run, without necessarily requiring user input.

News: A news reader that has a background process running to fetch breaking news.

Instant Message (IM): An IM application that sends heartbeat packets to the server periodically, typically every 5 to 20 seconds.

Micro-blog: A micro-blog application, which automatically fetches new tweets without user input.

Game with ad bar: A game that can run offline but with an advertisement bar that changes the content roughly once per minute.

Email: This application is run mostly in the background, synchronizing with an email server every five minutes.

Social Network: A user using the social network application to read the news feeds, clicks to see pictures, and posts comments. When running in the background, this appli-

115

cation updates only every 30 minutes. We did not collect much background traffic from it. We used the foreground traffic trace for a comparison trace.

Finance: An application for monitoring the stock market, which updates roughly once per second when running in the foreground.

We also collected real user data from six different users using Nexus S phones in T-Mobile's 3G network and from four different users using Galaxy Nexus phones in Verizon's 3G/LTE network. All the phones ran `tcpdump` in the background. Across all users, we collected 28 days of data. For each user, the amount of data collected varies from two to five days.

4.6.2 Comparison of Energy Savings
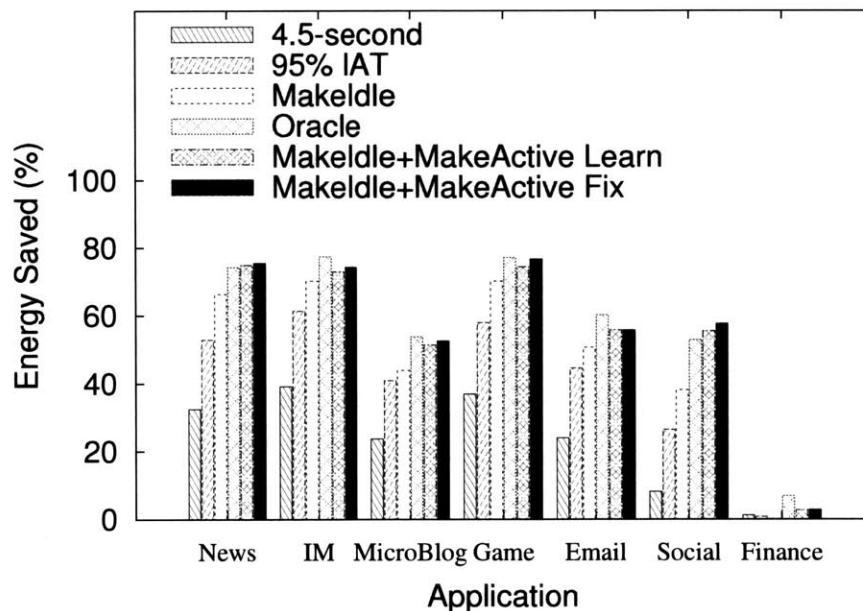
Figure 4-9: Energy savings for different applications. "4.5-second" sets the inactivity timer to 4.5 seconds. "95% IAT" uses the 95th percentile of packet inter-arrival time observed over the entire trace as the inactivity timer. "MakeIdle" shows the energy saved by our MakeIdle algorithm. "MakeIdle +MakeActive Learn" and "MakeIdle +MakeActive Fix" show the energy savings when running MakeIdle together with two different MakeActive algorithms: learning algorithm and fixed delay bound algorithm. Oracle shows the maximum achievable energy savings without delaying any traffic.
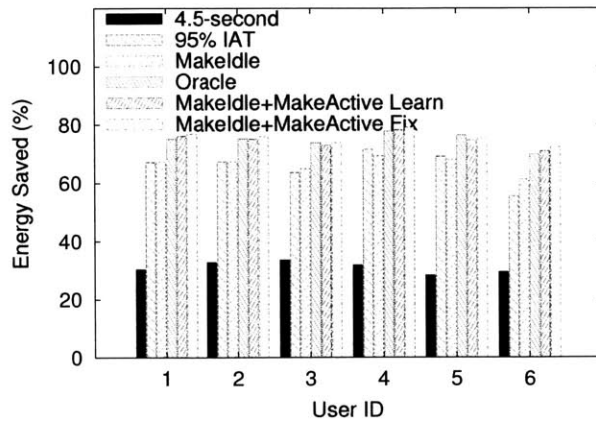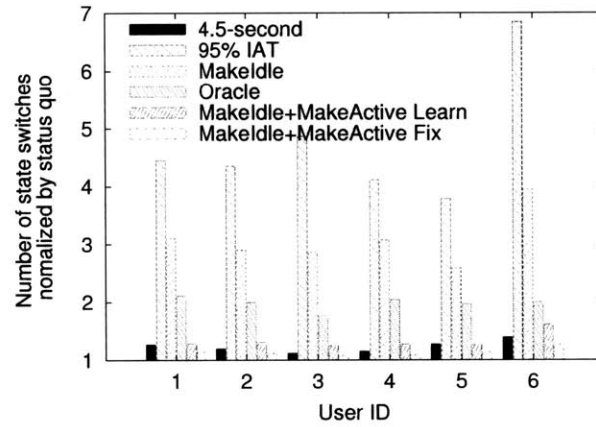
116

(a) Energy savings.

(b) Number of state switches normalized by status quo.
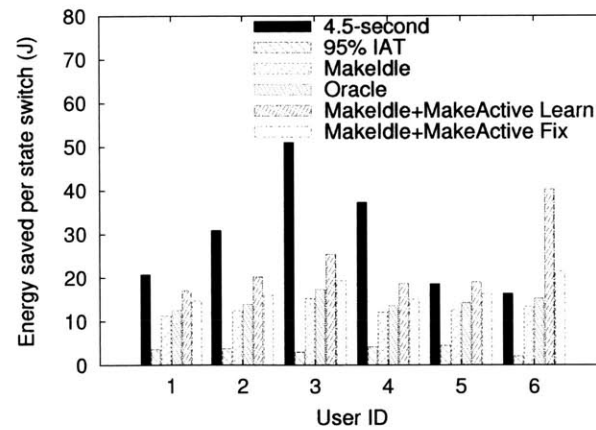
(c) Energy saved per state switch.

Figure 4-10: Energy savings and signaling overhead (number of state switches) across users in the Verizon 3G network.
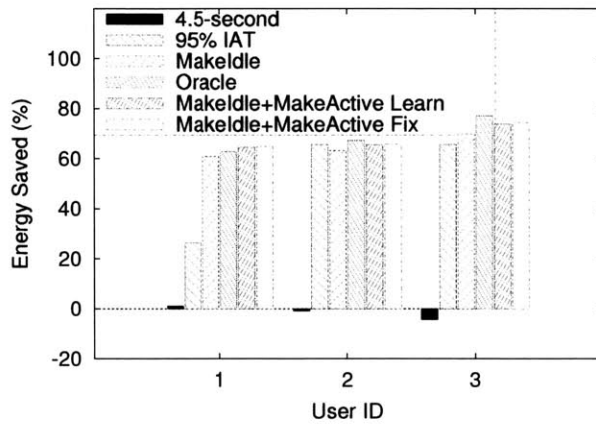
(a) Energy savings.
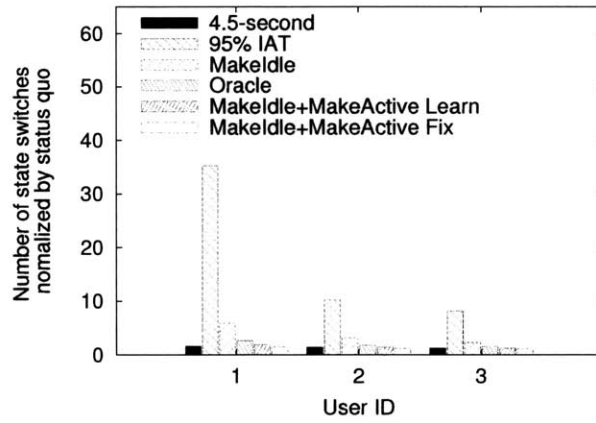
(b) Number of state switches normalized by status quo.
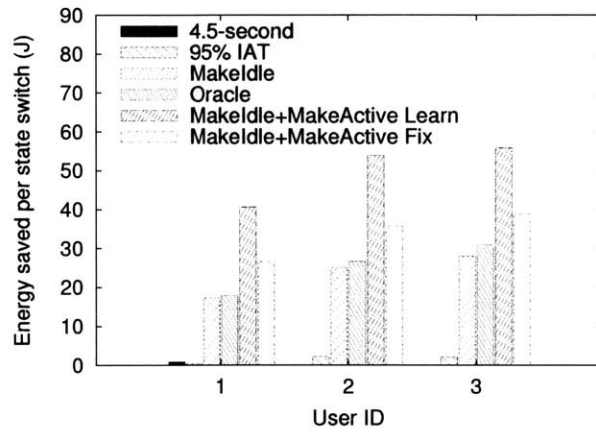
(c) Energy saved per state switch.

Figure 4-11: Energy savings and signaling overhead (number of state switches) across users in the Verizon LTE network.

We compared MakeIdle against MakeIdle together with MakeActive (shown as MakeIdle+MakeActive) and against two other schemes. The first other scheme is proposed in [29], in which a trace analysis found that 95% of the packet inter-arrival time values are smaller than 4.5 seconds. The proposal sets the inactivity timer to a fixed value, $t_1 + t_2 = 4.5$ seconds. We call this approach "4.5-second tail".

The second other scheme is that instead of using the value of 4.5 seconds, we drew the CDF of our traces and got the 95th percentile of packet inter-arrival time observed in each user's trace. We call this approach "95% IAT", which for the data shown in Figure 4-9 happened to be 1.67 seconds (the value does vary across users and also across applications). In our evaluation, we are granting this scheme significant leeway because we test the scheme over the same data on which it has been trained. Despite this advantage, we find that this scheme has significant limitations.

The "Oracle" is an algorithm in which the packet inter-arrival time is known before the packet comes, and the algorithm compares the inter-arrival time with the $t_{threshold}$ defined in §4.4.1. The Oracle scheme gives us an upper bound of how much energy can be saved without introducing extra delay. Our MakeIdle + MakeActive algorithm sometimes outperforms the Oracle because it can delay packets and further reduce the number of state switches.

Figure 4-9 shows that MakeIdle consistently achieves energy savings close to the Oracle scheme and outperforms the 4.5-second and 95% IAT schemes. When both MakeIdle and MakeActive are combined, the savings are greater.

The 95% IAT scheme gives little or negative savings for News and IM, while the other schemes provide significant positive savings. This is because the 95th percentile value of the inter-arrival time is highly variable and cannot guarantee savings in all situations. It is not a robust method.

Figures 4-10a and 4-11a show the estimated energy savings for each user in the Verizon 3G and Verizon LTE networks, respectively. In these results, the different schemes are as explained above, except that the 95% IAT scheme uses per-user (but not per-application) inter-arrival time CDFs. The gains of MakeIdle and MakeActive over the other schemes are substantial in most cases. In the LTE case, the 95% IAT scheme sometimes saves the most

energy (for user 2 and user 3), but it sometimes performs worse than MakeIdle (for user 1); it depends on the user, again showing a lack of robustness. Perhaps more importantly, the number of state switches is enormous compared to the other schemes, making it extremely unlikely to be useful in practice.

4.6.3 MakeIdle Evaluation

To understand why MakeIdle outperforms the other methods, we calculated the fraction of *false switches* and *missed switches* for each method. We used Oracle as ground truth and defined these ratios as follows:

$FalseSwitch(FalsePositive) = N_{FS}/(N_{FS} + N_{TN})$. Here, N_{FS} is the number of cases in which the algorithm switches the radio to Idle but Oracle decides to keep the radio in Active mode. N_{TN} is the number of cases in which both Oracle and the algorithm decide to keep the radio Active.

$MissedSwitch(FalseNegative) = N_{MS}/(N_{MS} + N_{TP})$. Here, N_{MS} is the number of cases where the algorithm decides to keep the radio in the Active mode but Oracle switches the radio to Idle. N_{TP} is the number of cases where both Oracle and the algorithm switch the radio to Idle. A high missed switch value means the algorithm tends to keep the radio in Active mode, which may not be energy efficient.

Figure 4-12 shows these two ratios for different data sets. Note that these values for MakeIdle are much smaller than for the other two algorithms.

Figure 4-13 shows the false positive and false negative rates (in percentage) as a function of the number of recent packets used to construct the distribution defined in §4.4.2. We found that the false negative rate is relatively constant, while the false positive rate decreases as the window size increases. For all the other results shown in §4.6, we used $n = 100$.

Another factor that affects battery consumption is the waiting time between a packet arrival and the time at which the algorithm actually switches the radio to Idle. For the 4.5-second tail scheme, the waiting time is always 4.5 seconds. Similarly, the waiting time for 95% IAT is 0.85 seconds for 3G and 0.01 seconds for LTE. In contrast, MakeIdle chooses
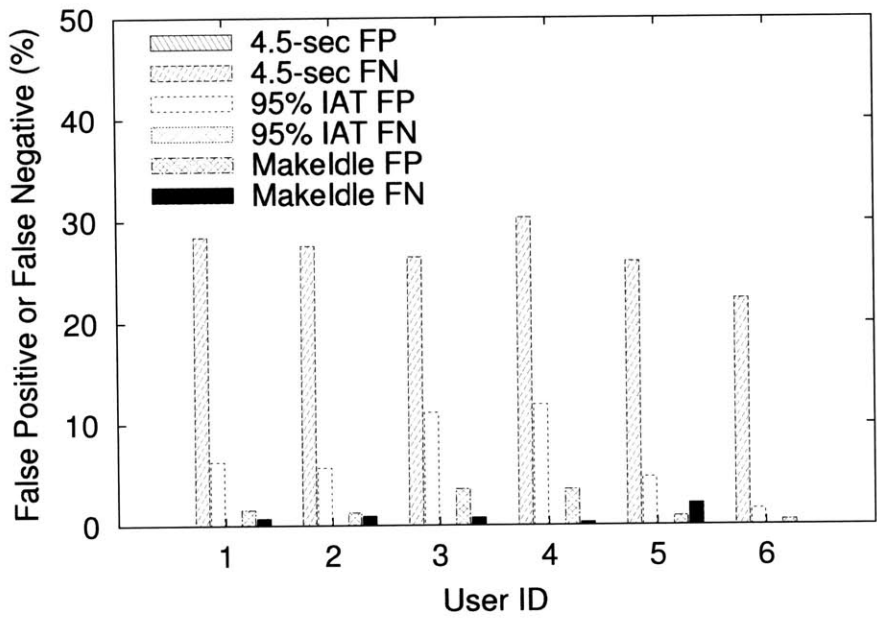
(a) Verizon 3G.
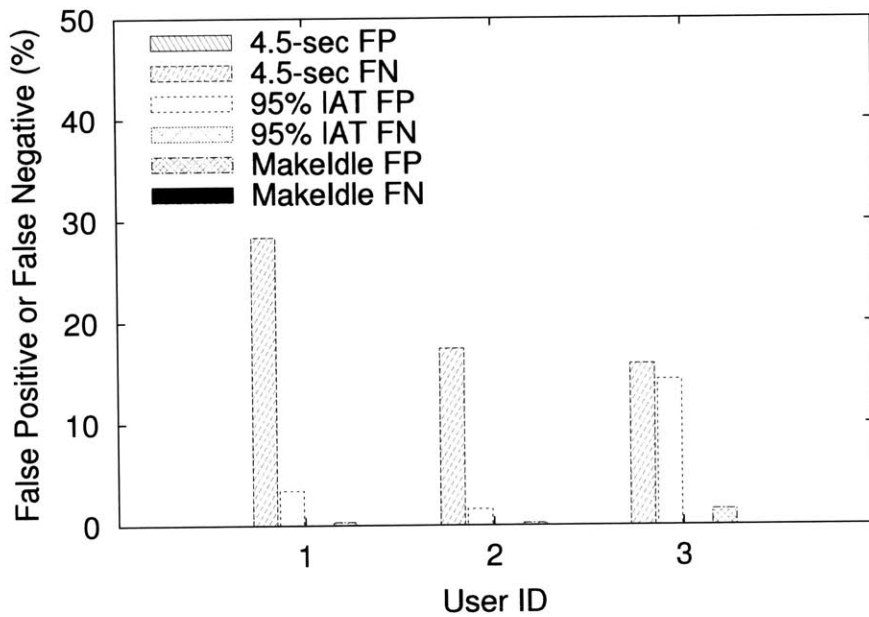
(b) Verizon LTE.

Figure 4-12: False ("FP" short for false positive) and missed switches ("FN" short for false negative).

the waiting time dynamically, achieving better gains. Figure 4-14 shows an example of waiting time changes in a user's trace in Verizon 3G network.
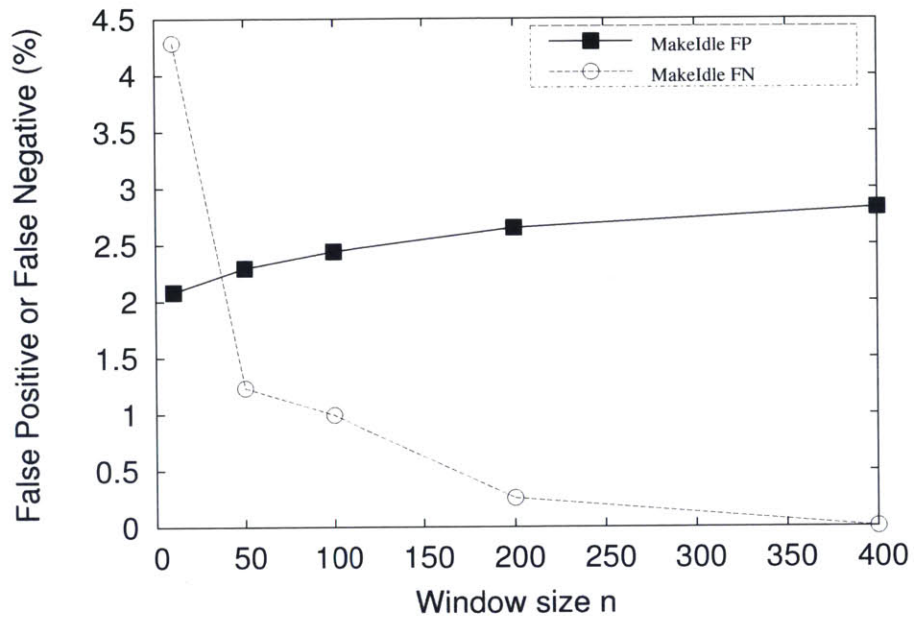
Figure 4-13: False ("FP") and missed switches ("FN") changes as the number of packets used to construct distribution (defined in § 4.4.2) changes.
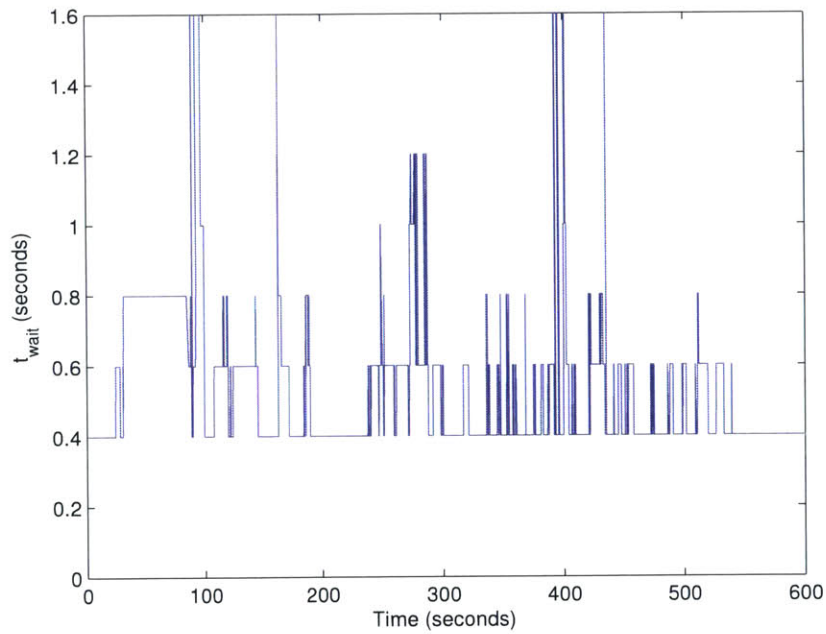
Figure 4-14: Waiting time changes in MakeIdle.

4.6.4 MakeActive Evaluation

Although shortening t_{wait} with the MakeIdle algorithm saves considerable amounts of energy, it may bring about more state switches between the Low-power Idle and Active states. But when there are multiple applications running at the same time, or when one application starts multiple connections, we can reduce the number of state switches by delaying the connections and batching them together using MakeActive.

Figures 4-10b and 4-11b show the number of state switches using different algorithms, normalized by the number measured in the status quo. Each user has several applications running on the phone. For MakeIdle only, in the 3G/LTE network, the number of state switches is at most four to five times higher than the status quo. For MakeIdle with MakeActive, either using the learning algorithm or the fixed-delay bound, the number of state switches is about the same as the status quo, meaning that by delaying traffic bursts, our algorithm can reduce the energy consumption without introducing any extra signaling overhead. Notice that for the 95% IAT algorithm in the LTE network, the number of state switches is as high as $35\times$ the status quo because the corresponding timer value is only 0.01 seconds. As a result, this method will always switch the radio to Idle even if there is only a small gap between packets. In a few cases, that does save energy, but at great expense.

In §4.5, we described both the fixed-delay bound and a learning algorithm. Figure 4-15 shows that using the learning algorithm reduces the average delay for each traffic burst by 50% compared to the fixed-delay bound, while both methods induce a comparable number of state switches (Figure 4-10b and Figure 4-11b). The learning algorithm is able to reduce the delay because the loss function (defined in §4.5.2) balances the tradeoff between the number of buffered bursts and the total delay. Figure 4-16 shows that due to the loss function, the algorithm will reduce the delay bound as the number of buffered bursts increase.

4.6.5 Different Carriers

To gain a better understanding on how different carriers' RRC state machine configurations affect the observed improvement, in this part of the evaluation we ran our trace-driven sim-
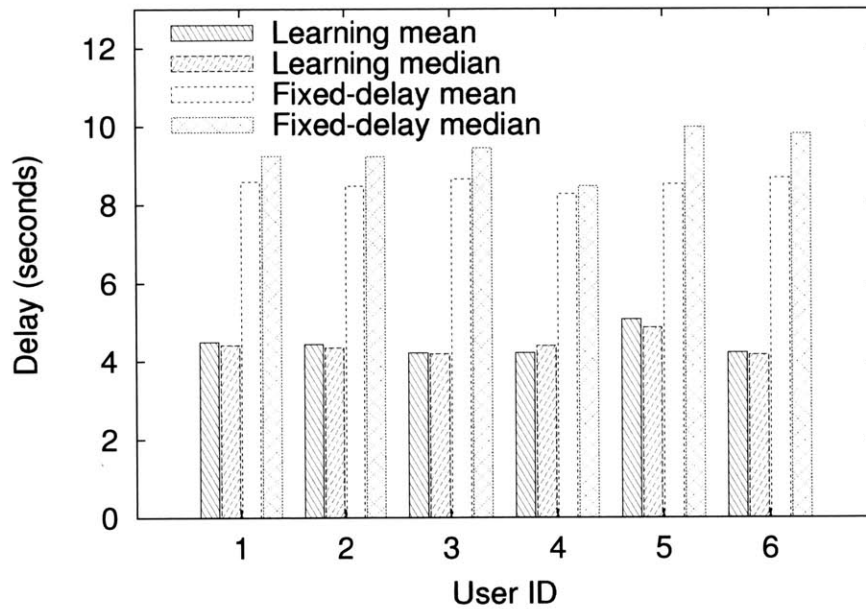
(a) Verizon 3G network.
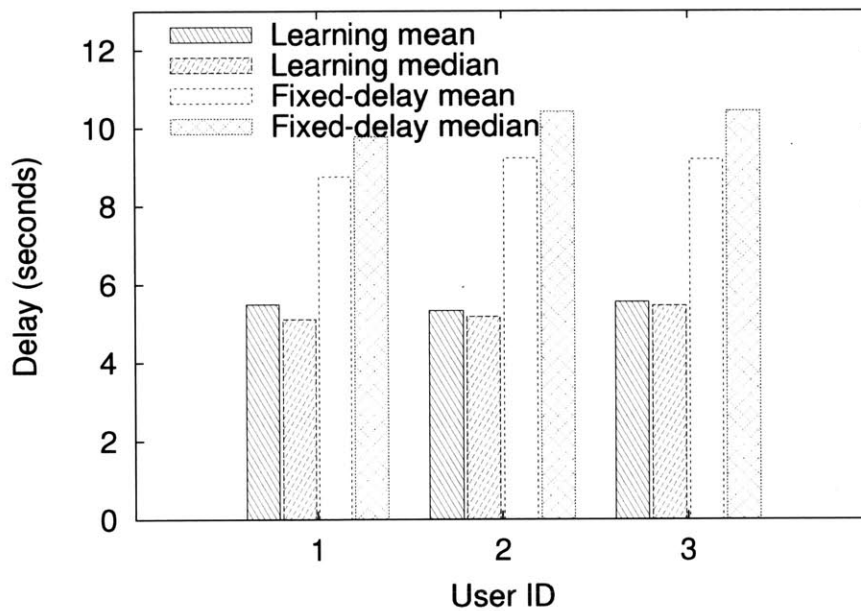
(b) Verizon LTE network.

Figure 4-15: Mean and median delays for traffic bursts using learning algorithm and fixed delay bound scheme.

ulation on different RRC profiles measured from the four major US carriers. In Table 4.2 we list the measured RRC parameters. There are two cases where the inactivity timer $t_2 = 0$
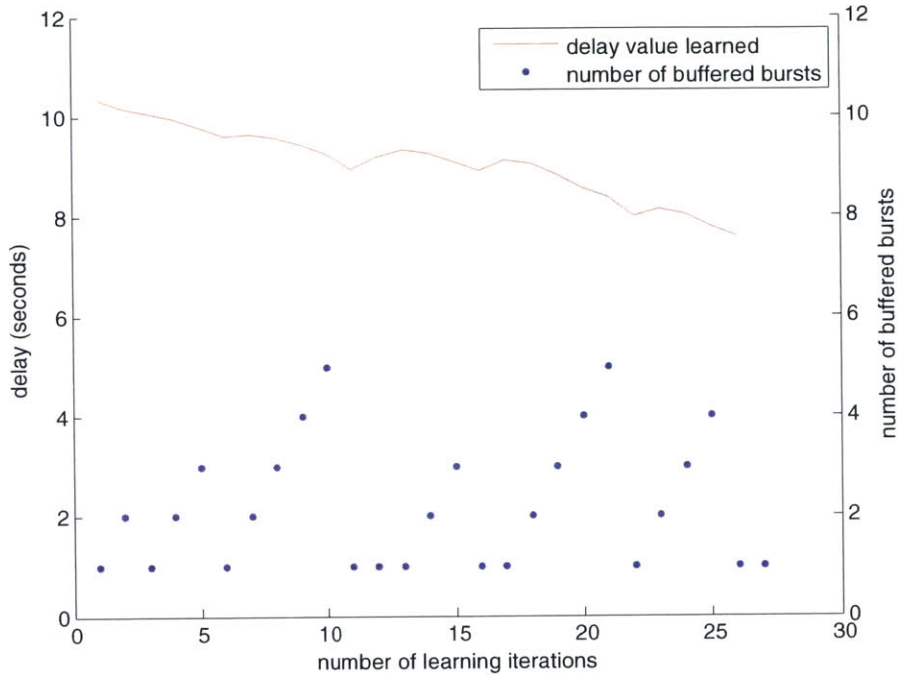
Figure 4-16: Delay value changes as the learning proceeds.

(effectively) because we cannot clearly distinguish t_1 and t_2 from the energy difference.

Network	P_{snd}	P_{rcv}	P_{t_1}	P_{t_2}	t_1	t_2
T-Mobile 3G	1,202	737	445	343	3.2	16.3
AT&T HSPA+	1,539	1,212	916	659	6.2	10.4
Verizon 3G	2,043	1,177	1,130	1,130	9.8	0
Verizon LTE	2,928	1,737	1,325	-	10.2	-

Table 4.2: Power and inactivity timer values for different networks. Power values are in mW; times are in seconds (measured in September 2011).

Network	Mean Delay	Median Delay
T-Mobile 3G	5.11	5.11
AT&T HSPA+	4.80	4.65
Verizon 3G	4.67	4.48
Verizon LTE	4.62	4.38

Table 4.3: The mean and median session delays brought by MakeIdle for different carriers (in seconds).

Figure 4-17 shows the percentage of energy saved compared to the status quo. Figure 4-18 shows the corresponding signaling overhead. We found that the MakeIdle+MakeActive

125
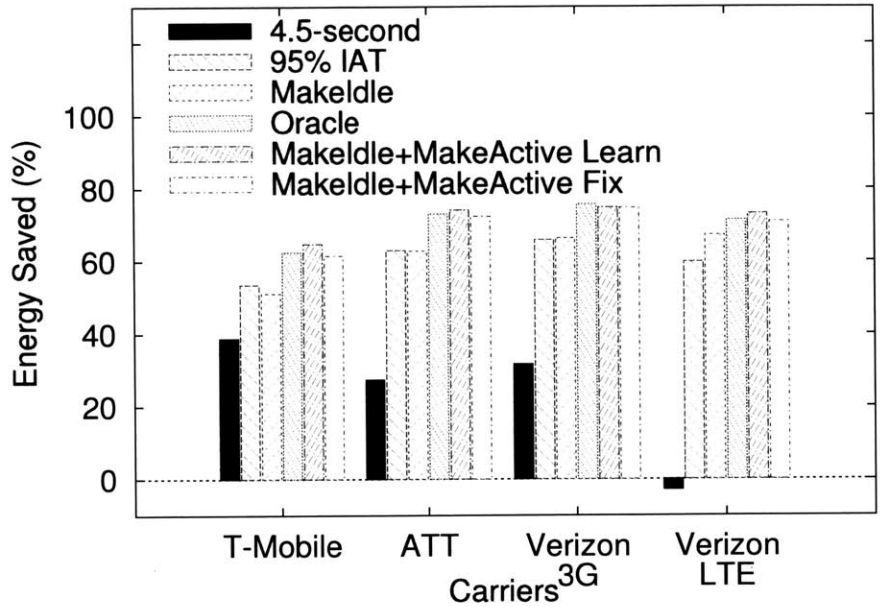
Figure 4-17: Energy saved for different carrier parameters using different methods. For MakeIdle, the maximum gain is 67% in the Verizon LTE network. For MakeIdle+MakeActive, the maximum gain is 75% achieved in Verizon 3G.
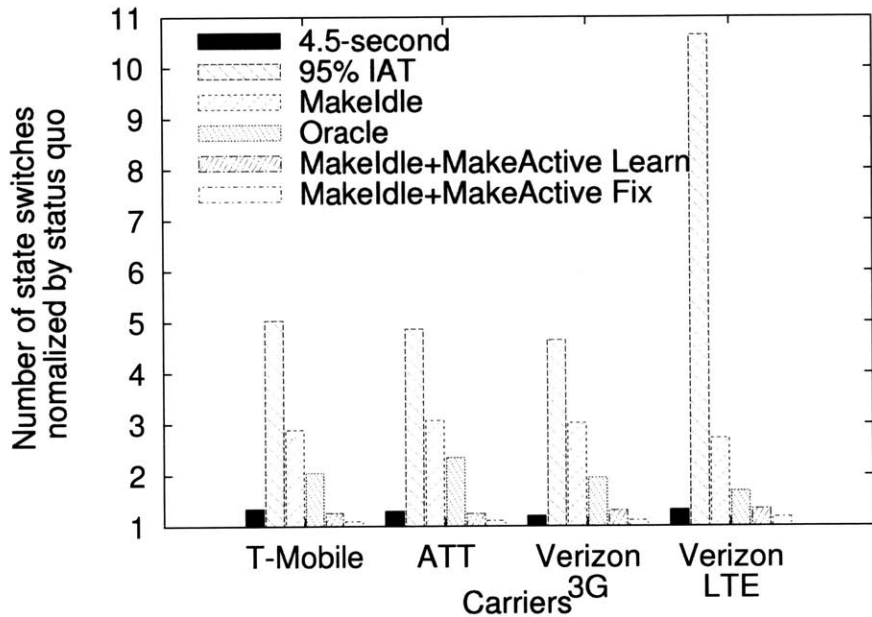
Figure 4-18: Number of state switches (signaling overhead) for different methods divided by number of state switches using the current inactivity timers.

method outperforms the 4.5-second tail method in all the carrier settings. Figure 4-18 shows the number of state switches (proportional to signaling overhead) of different schemes divided by the number of state switches without using any scheme.

The maximum signaling overhead for MakeIdle is less than $3.1\times$ the baseline where no fast dormancy is triggered. For MakeIdle+MakeActive, the signaling overhead reduces to only $1.33\times$ or less, a 62% reduction from the previous $3.1\times$, and is close to the signaling overhead of 4.5-second tail. The session delays brought by MakeActive are listed in Table 4.3.

In both Figures 4-17 and 4-18, the result shown as MakeIdle has no traffic batching, which corresponds to the case when all the traffic is treated as delay-sensitive, for example, web browsing. The MakeActive method is disabled in this case to make sure that the user's experience is not adversely affected. One possible method to decide when to disable MakeActive is for the control module to maintain a list of delay-sensitive or interactive applications; when any of these applications are running in the foreground, the system disables MakeActive.

Even without MakeActive, the reduction in energy consumption is still significant in all four carrier settings. The maximum gain is for Verizon LTE, where MakeIdle saves 67% energy over the status quo. With MakeIdle, the maximum gain is Verizon 3G, where the energy saving reaches 75%, and the corresponding median delay is 4.48 seconds.

4.6.6   Energy Overhead of Running Algorithms

To measure the energy overhead of running our methods, we implemented the algorithms on our test phones. We then generated traffic from the phones based on the user traces we collected. We ran the traffic generator with and without our methods enabled, ensuring that it generated the same traffic in all the experiments. We used the power monitor to measure the total energy consumed in both cases. The energy overhead for running our algorithm is 1.7% for AT&T HTC Vivid and 1.9% for Verizon Galaxy Nexus.

| (a) Periodic Ping | (b) Bulk (1 MByte) Download |
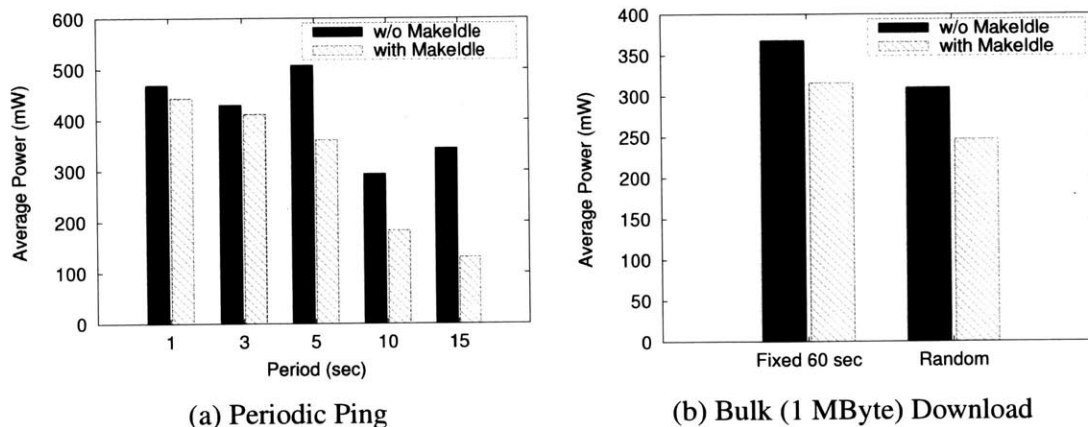
Figure 4-19: Average power level measured when a Sony Xperia phone was transferring data with and without MakeIdle enabled.

4.6.7 Implementation Results

Two years after our MakeIdle and MakeActive algorithms were developed, fast dormancy was enabled in the US and we implemented MakeIdle with the help of our industrial collaborator, Foxconn. To achieve better performance, we implemented our algorithm at the cellular driver layer, a non-open source part of the Android OS. We installed this modified driver on a Sony Xperia phone connected to AT&T 3G network. We measured the energy consumption when the phone transferred data with the following traffic patterns:

1. Periodic Ping with various periods,

2. Bulk (1 MByte) downloads with fixed idle interval between each two downloads, and

3. Bulk (1 MByte) downloads with random idle interval.

Figure 4-19 shows the average power level when the phone was transferring data with different patterns. To calculate the power level, we measured the amount of energy consumed during the transfer, average over the measuring time period. Thus, the energy overhead of algorithm computation is also included. For comparison, we also measured the average power level when the phone was loaded with the unmodified driver and was transferring data with the same traffic pattern. We find that for periodic ping traffic, MakeIdle can reduce energy consumption by up to 62% (period set to 15 seconds). For bulk download, the energy reductions are 15% for fixed 60-second idle interval and 20% for random idle interval.

128

4.7 Related Work

We divide related work into measurement studies of 3G energy consumption and approaches to reduce that energy, 3G usage profiling, and Wi-Fi power saving methods.

4.7.1 3G Energy Mitigation Strategies

Past work aimed at eliminating the tail energy falls into three categories: inactivity timer reconfiguration, tail cutting, and tail sharing.

Inactivity timer reconfiguration. Lee et al. [40] developed analytic models for energy consumption in WCDMA and CDMA2000 and showed that the inactivity timer should be dynamically configured. Falaki et al. [29] proposed an empirical method by plotting the CDF of packet inter-arrival times for traces collected on smartphones communicating over 3G radio over a long period of time (several days). They found that 95% of the packet inter-arrival time values are smaller than 4.5 seconds, and proposed setting the inactivity timer to a fixed value, $t_1 + t_2 = 4.5$ seconds. Our approach finds a dynamic inactivity timer value using traffic pattern information within a short period of time.

Tail cutting. Qian et al. [66] gave an algorithm, *TOP*, to help the device decide when to trigger fast dormancy based on the information provided by applications running on the device. Their algorithm requires the application to predict when the next packet will come and report it to the OS. This approach requires modifications to the applications, and it is not clear how each application should make these predictions. Our work requires no modification to the application code and does not require the application to predict its traffic.

Traffic batching. Balasubramanian et al. [15] propose an application-layer protocol, *TailEnder*, to coalesce separate data transfers by delaying some of them. For delay-tolerant applications such as email, TailEnder allows applications to set a deadline for the incoming transfer requests; they suggest and evaluate a relatively long delay of 10 minutes for such applications. For applications that can benefit from prefetching, TailEnder prefetches 10 web documents for each user query. Their design needs to re-implement the application and let each application propose its own delay tolerant timers, whereas our design is able

129

to "pause" the traffic transmission at the OS layer.

Liu et al. [41] proposed *TailTheft*, a traffic queuing and scheduling mechanism to batch traffic among different applications and share the tail energy among them. One idea of this work is to set up a timeout value for delay-tolerant transfers and transfer data when timeouts or other delay-sensitive transfers have triggered the radio to Active mode. Similar to *TailEnder*, they require the application to specify how much delay is acceptable.

Another traffic batching approach is prefetching. Qian et al. [65] proposed a prefetching algorithm for YouTube, which erases the tail between transfers of video pieces.

4.7.2 3G Resource Usage Profiling

Qian et al. [64] designed an algorithm to infer RRC state machine states using packet traces. The per-application analysis shows that some of the popular mobile applications have traffic patterns that are not energy-efficient, due to low bit-rate transmission, inefficient prefetching, and aggressive refresh.

4.7.3 Wi-Fi Power-Saving Algorithms

Much prior work has focused on Wi-Fi power-saving algorithms [38, 39, 69]. The problem in Wi-Fi networks is qualitatively different from 3G; in Wi-Fi, the time and energy consumed to transition between states is negligible; what is important is to dynamically determine the best sleep duration when the Wi-Fi radio is off. In this state, no packets can be delivered, but the access point will be able to buffer them; the problem is finding the longest sleep time that ensures that no packets are delayed (say, by a specified maximum delay). In the 3G context, changing the state of the radio consumes time, energy, and network signaling overhead, but there is no risk of receiving packets with excessive delay because the base station is able to notify a mobile device that packets are waiting for it even if the device is in Idle state. Thus, we cannot simply apply Wi-Fi power-saving algorithms to 3G networks. Also, machine learning algorithms have been applied to the 802.11 power saving mode configuration problem [46], but the problem setup is different for the 3G energy environment because of different tradeoffs we aim to balance.

4.7.4 Power-Saving for Processors

Though not directly related to the problem we address, previous work on processor power-saving has used a similar model to ours in which the different power states and transitions between different states are abstracted as a state machine [20]. Here, the power-saving mechanisms are categorized into static methods and adaptive methods, with the adaptive methods using a nonlinear regression over previous idle/active periods and knowledge of how successful previous power-saving decisions were.

4.8 Chapter Summary

3G/LTE energy consumption is widely recognized to be a significant problem [15]. We developed a system to reduce the energy consumption using knowledge of the network workload. In evaluating the methods on real usage data from nine users over 28 total days on four different carriers, we find that the energy savings range between 51% and 66% across the carriers for 3G, and is 67% on the Verizon LTE network. When allowing for delays of a few seconds (acceptable for background applications), the energy savings increase to between 62% and 75% for 3G, and 71% for LTE. The increased delays reduce the number of state switches to be the same as in current networks with existing inactivity timers.

The key idea in this chapter is to adapt the state of the radio to network traffic. To put the 66% saving (without any delays) or 75% saving (with delay) in perspective, we note that according to the Nexus 5 specifications, the reduction in lifetime from using the 3G radio is 10 hours; while it is not clear what application mix produces these numbers, one might speculate that saving 66% of the energy might correspond to an increase in lifetime by about 66% of 10 hours, or about 6.6 hours.

Chapter 5

Conclusion

We conclude the dissertation with a summary of our contributions and discussion of future work.

5.1 Contributions

This dissertation makes the following contributions:

1. Our measurement study analyzes the wireless network performance of mobile devices in the real world. This measurement study also demonstrates significant potential improvement if network selection is done properly.

2. The design and implementation of Delphi demonstrated a way to coordinate different concerns when making network interface selections. Inside Delphi, we employ machine learning methods to make network selections. The machine learning models are trained using network performance data we collected during the measurement study. As the wireless networks keep advancing, in the future, even the specific parameters we trained for the current solution, or even the machine learning algorithm, may not be applicable to make good network selections; however, our modular design makes sure that the algorithms can be easily replaced. Thus, as long as there are co-existing networks whose performances are not evenly distributed spatially or temporally, Delphi's framework can always be applicable.

3. Both our network selection and energy efficiency solutions require no modification

to the application running on the mobile devices. Thus, they can be easily deployed and improve the performance and user experience of millions of apps already in the app market.

5.2 Future Work

This dissertation opens up the following directions of future research directions:

Real-world Network Monitoring: As both Wi-Fi and cellular network technologies keep advancing, it is necessary to keep measuring and monitoring the network performance for end users. Also, as content distribution networks (CDN) are widely used, mobile devices are more likely to interact with servers that are geographically close to them. Thus, to reveal the end-to-end network performance, CDN-like measurement server networks should be deployed.

Network Performance Prediction: As we show in the dissertation, Delphi's improvement decreases when mobile devices enter new locations. One direction that can be further explored is to enhance Delphi's learning capability by using online learning or crowd-sourced learning mechanisms. This would allow mobile devices to make better network selection decisions when they enter locations for the first time. Also, applications could care about other metrics such as average per-packet delay, and tail per-packet delay or more app-centric metrics such as page-load time for web pages or minimizing the risk of a stall for streaming video. We view Delphi as a first step in answering these more involved questions. One direction of our future work is to provide expressive APIs for applications to express their specific needs to Delphi.

Appendix A

Bank of Experts

Here we show how *bank of experts* [44, 47] works. We bound the maximum delay to n seconds. Each expert "proposes" a delay value T_i:

$$T_i = i, \ i \in 1 \ldots n.$$

The output of the algorithm is the weighted average over all the experts:

$$T_t = \sum_{i=1}^{n} p_t(i) T_i$$

For each iteration of the updates, the algorithm calculates the probability of each possible hidden state (in our case, the identity of the expert) based on some observation y_t. Here, we can define the probability of predicting observation y_t as $P(y_t|T_i) = e^{-L(i,t)}$. The observation is the number of sessions we batched at time t, and $L(i,t)$ is the loss function. Then we can apply the following equation to get the weight $p_t(i)$:

$$p_t(i) = \frac{1}{Z_t} \sum_{j=1}^{n} p_{t-1}(j) e^{-L(j,t-1)} P(i|j, \alpha).$$

Here, Z_t is a normalization factor that makes sure $\sum_i p_t i = 1$. The $P(i|j, \alpha)$ shows the probability of switching between experts. There are different versions to solve this part. The one we chose [32] supports switching between the experts and is suitable for cases

135

where the observation may change rapidly, which matches the bursty character of network traffic. $P(i|j,\alpha)$ is defined as:

$$P(i|j,\alpha) = \begin{cases} (1-\alpha) & i = j \\ \frac{\alpha}{n-1} & i \neq j \end{cases}$$

$0 \leq \alpha \leq 1$ is a parameter that determines how quickly the algorithm changes the best experts. α close to 1 means the network condition changes rapidly and the best expert always changes. One problem with this algorithm is that it is hard to choose a good α. In reality, α should not be a fixed value since the network traffic pattern may change rapidly or remain stationary. We use a more adaptive algorithm, Learn-α [45, 47], to dynamically choose α.

The basic idea is to first assign m α-experts and use the algorithm above to learn the proper value of α in each iteration, and then use the up-to-date α to learn T_t [45, 47]. The final equation for this "two-layer learning" is:

$$T_t = \sum_{j=1}^{m} \sum_{i=1}^{n} p_t'(j) p_{t,j}(i) T_i \tag{A.1}$$

Here, $p_t'(j)$ is the weight for the jth α-expert, which is given by:

$$p_t'(j) = \frac{1}{Z_t} p_{t-1}'(j) e^{-L(\alpha_j, t-1)} \tag{A.2}$$

This equation shows that $p_t'(j)$ is updated from the previous value $p_{t-1}'(j)$; the initial values are: $p_1'(j) = 1/m$. $-L(\alpha_j, t-1)$ is the α loss function, defined as:

$$L(\alpha_j, t) = -\log \sum_{i=1}^{n} p_{t,j}(i) e^{-L(i,t)} \tag{A.3}$$

Here, $L(i,t)$ is the loss function, discussed in §4.5.2. t is the present time; the loss function value for the current iteration is calculated from information learned at time $t - 1$.

Bibliography

[1] IEEE P802.11ac. Specification Framework for TGac. IEEE 802.11-09/0992r21, 2011.

[2] LTE-Advanced.

[3] 3GPP Release 7: UE Fast Dormancy behavior, 2007. 3GPP discussion and decision notes R2-075251.

[4] 3GPP Release 8: 3GPP TS 25.331, 2008.

[5] Data Service Options for Spread Spread Spectrum Systems: Service Options 33 and 66, May 2006.

[6] Recognizing the User's Current Activity. http://developer.android.com/training/location/activity-recognition.html.

[7] AGARWAL, Y., PERING, T., WANT, R., AND GUPTA, R. SwitchR: Reducing System Power Consumption in a Multi-Client, Multi-Radio Environment. In *Wearable Computers* (2008).

[8] ios: Using airdrop. http://support.apple.com/kb/HT5887.

[9] Top Sites in United States. http://www.alexa.com/topsites/countries/US.

[10] ANANTHANARAYANAN, G., PADMANABHAN, V. N., RAVINDRANATH, L., AND THEKKATH, C. A. Combine: Leveraging the Power of Wireless Peers through Collaborative Downloading. In *MobiSys* (2007).

[11] ANANTHANARAYANAN, G., AND STOICA, I. Blue-Fi: Enhancing Wi-Fi Performance Using Bluetooth Signals. In *MobiSys* (2009).

[12] Android telephony manager api. http://developer.android.com/reference/android/telephony/TelephonyManager.html.

[13] BAHL, P., ADYA, A., PADHYE, J., AND WALMAN, A. Reconsidering Wireless Systems with Multiple Radios. *CCR* (2004).

[14] BALASUBRAMANIAN, N., BALASUBRAMANIAN, A., AND VENKATARAMANI, A. Energy Consumption in Mobile Phones: A Measurement Study and Implications for Network Applications. In *IMC* (2009).

[15] BALASUBRAMANIAN, N., BALASUBRAMANIAN, A., AND VENKATARAMANI, A. Energy Consumption in Mobile Phones: A Measurement Study and Implications for Network Applications. In *IMC* (2009).

[16] BALASUBRAMANIAN, N., BALASUBRAMANIAN, A., AND VENKATARAMANI, A. Energy Consumption in Mobile Phones: a Measurement Study and Implications for Network Applications. In *IMC* (2009).

[17] BARI, F., AND LEUNG, V. Automated Network Selection in a Heterogeneous Wireless Network Environment. *Network, IEEE* (2007).

[18] BARLOW-BIGNELL, J., DA SILVA, C., GJENGSET, J., AND OLIHA, P. Wireless Interference and Multipath TCPReducing 3G energy consumption on mobile devices, 2013.

[19] BARRÉ, S., PAASCH, C., AND BONAVENTURE, O. Multipath TCP: from Theory to Practice. In *NETWORKING 2011*. Springer, 2011, pp. 444–457.

[20] BENINI, L., BOGLIOLO, A., AND MICHELI, G. D. A Survey of Design Techniques for System-Level Dynamic Power Management. *Very Large Scale Integration (VLSI) Systems, IEEE Transactions on* (2000).

[21] CARTER, C., KRAVETS, R., AND TOURRILHES, J. Contact Networking: a Localized Mobility System. In *MobiSys* (2003).

[22] CHAKRABORTY, A., NAVDA, V., PADMANABHAN, V. N., AND RAMJEE, R. Coordinating Cellular Background Transfers Using LoadSense. In *MobiCom* (2013).

[23] CHANDRA, R., AND BAHL, P. MultiNet: Connecting to Multiple IEEE 802.11 Networks Using a Single Wireless Card. In *INFOCOM* (2004).

[24] CHEN, Y.-C., LIM, Y., GIBBENS, R. J., NAHUM, E. M., KHALILI, R., AND TOWSLEY, D. A Measurement-based Study of Multipath TCP Performance over Wireless Networks. In *IMC* (2013).

[25] DAI, S., TONGAONKAR, A., WANG, X., NUCCI, A., AND SONG, D. Networkprofiler: Towards Automatic Fingerprinting of Android Apps. In *INFOCOM* (2013).

[26] DENG, S., AND BALAKRISHNAN, H. Traffic-Aware Techniques to Reduce 3G/LTE Wireless Energy Consumption. In *CoNEXT* (2012).

[27] DENG, S., NETRAVALI, R., SIVARAMAN, A., AND BALAKRISHNAN, H. WiFi, LTE, or Both? Measuring Multi-Homed Wireless Internet Performance. In *IMC* (2014).

[28] DESHPANDE, P., HOU, X., AND DAS, S. R. Performance Comparison of 3G and Metro-Scale WiFi for Vehicular Network Access. In *IMC* (2010).

[29] FALAKI, H., LYMBEROPOULOS, D., MAHAJAN, R., KANDULA, S., AND ESTRIN, D. A First Look at Traffic on Smartphones. In *IMC* (2010).

[30] Faster connections, longer-lasting batteries: A fifth of all smartphones now benefit from Network Controlled Fast Dormancy. https://blog.networks.nokia.com/mobile-networks/2011/11/28/faster-connections-longer-lasting-batteries-a-fifth-of-all-smartphones-now-benefit-from-network-controlled-fast-dormancy/.

[31] UE "Fast Dormancy" behavior, 2007. 3GPP Discussion and Decision Notes R2-075251.

[32] HERBSTER, M., AND WARMUTH, M. K. Tracking the best expert. *Machine Learning 32* (1998), 151–178.

[33] HIGGINS, B. D., REDA, A., ALPEROVICH, T., FLINN, J., GIULI, T. J., NOBLE, B., AND WATSON, D. Intentional Networking: Opportunistic Exploitation of Mobile Network Diversity. In *MobiCom* (2010).

[34] HUANG, J., QIAN, F., GERBER, A., MAO, Z. M., SEN, S., AND SPATSCHECK, O. A Close Examination of Performance and Power Characteristics of 4G LTE Networks. In *MobiSys* (2012).

[35] JIANG, H., LIU, Z., WANG, Y., LEE, K., AND RHEE, I. Understanding Bufferbloat in Cellular Networks. In *CellNet* (2012).

[36] KANDULA, S., LIN, K. C.-J., BADIRKHANLI, T., AND KATABI, D. FatVAP: Aggregating AP Backhaul Capacity to Maximize Throughput. In *NSDI* (2008).

[37] KHALILI, R., GAST, N., POPOVIC, M., UPADHYAY, U., AND LE BOUDEC, J.-Y. MPTCP is Not Pareto-Optimal: Performance Issues and a Possible Solution. In *CoNEXT* (2012).

[38] KRASHINSKY, R., AND BALAKRISHNAN, H. Minimizing Energy for Wireless Web Access with Bounded Slowdown. In *MobiCom* (2002).

[39] KRASHINSKY, R., AND BALAKRISHNAN, H. Minimizing Energy for Wireless Web Access with Bounded Slowdown. *ACM Wireless Networks* (2005).

[40] LEE, C.-C., YEH, J.-H., AND CHEN, J.-C. Impact of inactivity timer on energy consumption in WCDMA and CDMA2000. In *IEEE Wireless Telecomm. Symp.(WTS)* (2004).

[41] LIU, H., ZHANG, Y., AND ZHOU, Y. TailTheft: Leveraging the Wasted Time for Saving Energy in Cellular Communications. In *MobiArch* (2011).

[42] MAHINDRA, R., VISWANATHAN, H., SUNDARESAN, K., ARSLAN, M. Y., AND RANGARAJAN, S. A Practical Traffic Management System for Integrated LTE-WiFi Networks. In *MobiCom* (2014).

[43] Monsoon power monitor. http://www.msoon.com/LabEquipment/PowerMonitor/.

[44] MONTELEONI, C. Online Learning of Non-stationary Sequences. In *AI Technical Report 2003-011, S.M. Thesis* (Artificial Intelligence Laboratory, Massachusetts Institute of Technology, 2003).

[45] MONTELEONI, C. Online learning of non-stationary sequences. In *AI Technical Report 2003-011, S.M. Thesis* (Artificial Intelligence Laboratory, Massachusetts Institute of Technology, May 2003).

[46] MONTELEONI, C., BALAKRISHNAN, H., FEAMSTER, N., AND JAAKKOLA, T. Managing the 802.11 Energy/Performance Tradeoff with Machine Learning. Tech. Rep. MIT-LCS-TR-971, MIT CSAIL, 2004.

[47] MONTELEONI, C., AND JAAKKOLA, T. Online Learning of Non-stationary Sequences. In *Neural Information Processing Systems 16* (2003).

[48] MPTCP for Android. http://multipath-tcp.org/pmwiki.php/Users/Android.

[49] Apple iOS 7 Surprises as First with New Multipath TCP Connections. http://www.networkworld.com/news/2013/091913-ios7-multipath-273995.html.

[50] Configure MPTCP Routing. `http://multipath-tcp.org/pmwiki.php/Users/ConfigureRouting`.

[51] MPTCP v0.88 Release. `http://multipath-tcp.org/pmwiki.php?n=Main.Release88`.

[52] MultiPath TCP - Linux Kernel Implementation. http://www.multipath-tcp.org/.

[53] NETRAVALI, R., SIVARAMAN, A., WINSTEIN, K., DAS, S., GOYAL, A., AND BALAKRISHNAN, H. Mahimahi: A Lightweight Toolkit for Reproducible Web Measurement (Demo). In *SIGCOMM* (2014).

[54] NIRJON, S., NICOARA, A., HSU, C.-H., SINGH, J., AND STANKOVIC, J. Multi-Nets: Policy Oriented Real-Time Switching of Wireless Interfaces on Mobile Devices. In *RTAS* (2012).

[55] NIYATO, D., AND HOSSAIN, E. Dynamics of Network Selection in Heterogeneous Wireless Networks: An Evolutionary Game Approach. *IEEE Transactions on Vehicular Technology* (2009).

[56] OLSHEN, L., AND STONE, C. J. Classification and Regression Trees. *Wadsworth International Group* (1984).

[57] PAASCH, C., DETAL, G., DUCHENE, F., RAICIU, C., AND BONAVENTURE, O. Exploring Mobile/WiFi Handover with MultiPath TCP. In *CellNet* (2012).

[58] PAASCH, C., FERLIN, S., ALAY, O., AND BONAVENTURE, O. Experimental Evaluation of Multipath TCP Schedulers. In *ACM SIGCOMM Capacity Sharing Workshop (CSWS)* (2014), ACM.

140

[59] PAREKH, A., AND GALLAGER, R. A Generalized Processor Sharing Approach to Flow Control in Integrated Services Networks: the Single-Node Case. *Networking, IEEE/ACM Transactions on* (1993).

[60] PEDREGOSA, F., VAROQUAUX, G., GRAMFORT, A., MICHEL, V., THIRION, B., GRISEL, O., BLONDEL, M., PRETTENHOFER, P., WEISS, R., DUBOURG, V., VANDERPLAS, J., PASSOS, A., COURNAPEAU, D., BRUCHER, M., PERROT, M., AND DUCHESNAY, E. Scikit-learn: Machine learning in Python. *Journal of Machine Learning Research* (2011).

[61] PERING, T., AGARWAL, Y., GUPTA, R., AND WANT, R. Coolspots: Reducing the Power Consumption of Wireless Mobile Devices with Multiple Radio Interfaces. In *MobiSys* (2006).

[62] PERKINS, C. E. Mobile IP. *Communications Magazine, IEEE* (1997).

[63] PLUNTKE, C., EGGERT, L., AND KIUKKONEN, N. Saving Mobile Device Energy with MultiPath TCP. In *MobiArch* (2011).

[64] QIAN, F., WANG, Z., GERBER, A., MAO, Z., SEN, S., AND SPATSCHECK, O. Profiling Resource Usage for Mobile Applications: a Cross-Layer Approach. In *MobiSys* (2011).

[65] QIAN, F., WANG, Z., GERBER, A., MAO, Z. M., SEN, S., AND SPATSCHECK, O. Characterizing radio resource allocation for 3G networks. In *IMC* (2010).

[66] QIAN, F., WANG, Z., GERBER, A., MAO, Z. M., SEN, S., AND SPATSCHECK, O. TOP: Tail Optimization Protocol For Celluar Radio Resource Allocation. In *ICNP* (2010).

[67] RAICIU, C., NICULESCU, D., BAGNULO, M., AND HANDLEY, M. J. Opportunistic Mobility with MultiPath TCP. In *MobiArch* (2011).

[68] ROSEN, S., LEE, S.-J., LEE, J., CONGDON, P., MORLEY MAO, Z., AND BURDEN, K. MCNet: Crowdsourcing Wireless Performance Measurements through the Eyes of Mobile Devices. *Communications Magazine, IEEE* (2014).

[69] SIMUNIC, T., BENINI, L., GLYNN, P. W., AND MICHELI, G. D. Dynamic power management for portable systems. In *MobiCom* (2000).

[70] SNOEREN, A. C., AND BALAKRISHNAN, H. An End-to-end Approach to Host Mobility. In *MobiCom* (2000).

[71] SOMMERS, J., AND BARFORD, P. Cell vs. WiFi: on the Performance of Metro Area Mobile Connections. In *IMC* (2012).

[72] SONG, Q., AND JAMALIPOUR, A. Network Selection in an Integrated Wireless LAN and UMTS Environment Using Mathematical Modeling and Computing Techniques. *IEEE Wireless Communications* (2005).

[73] SSL Proxy: Man-in-the-middle. `http://crypto.stanford.edu/ssl-mitm/`.

[74] Cisco visual networking index: Global mobile data traffic forecast update, 2014-2019. `http://www.cisco.com/c/en/us/solutions/collateral/service-provider/visual-networking-index-vni/white_paper_c11-520862.html`.

[75] WiFi direct description. `http://en.wikipedia.org/wiki/Pearson_product-moment_correlation_coefficient`.

[76] WINSTEIN, K., AND BALAKRISHNAN, H. Mosh: An Interactive Remote Shell for Mobile Clients. In *USENIX ATC* (2012).

[77] WISCHIK, D., RAICIU, C., GREENHALGH, A., AND HANDLEY, M. Design, Implementation and Evaluation of Congestion Control for Multipath TCP. In *NSDI* (2011).

[78] XU, Q., MEHROTRA, S., MAO, Z., AND LI, J. PROTEUS: Network Performance Forecast for Real-Time, Interactive Mobile Applications. In *MobiSys* (2013).

[79] YAP, K.-K., HUANG, T.-Y., YIAKOUMIS, Y., CHINCHALI, S., MCKEOWN, N., AND KATTI, S. Scheduling Packets over Multiple Interfaces While Respecting User Preferences. In *CoNEXT* (2013).

[80] YAP, K.-K., MCKEOWN, N., AND KATTI, S. Multi-Server Generalized Processor Sharing. In *ITC* (2012).

[81] YEH, J.-H., CHEN, J.-C., AND LEE, C.-C. Comparative Analysis of Energy-Saving Techniques in 3GPP and 3GPP2 Systems. *IEEE Trans. on Vehicular Technology* (2009).

[82] YEH, J.-H., LEE, C.-C., AND CHEN, J.-C. Performance analysis of energy consumption in 3GPP networks. In *IEEE Wireless Telecomm. Symp. (WTS)* (2004).

[83] Google's next bid to lower mobile data costs: Zero rating. `https://www.theinformation.com/Google-s-Next-Bid-to-Lower-Mobile-Data-Costs-Zero-Rating`.

[84] ZHAO, X., CASTELLUCCIA, C., AND BAKER, M. Flexible Network Support for Mobility. In *MobiCom* (1998).